SUSAN HOLMES & WOLFGANG HUBER ©

MODERN STATISTICS FOR MODERN BIOLOGY

Contents

Chapter 3
High Quality Graphics in R

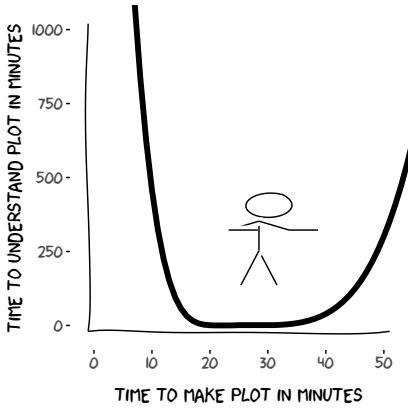

Figure 3.1: An elementary law of visualization.

There are (at least) two types of data visualization. The first enables a scientist to effectively explore data and make discoveries about the complex processes at work. The other type of visualization provides informative, clear and visually attractive illustrations of her results that she can show to others and eventually include in a publication.

Both of these types of visualizations can be made with R. In fact, R offers multiple graphics systems. This is because R is extensible, and because progress in R graphics has proceeded largely not by replacing the old functions, but by adding packages. Each of the different graphics systems has its advantages and limitations. In this chapter we'll use two of them. First, we have a cursory look at the base R plotting functions[1]. Subsequently we will switch to *ggplot2*.

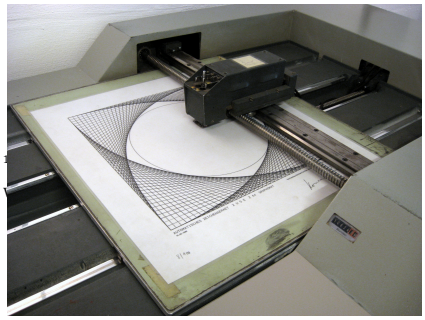
Figure 3.2: The ZUSE Plotter Z64 (presented in 1961). Source: `https://en.wikipedia.org/wiki/Plotter`.

Base R graphics were historically first: simple, procedural, canvas-oriented. There are specialized functions for different types of plots. These are easy to call – but when you want to combine them to build up more complex plots, or exchange one for another, this quickly gets messy to program, or even impossible. The user plots (the word stems back to some of the first graphics devices – see Figure 3.2) directly onto a (conceptual) canvas. She explicitly needs to deal with decisions such as how many inches to allocate to margins, axes labels, titles, legends, subpanels; once something is "plotted" it cannot be easily moved or erased.

There is a more high-level approach: in the **grammar of graphics**, graphics are built up from modular logical pieces, so that we can easily try different visualization types for our data in an intuitive and easily deciphered way, like we can switch in and out parts of a sentence in human language. There is no concept of a canvas or a plotter, rather, the user gives *ggplot2* a high-level description of the plot she wants, in the form of an R object, and the rendering engine takes a wholistic view on the scene to lay out the graphics and render them on the output device.

We'll explore **faceting**, for showing more than 2 variables at a time. Sometimes this is also called lattice[2] graphics, and it allows us to visualise data in up to four or five dimensions.

[2] The first major R package to implement this was *lattice*; nowadays much of such functionality is also provided through *ggplot2*.

3.1 Goals for this chapter

- Learn how to rapidly and flexibly explore datasets by visualization.
- Create beautiful and intuitive plots for scientific presentations and publications.
- Review the basics of *base* R plotting.
- Understand the logic behind the **grammar of graphics** concept.
- Introduce *ggplot2*'s `ggplot` function.
- See how to plot 1D, 2D, 3-5D data, and understand faceting.
- Creating "along-genome" plots for molecular biology data (or along other sequences, e. g., peptides).
- Discuss our options of interactive graphics.

3.2 Base R plotting

The most basic function is `plot`. In the code below, the output of which is shown in Figure 3.3, it is used to plot data from an enzyme-linked immunosorbent assay (ELISA) assay. The assay was used to quantify the activity of the enzyme deoxyribonuclease (DNase), which degrades DNA. The data are assembled in the R object `DNase`, which conveniently comes with base R. `DNase` is a dataframe whose columns are `Run`, the assay run; `conc`, the protein concentration that was used; and `density`, the measured optical density.

```
head(DNase)
```

```
##   Run       conc density
## 1   1 0.04882812   0.017
## 2   1 0.04882812   0.018
## 3   1 0.19531250   0.121
## 4   1 0.19531250   0.124
## 5   1 0.39062500   0.206
## 6   1 0.39062500   0.215
```

```
plot(DNase$conc, DNase$density)
```

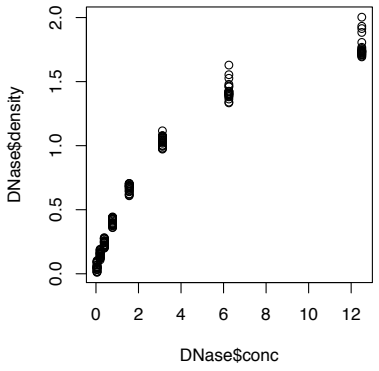

Figure 3.3: Plot of concentration vs. density for an ELISA assay of DNase.

This basic plot can be customized, for example by changing the plot symbol and axis labels using the parameters `xlab`, `ylab` and `pch` (plot character), as shown in Figure 3.4. Information about the variables is stored in the object `DNase`, and we can access it with the `attr` function.

```
plot(DNase$conc, DNase$density,
  ylab = attr(DNase, "labels")$y,
  xlab = paste(attr(DNase, "labels")$x, attr(DNase, "units")$x),
  pch = 3,
  col = "blue")
```

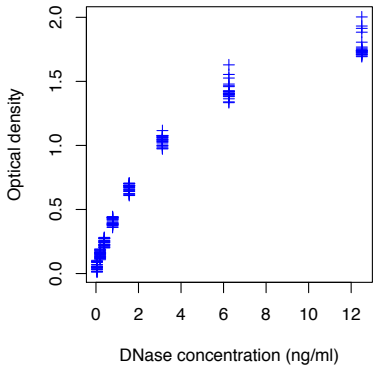

Figure 3.4: Same data as in Figure 3.3 but with better axis labels and a different plot symbol.

▶ Question **3.2.1.** Annotating dataframe columns with "metadata" such as longer descriptions, physical units, provenance information, etc., seems like a useful feature. Is this way of storing such information, as in the `DNase` object, standardized or common across the R ecosystem? Are there other standardized or common ways for doing this?

▶ Answer **3.2.1.** Have a look at the *DataFrame* class in the Bioconductor package *S4Vectors*. Among other things it is used to annotate the rows and columns of a *SummarizedExperiment*[3].

Besides scatterplots, we can also use built-in functions to create histograms and boxplots (Figure 3.5).

```
hist(DNase$density, breaks=25, main = "")
```

```
boxplot(density ~ Run, data = DNase)
```

Boxplots are convenient for showing multiple distributions next to each other in a compact space, and they are universally preferable to the barplots with error bars sometimes still seen in biological papers. We will see more about plotting multiple univariate distributions in Section 3.6.

The base R plotting functions are great for quick interactive exploration of data; but we run soon into their limitations if we want to create more sophisticated displays. We are going to use a visualization framework called the grammar of graphics, implemented in the package *ggplot2*, that enables step by step construction of high quality graphics in a logical and elegant manner. First let us introduce and load an example dataset.

[3] So the meatadata of the *DataFrame* that itself serves as metadata to the matrix in a *SummarizedExperiment* could be called metametadata. This recursion can be repeated ad infinitum. Some people dislike the "meta" prefix since it is more a subjective comment on rather than an objective property of a datum.

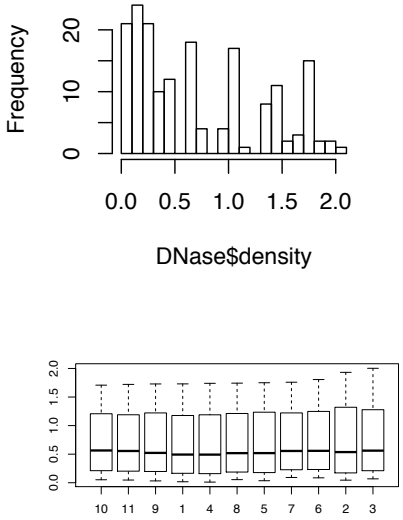

Figure 3.5: Histogram of the density from the ELISA assay, and boxplots of these values stratified by the assay run. The boxes are ordered along the axis in lexicographical order because the runs were stored as text strings. We could use R's type conversion functions to achieve numerical ordering.

3.3 An example dataset

To properly testdrive the *ggplot2* functionality, we are going to need a dataset that is big enough and has some complexity so that it can be sliced and viewed from many different angles. We'll use a gene expression microarray dataset that reports the transcriptomes of around 100 individual cells from mouse embryos at different time points in early development. The mammalian embryo starts out as a single cell, the fertilized egg. Through synchronized waves of cell divisions, the egg multiplies into a clump of cells that at first show no discernible differences between them. At some point, though, cells choose different lineages. By further and further specification, the different cell types and tissues arise that are needed for a full organism. The aim of the experiment, explained by Ohnishi et al. (2014), was to investigate the gene expression changes associated with the first symmetry breaking event in the embryo. We'll further explain the data as we go. More details can be found in the paper and in the documentation of the Bioconductor data package *Hiiragi2013*. We first load the package and the data:

```
library("Hiiragi2013")
data("x")
dim(exprs(x))
```

```
## [1] 45101   101
```

You can print out a more detailed summary of the *ExpressionSet* object `x` by just typing `x` at the R prompt. The 101 columns of the data matrix (accessed above through the `exprs` function) correspond to the samples (and each of these to a single cell), the 45101 rows correspond to the genes probed by the array, an Affymetrix mouse4302

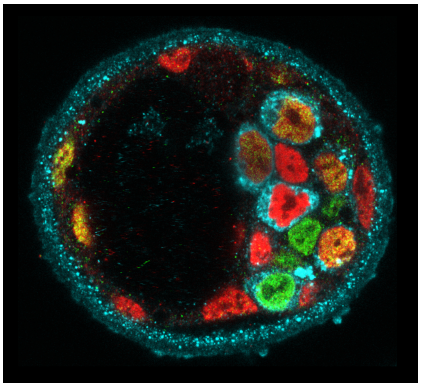

Figure 3.6: Single-section immunofluorescence image of the E3.5 mouse blastocyst stained for Serpinh1, a marker of primitive endoderm (blue), Gata6 (red) and Nanog (green).

array. The data were normalized using the RMA method (Irizarry et al., 2003). The raw data are also available in the package (in the data object a) and at EMBL-EBI's ArrayExpress database under the accession code E-MTAB-1681.

Let's have a look at what information is available about the samples.[4]

```
head(pData(x), n = 2)
```

```
##         File.name Embryonic.day Total.number.of.cells lineage
## 1 E3.25  1_C32_IN         E3.25                    32
## 2 E3.25  2_C32_IN         E3.25                    32
##         genotype   ScanDate sampleGroup sampleColour
## 1 E3.25       WT 2011-03-16       E3.25      #CAB2D6
## 2 E3.25       WT 2011-03-16       E3.25      #CAB2D6
```

The information provided is a mix of information about the cells (i.e., age, size and genotype of the embryo from which they were obtained) and technical information (scan date, raw data file name). By convention, time in the development of the mouse embryo is measured in days, and reported as, for instance, `E3.5`. Moreover, in the paper the authors divided the cells into 8 biological groups (`sampleGroup`), based on age, genotype and lineage, and they defined a color scheme to represent these groups (`sampleColour`[5]). Using the `group_by` and `summarise` functions from the package *dplyr*, we'll define a little dataframe `groups` that contains summary information for each group: the number of cells and the preferred color.

```
library("dplyr")
groups = group_by(pData(x), sampleGroup) %>%
  summarise(n = n() , color = unique(sampleColour))
groups
```

```
## # A tibble: 8 x 3
##       sampleGroup     n   color
##             <chr> <int>   <chr>
## 1           E3.25    36 #CAB2D6
## 2 E3.25 (FGF4-KO)    17 #FDBF6F
## 3      E3.5 (EPI)    11 #A6CEE3
## 4  E3.5 (FGF4-KO)     8 #FF7F00
## 5       E3.5 (PE)    11 #B2DF8A
## 6      E4.5 (EPI)     4 #1F78B4
## 7  E4.5 (FGF4-KO)    10 #E31A1C
## 8       E4.5 (PE)     4 #33A02C
```

The cells in the groups whose name contains `FGF4-KO` are from embryos in which the FGF4 gene, an important regulator of cell differentiation, was knocked out. Starting from E3.5, the wildtype cells (without the FGF4 knock-out) undergo the first symmetry breaking event and differentiate into different cell lineages, called pluripotent epiblast (EPI) and primitive endoderm (PE).

3.4 ggplot2

ggplot2 is a package by Hadley Wickham (Wickham, 2016) that implements the idea

[4] The notation #CAB2D6 is a hexadecimal representation of the RGB coordinates of a color; more on this in Section 3.10.2.

[5] This identifier in the dataset uses the British spelling. Everywhere else in this chapter, we use the US spelling (color). The *ggplot2* package generally accepts both spellings.

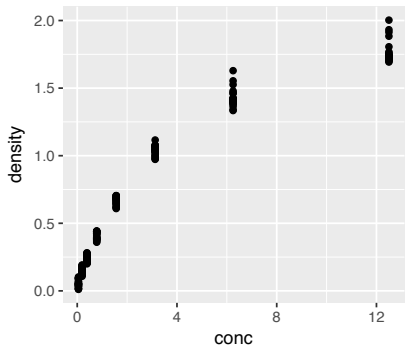

Figure 3.7: Our first *ggplot2* figure, similar to the base graphics Figure 3.3.

of **grammar of graphics** – a concept created by Leland Wilkinson in his eponymous book (Wilkinson, 2005). Comprehensive documentation for the package can be found on its website. The online documentation includes example use cases for each of the graphic types that are introduced in this chapter (and many more) and is an invaluable resource when creating figures.

Let's start by loading the package and redoing the simple plot of Figure 3.3.

```
library("ggplot2")
ggplot(DNase, aes(x = conc, y = density)) + geom_point()
```

We just wrote our first "sentence" using the grammar of graphics. Let us deconstruct this sentence. First, we specified the dataframe that contains the data, `DNase`. Then we told `ggplot` via the `aes`[6] argument which variables we want on the x- and y-axes, respectively. Finally, we stated that we want the plot to use points, by adding the result of calling the function `geom_point`.

Now let's turn to the mouse single cell data and plot the number of samples for each of the 8 groups using the `ggplot` function. The result is shown in Figure 3.8.

```
ggplot(data = groups, aes(x = sampleGroup, y = n)) +
  geom_bar(stat = "identity")
```

With `geom_bar` we now told `ggplot` that we want each data item (each row of `groups`) to be represented by a bar. Bars are one geometric object (**geom**) that `ggplot` knows about. We've already seen another geom in Figure 3.7: points. We'll encounter many other possible geometric objects later. We used the `aes` to indicate that we want the groups shown along the x-axis and the sizes along the y-axis. Finally, we provided the argument `stat = "identity"` (in other words, do nothing) to the `geom_bar` function, since otherwise it would try to compute a histogram of the data (the default value of `stat` is `"count"`). `stat` is short for **statistic**, which is what we call any function of data. Besides the identity and count statistic, there are others, such as smoothing, averaging, binning, or other operations that reduce the data in some way.

These concepts –data, geometrical objects, statistics– are some of the ingredients of the grammar of graphics, just as nouns, verbs and adverbs are ingredients of an English sentence.

▶ Question **3.4.1.**

Flip the x- and y-aesthetics to produce a horizontal barplot.

The plot in Figure 3.8 is not bad, but there are several potential improvements. We can use color for the bars to help us quickly see which bar corresponds to which group. This is particularly useful if we use the same color scheme in several plots. To this end, let's define a named vector `groupColor` that contains our desired colors for each possible value of `sampleGroup`.[7]

```
groupColor = setNames(groups$color, groups$sampleGroup)
```

Another thing that we need to fix is the readability of the bar labels. Right now

[6] This stands for **aesthetic**, a terminology that will become clearer below.

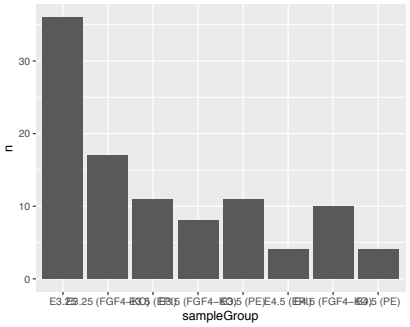

Figure 3.8: A barplot, produced with the `ggplot` function from the table of group sizes in the mouse single cell data.

[7] The information is completely equivalent to that in the `sampleGroup` and `color` columns of the dataframe `groups`, we're just adapting to the fact that *ggplot2* expects this information in the form of a named vector.

they are running into each other — a common problem when you have descriptive names.

```
ggplot(groups, aes(x = sampleGroup, y = n, fill = sampleGroup)) +
  geom_bar(stat = "identity") +
  scale_fill_manual(values = groupColor, name = "Groups") +
  theme(axis.text.x = element_text(angle = 90, hjust = 1))
```

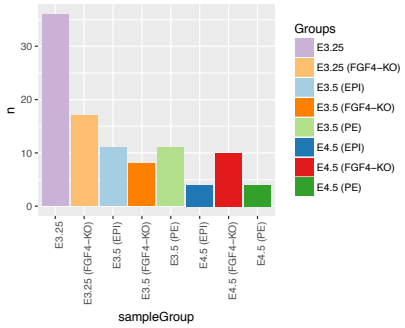

Figure 3.9: Similar to Figure 3.8, but with colored bars and better bar labels.

This is now already a longer and more complex sentence. Let us dissect it. We added an argument, `fill` to the `aes` function that states that we want the bars to be colored (filled) based on `sampleGroup` (which in this case co-incidentally is also the value of the `x` argument, but that need not be so). Furthermore we added a call to the `scale_fill_manual` function, which takes as its input a color map – i. e., the mapping from the possible values of a variable to the associated colors – as a named vector. We also gave this color map a title (note that in more complex plots, there can be several different color maps involved). Had we omitted the call to `scale_fill_manual`, *ggplot2* would have used its choice of default colors. We also added a call to `theme` stating that we want the x-axis labels rotated by 90 degrees and right-aligned (`hjust`; the default would be to center).

3.4.1 Data flow

ggplot2 expects your data in a dataframe[8]. If they are in a matrix, in separate vectors, or other types of objects, you will have to convert them. The packages *dplyr* and *broom*, among others, offer facilities to this end, we'll discuss this more in Section 14.11, and you'll see examples of such conversions sprinkled throughout the book.

[8] This includes the base R *data.frame* as well as the *tibble* (and synonymous *data_frame*) classes from the *tibble* package in the tidyverse.

The result of a call to the `ggplot` is a *ggplot* object. Let's recall a piece of code from above:

```
gg = ggplot(DNase, aes(x = conc, y = density)) + geom_point()
```

We have now assigned the output of `ggplot` to the object `gg`, instead of sending it directly to the console, where it was "printed" and produced Figure 3.7. The situation is completely analogously to what you are used to from working with the R console: when you enter an expression like `1+1` and hit "Enter", the result is printed. When the expression is an assignment, such as `s = 1+1`, the side effect takes place (the name `"s"` is bound to an object in memory that represents the value of `1+1`), but nothing is printed. Similarly, when an expression is evaluated as part of a script called with `source`, it is not printed. Thus, the above code also does not create any graphic output, since no `print` method is invoked. To print the `gg`, type its name (in an interactive session) or call `print` on it:

```
gg
print(gg)
```

3.4.2 Saving figures

ggplot2 has a built-in plot saving function called `ggsave`:

```
ggsave("DNAse-histogram-demo.pdf", plot = gg)
```

There are two major ways of storing plots: vector graphics and raster (pixel) graphics. In vector graphics, the plot is stored as a series of geometrical primitives such as points, lines, curves, shapes and typographic characters. The prefered format in R for saving plots into a vector graphics format is PDF. In raster graphics, the plot is stored in a dot matrix data structure. The main limitation of raster formats is their limited resolution, which depends on the number of pixels available. In R, the most commonly used device for raster graphics output is `png`. Generally, it's preferable to save your graphics in a vector graphics format, since it is always possible later to convert a vector graphics file into a raster format of any desired resolution, while the reverse is fundamentally limited by the resolution of the original file. And you don't want the figures in your talks or papers look poor because of pixelization artefacts!

3.5 The grammar of graphics

The components of *ggplot2*'s grammar of graphics are

1. one or more datasets,
2. one or more geometric objects that serve as the visual representations of the data, – for instance, points, lines, rectangles, contours,
3. descriptions of how the variables in the data are mapped to visual properties (aesthetics) of the geometric objects, and an associated scale (e. g., linear, logarithmic, rank),
4. one or more coordinate systems,
5. statistical summarization rules,
6. a facet specification, i. e. the use of multiple similar subplots to look at subsets of the same data,
7. optional parameters that affect the layout and rendering, such text size, font and alignment, legend positions, and the like.

In the examples above, Figures 3.8 and 3.9, the dataset was `groupsize`, the variables were the numeric values as well as the names of `groupsize`, which we mapped to the aesthetics y-axis and x-axis respectively, the scale was linear on the y and rank-based on the x-axis (the bars are ordered alphanumerically and each has the same width), the geometric object was the rectangular bar.

Items 4.–7. in the above list are optional. If you don't specify them, then the Cartesian is used as the coordinate system, the statistical summary is the trivial one (i. e., the identity), and no facets or subplots are made (we'll see examples later on, in Section 3.8). The first three items are mandatory, you always need to specify at least one of them: they are the minimal components of a valid *ggplot2* "sentence".

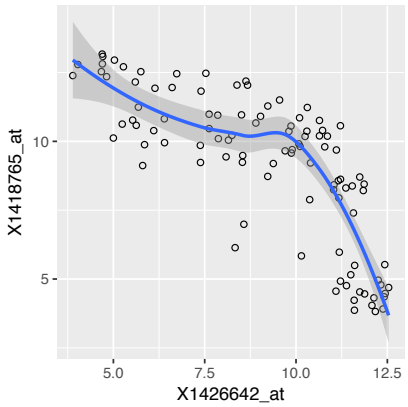

Figure 3.10: A scatterplot with three layers that show different statistics of the same data: points, a smooth regression line, and a confidence band.

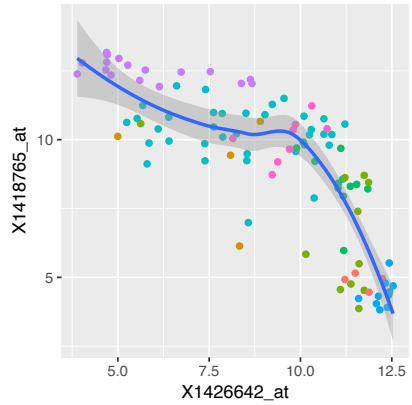

Figure 3.11: As Figure 3.10, but in addition with points colored by the sample group (as in Figure 3.9). We can now see that the expression values of the gene Timd2 (whose mRNA is targeted by the probe 1418765_at) are consistently high in the early time points, whereas its expression goes down in the EPI samples at days 3.5 and 4.5. In the FGF4-KO, this decrease is delayed - at E3.5, its expression is still high. Conversely, the gene Fn1 (1426642_at) is off in the early timepoints and then goes up at days 3.5 and 4.5. The PE samples (green) show a high degree of

In fact, *ggplot2*'s implementation of the grammar of graphics allows you to use the same type of component multiple times, in what are called layers (Wickham, 2010). For example, the code below uses three types of geometric objects in the same plot, for the same data: points, a line and a confidence band.

```
# dftx = as_tibble(t(exprs(x))) %>% cbind(pData(x))
dftx = data.frame(t(exprs(x)), pData(x))
ggplot( dftx, aes( x = X1426642_at, y = X1418765_at)) +
  geom_point( shape = 1 ) +
  geom_smooth( method = "loess" )
```

Here we had to assemble a copy of the expression data (`exprs(x)`) and the sample annotation data (`pData(x)`) all together into the dataframe `dftx` – since this is the data format that *ggplot2* functions most easily take as input (more on this in Section 14.11).

We can further enhance the plot by using colors – since each of the points in Figure 3.10 corresponds to one sample, it makes sense to use the `sampleColour` information in the object `x`.

```
ggplot( dftx, aes( x = X1426642_at, y = X1418765_at ))  +
  geom_point( aes( color = sampleColour), shape = 19 ) +
  geom_smooth( method = "loess" ) +
  scale_color_discrete( guide = FALSE )
```

▶ Question **3.5.1.** In the code above we defined the `color` aesthetics (`aes`) only for the `geom_point` layer, while we defined the `x` and `y` aesthetics for all layers. What happens if we set the `color` aesthetics for all layers, i. e., move it into the argument list of `ggplot`? What happens if we omit the call to `scale_color_discrete`?

▶ Question **3.5.2.** Is it always meaningful to visualize scatterplot data together with a regression line as in Figures 3.10 and 3.11?

As a small side remark, if we want to find out which genes are targeted by these probe identifiers, and what they might do, we can call.[9]

```
library("mouse4302.db")
```

```
AnnotationDbi::select(mouse4302.db,
   keys = c("1426642_at", "1418765_at"), keytype = "PROBEID",
   columns = c("SYMBOL", "GENENAME"))
```

```
##      PROBEID SYMBOL
## 1 1426642_at    Fn1
## 2 1418765_at  Timd2
##                                          GENENAME
## 1                                     fibronectin 1
## 2 T cell immunoglobulin and mucin domain containing 2
```

Often when using `ggplot` you will only need to specify the data, aesthetics and a geometric object. Most geometric objects implicitly call a suitable default statistical summary of the data. For example, if you are using `geom_smooth`, *ggplot2* by default uses `stat = "smooth"` and then displays a line; if you use `geom_histogram`, the

[9] Note that here were need to use the original feature identifiers (e. g., "1426642_at", without the leading "X"). This is the notation used by the microarray manufacturer, by the Bioconductor annotation packages, and also inside the object `x`. The leading "X" that we used above when working with `dftx` was inserted during the creation of `dftx` by the constructor fuction `data.frame`, since its argument `check.names` is set to `TRUE` by default. Alternatively, we could have kept the original identifer notation by setting `check.names=FALSE`, but then we would need to work with the backticks, such as `aes( x = `1426642_at`, ...)`, to make sure R understands the identifiers correctly.

data are binned, and the result is displayed in barplot format. Here's an example:

```
dfx = as.data.frame(exprs(x))
ggplot(dfx, aes(x = `20 E3.25`)) + geom_histogram(binwidth = 0.2)
```

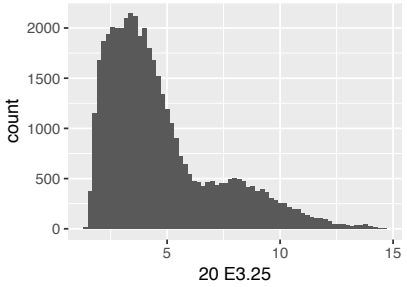

Figure 3.12: Histogram of probe intensities for one particular sample, cell number 20, which was from day E3.25.

▶ Question **3.5.3.** What is the difference between the objects `dfx` and `dftx`? Why did we need to create both of the?

Let's come back to the barplot example from above.

```
pb = ggplot(groups, aes(x = sampleGroup, y = n))
```

This creates a plot object `pb`. If we try to display it, it creates an empty plot, because we haven't specified what geometric object we want to use. All that we have in our `pb` object so far are the data and the aesthetics (Fig. 3.13)

```
class(pb)

## [1] "gg"     "ggplot"

pb
```

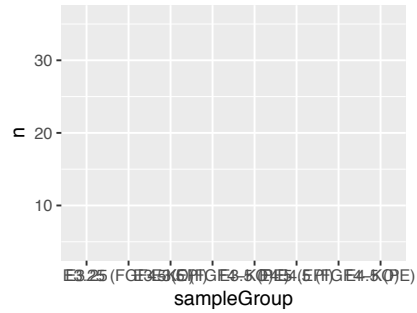

Figure 3.13: `pb`: without a geometric object, the plot remains empty.

Now we can literally add on the other components of our plot through using the + operator (Fig. 3.14):

```
pb = pb + geom_bar(stat = "identity")
pb = pb + aes(fill = sampleGroup)
pb = pb + theme(axis.text.x = element_text(angle = 90, hjust = 1))
pb = pb + scale_fill_manual(values = groupColor, name = "Groups")
pb
```

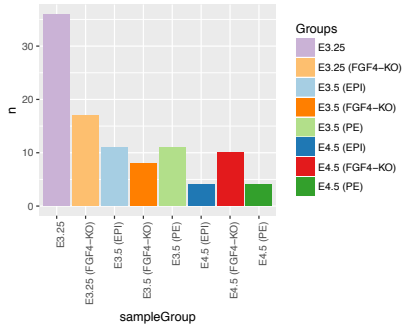

Figure 3.14: The graphics object `bp` in its full glory.

This step-wise buildup –taking a graphics object already produced in some way and then further refining it– can be more convenient and easy to manage than, say, providing all the instructions upfront to the single function call that creates the graphic. We can quickly try out different visualization ideas without having to rebuild our plots each time from scratch, but rather store the partially finished object and then modify it in different ways. For example we can switch our plot to polar coordinates to create an alternative visualization of the barplot.

```
pb.polar = pb + coord_polar() +
  theme(axis.text.x = element_text(angle = 0, hjust = 1),
        axis.text.y = element_blank(),
        axis.ticks = element_blank()) +
  xlab("") + ylab("")
pb.polar
```

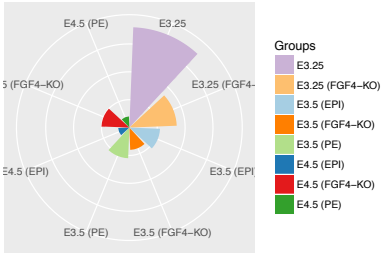

Figure 3.15: A barplot in a polar coordinate system.

Note above that we can override previously set `theme` parameters by simply setting them to a new value – no need to go back to recreating `pb`, where we originally set them.

3.6 Visualization of 1D data

A common task in biological data analysis is the comparison between several samples of univariate measurements. In this section we'll explore some possibilities for visual-

izing and comparing such samples. As an example, we'll use the intensities of a set of four genes Fgf4, Gata4, Gata6 and Sox2[10]. On the array, they are represented by

```
selectedProbes = c( Fgf4 = "1420085_at", Gata4 = "1418863_at",
                    Gata6 = "1425463_at",  Sox2 = "1416967_at")
```

[10] You can read more about these genes in the paper associated with the data.

To extract data from this representation and convert them into a dataframe, we use the function `melt` from the *reshape2* package[11].

```
library("reshape2")
genes = melt(exprs(x)[selectedProbes, ], varnames = c("probe", "sample"))
head(genes)
```

```
##        probe  sample    value
## 1 1420085_at 1 E3.25 3.027715
## 2 1418863_at 1 E3.25 4.843137
## 3 1425463_at 1 E3.25 5.500618
## 4 1416967_at 1 E3.25 1.731217
## 5 1420085_at 2 E3.25 9.293016
## 6 1418863_at 2 E3.25 5.530016
```

[11] We'll talk more about the concepts and mechanics of different data representations in Section 14.11.

For good measure, we also add a column that provides the gene symbol along with the probe identifiers.

```
genes$gene = names(selectedProbes)[ match(genes$probe, selectedProbes) ]
```

3.6.1 Barplots

A popular way to display data such as in our dataframe `genes` is through barplots. See Fig. 3.16.

```
ggplot(genes, aes( x = gene, y = value)) +
  stat_summary(fun.y = mean, geom = "bar")
```

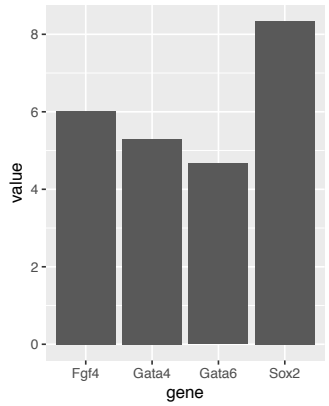

Figure 3.16: Barplots showing the means of the distributions of expression measurements from 4 probes.

In Figure 3.16, each bar represents the mean of the values for that gene. Such plots are seen a lot in the biological sciences, as well as in the popular media. The data summarization into only the mean looses a lot of information, and given the amount of space it takes, a barplot can be a poor way to visualise data[12].

[12] In fact, if the mean is not an appropriate summary, such as for highly skewed distributions, or datasets with outliers, the barplot can be outright misleading.

Sometimes we want to add error bars, and one way to achieve this in *ggplot2* is as follows.

```
library("Hmisc")
ggplot(genes, aes( x = gene, y = value, fill = gene)) +
  stat_summary(fun.y = mean, geom = "bar") +
  stat_summary(fun.data = mean_cl_normal, geom = "errorbar",
               width = 0.25)
```

Here, we see again the principle of layered graphics: we use two summary functions, `mean` and `mean_cl_normal`, and two associated geometric objects, `bar` and `errorbar`. The function `mean_cl_normal` is from the *Hmisc* package and computes the standard error (or **c**onfidence **l**imits) of the mean; it's a simple function, and we

could also compute it ourselves using base R expressions if we wished to do so. We also colored the bars to make the plot more pleasant.

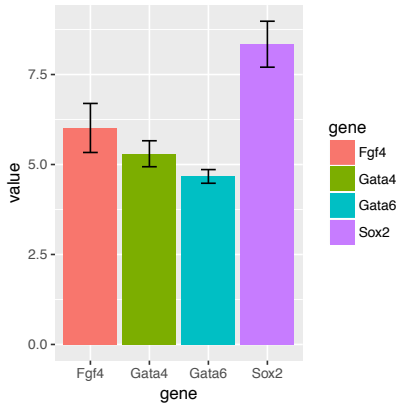

Figure 3.17: Barplots with error bars indicating standard error of the mean.

3.6.2 Boxplots

It's easy to show the same data with boxplots.

```
p = ggplot(genes, aes( x = gene, y = value, fill = gene))
p + geom_boxplot()
```

Compared to the barplots, this takes a similar amount of space, but is much more informative. In Figure 3.18 we see that two of the genes (Gata4, Gata6) have relatively concentrated distributions, with only a few data points venturing out to the direction of higher values. For Fgf4, we see that the distribution is right-skewed: the median, indicated by the horizontal black bar within the box is closer to the lower (or left) side of the box. Analogously, for Sox2 the distribution is left-skewed.

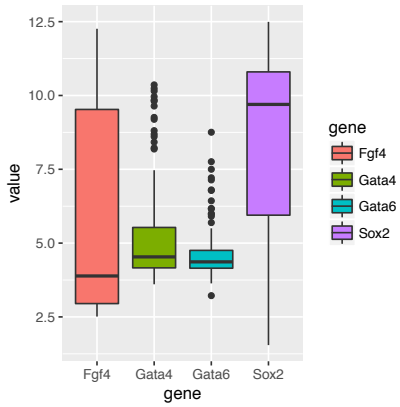

Figure 3.18: Boxplots.

3.6.3 Violin plots

A variation of the boxplot idea, but with an even more direct representation of the shape of the data distribution, is the violin plot. Here, the shape of the violin gives a rough impression of the distribution density.

```
p + geom_violin()
```

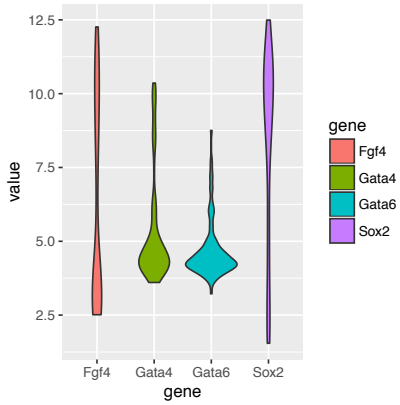

Figure 3.19: Violin plots.

3.6.4 Dot plots and beeswarm plots

If the number of data points is not too large, it is possible to show the data points directly, and it is good practice to do so, compared to using more abstract summaries. However, plotting the data directly will often lead to overlapping points, which can be visually unpleasant, or even obscure the data. We can try to layout the points so that they are as near possible to their proper locations without overlap (Wilkinson, 1999).

```
p + geom_dotplot(binaxis = "y", binwidth = 1/6,
       stackdir = "center", stackratio = 0.75,
       aes(color = gene))
```

The plot is shown in the left panel of Figure 3.20. The y-coordinates of the points are discretized into bins (above we chose a bin size of 1/6), and then they are stacked next to each other.

An alternative is provided by the package *ggbeeswarm*, which provides `geom_beeswarm`.

```
library("ggbeeswarm")
p + geom_beeswarm(aes(color = gene))
```

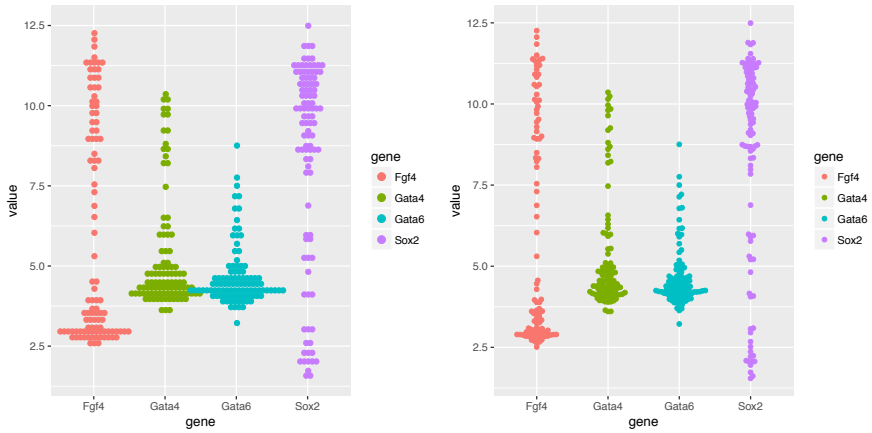

Figure 3.20: Left: dot plots, made using `geom_dotplot` from *ggplot2*. Right: beeswarm plots, made using `geom_beeswarm` from *ggbeeswarm*.

The plot is shown in the right panel of Figure 3.20. The layout algorithm tries to avoid overlaps between the points. If a point were to overlap an existing point, it is shifted sideways (along the x-axis) by a small amount sufficient to avoid overlap. Some twiddling with layout parameters is usually needed for each new dataset to make a dot plot or a beeswarm plot look good.

3.6.5 Density plots

Yet another way to represent the same data is by density plots (Figure 3.21).

```
ggplot(genes, aes( x = value, color = gene)) + geom_density()
```

Density estimation has a number of complications, in particular, the need for choosing a smoothing window. A window size that is small enough to capture peaks in the dense regions of the data may lead to instable ("wiggly") estimates elsewhere. On the other hand, if the window is made bigger, pronounced features of the density, such as sharp peaks, may be smoothed out. Moreover, the density lines do not convey the information on how much data was used to estimate them, and plots like Figure 3.21 can be especially problematic if the sample sizes for the curves differ.

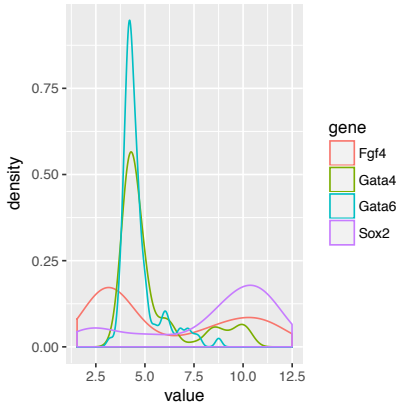

Figure 3.21: Density plots.

3.6.6 ECDF plots

The mathematically most convenient way to describe the distribution of a one-dimensional random variable X is its cumulative distribution function (CDF), i. e., the function

$$F(x) = P(X \leq x), \tag{3.1}$$

where x takes all values along the real axis. The density of X is then the derivative of F, if it exists[13]. The definition of the CDF can also be applied to finite samples of X, i. e., samples $x_1, \ldots, x_n$. The empirical cumulative distribution function (ECDF) is

[13] By its definition, F tends to 0 for small x ($x \to -\infty$) and to 1 for large x ($x \to +\infty$).

simply (Figure 3.22):

$$F_n(x) = \frac{1}{n}\sum_{i=1}^{n} \mathbb{1}_{x \le x_i}. \tag{3.2}$$

```
ggplot(genes, aes( x = value, color = gene)) + stat_ecdf()
```

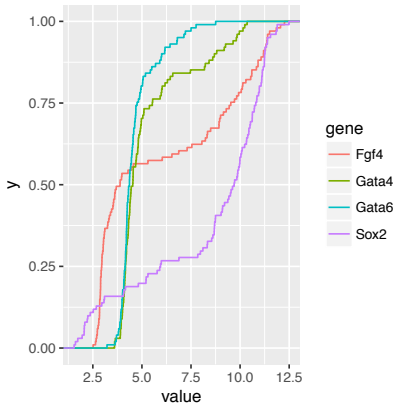

Figure 3.22: Empirical cumulative distribution functions (ECDF).

The ECDF has several nice properties:

- It is lossless - the ECDF $F_n(x)$ contains all the information contained in the original sample $x_1, \ldots, x_n$ (except the –unimportant– order of the values).
- As n grows, the ECDF $F_n(x)$ converges to the true CDF $F(x)$. Even for limited sample sizes n, the difference between the two functions tends to be small. Note that this is not the case for the empirical density! Without smoothing, the empirical density of a finite sample is a sum of Dirac delta functions, which is difficult to visualize and quite different from any underlying smooth, true density. With smoothing, the difference can be less pronounced, but is difficult to control, as we discussed above.

3.6.7 The effect of transformations on densities

It is tempting to look at histograms or density plots and inspect them for evidence of bimodality (or multimodality) as an indication of some underlying biological phenomenon. Before doing so, it is important to remember that the number of modes of a density depends on scale transformations of the data, via the **chain rule**. A simple example, with a mixture of two normal distributions, is shown in Figure 3.23.

```
sim <- data_frame(
   x = exp(rnorm(
     n    = 1e5,
     mean = sample(c(2, 5), size = 1e5, replace = TRUE))))

ggplot(sim, aes(x)) +
    geom_histogram(binwidth = 10, boundary = 0) + xlim(0, 400)
ggplot(sim, aes(log(x))) + geom_histogram(bins = 30)
```

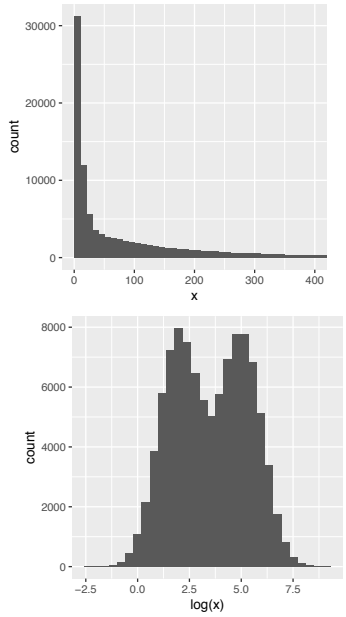

Figure 3.23: Histograms of the same data, with and without logarithmic transformation. The number of modes is different.

▶ Question **3.6.1.** Consider a log-normal mixture model as in the code above. What is the density function of X? What is the density function of $log(X)$? How many modes do these densities have, as a function of the parameters of the mixture model (mean and standard deviation of the component normals, and mixture fraction)?

3.7 Visualization of 2D data: scatterplots

Scatterplots are useful for visualizing treatment–response comparisons (as in Figure 3.4), associations between variables (as in Figure 3.11), or paired data (e. g., a disease biomarker in several patients before and after treatment). We use the two

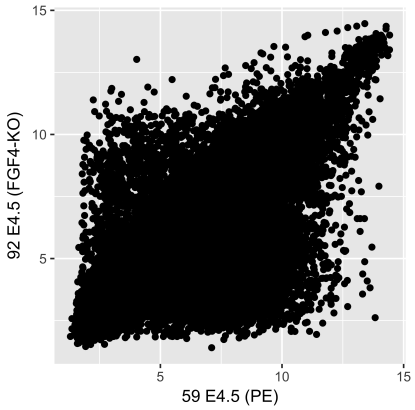

Figure 3.24: Scatterplot of 45101 expression measurements for two of the samples.

dimensions of our plotting paper, or screen, to represent the two variables. Let us take a look at differential expression between a wildtype and an FGF4-KO sample.

```
scp = ggplot(dfx, aes(x = `59 E4.5 (PE)` ,
                      y = `92 E4.5 (FGF4-KO)`))
scp + geom_point()
```

The labels `59 E4.5 (PE)` and `92 E4.5 (FGF4-KO)` refer to column names (sample names) in the dataframe `dfx`, which we created above. Since they contain special characters (spaces, parentheses, hyphen) and start with numerals, we need to enclose them with the downward sloping quotes to make them syntactically digestible for R. The plot is shown in Figure 3.24. We get a dense point cloud that we can try and interpret on the outskirts of the cloud, but we really have no idea visually how the data are distributed within the denser regions of the plot.

One easy way to ameliorate the overplotting is to adjust the transparency (alpha value) of the points by modifying the `alpha` parameter of `geom_point` (Figure 3.25).

```
scp  + geom_point(alpha = 0.1)
```

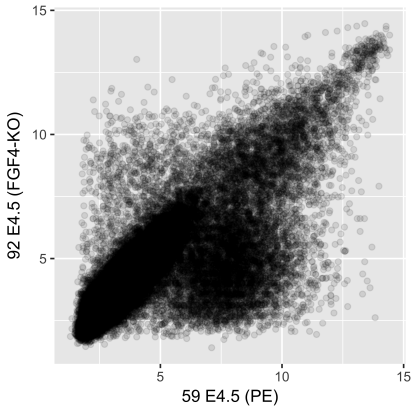

Figure 3.25: As Figure 3.24, but with semi-transparent points to resolve some of the over-plotting.

This is already better than Figure 3.24, but in the more dense regions even the semi-transparent points quickly overplot to a featureless black mass, while the more isolated, outlying points are getting faint. An alternative is a contour plot of the 2D density, which has the added benefit of not rendering all of the points on the plot, as in Figure 3.26.

```
scp + geom_density2d()
```

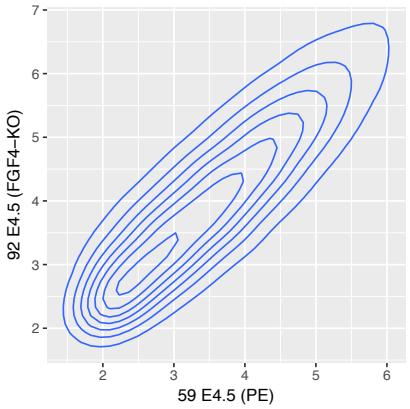

Figure 3.26: As Figure 3.24, but rendered as a contour plot of the 2D density estimate.

However, we see in Figure 3.26 that the point cloud at the bottom right (which contains a relatively small number of points) is no longer represented. We can somewhat overcome this by tweaking the bandwidth and binning parameters of `geom_density2d` (Figure 3.27, left panel).

```
scp + geom_density2d(h = 0.5, bins = 60)
```

We can fill in each space between the contour lines with the relative density of points by explicitly calling the function `stat_density2d` (for which `geom_density2d` is a wrapper) and using the geometric object **polygon**, as in the right panel of Figure 3.27.

```
library("RColorBrewer")
colorscale = scale_fill_gradientn(
    colors = rev(brewer.pal(9, "YlGnBu")),
    values = c(0, exp(seq(-5, 0, length.out = 100))))

scp + stat_density2d(h = 0.5, bins = 60,
          aes( fill = ..level..), geom = "polygon") +
  colorscale + coord_fixed()
```

We used the function `brewer.pal` from the package *RColorBrewer* to define the color scale, and we added a call to `coord_fixed` to fix the aspect ratio of the plot, to make sure that the mapping of data range to x- and y-coordinates is the same for the two variables. Both of these issues merit a deeper look, and we'll talk more about plot

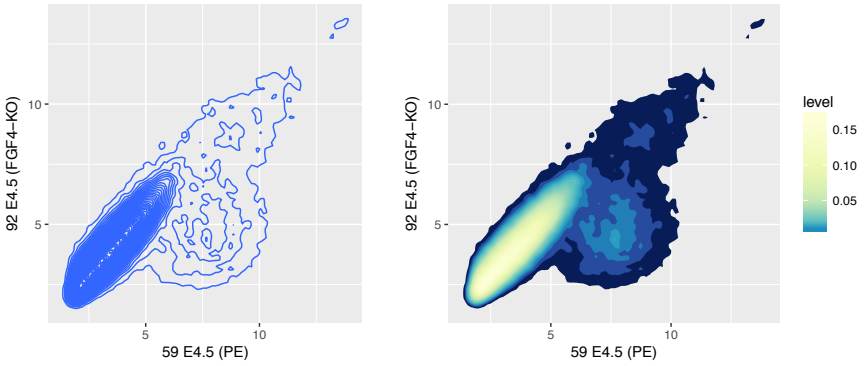

Figure 3.27: Left: as Figure 3.26, but with smaller smoothing bandwidth and tighter binning for the contour lines. Right: with color filling.

shapes in Section 3.7.1 and about colors in Section 3.9.

The density based plotting methods in Figure 3.27 are more visually appealing and interpretable than the overplotted point clouds of Figures 3.24 and 3.25, though we have to be careful in using them as we loose a lot of the information on the outlier points in the sparser regions of the plot. One possibility is using `geom_point` to add such points back in.

But arguably the best alternative, which avoids the limitations of smoothing, is hexagonal binning (Carr et al., 1987).

```
scp + geom_hex() + coord_fixed()
scp + geom_hex(binwidth = c(0.2, 0.2)) + colorscale +
  coord_fixed()
```

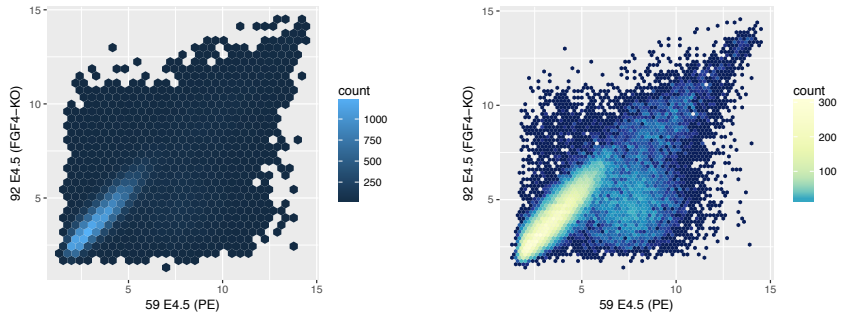

Figure 3.28: Hexagonal binning. Left: default parameters. Right: finer bin sizes and customized color scale.

3.7.1 Plot shapes

Choosing the proper shape for your plot is important to make sure the information is conveyed well. By default, the shape parameter, that is, the ratio, between the height of the graph and its width, is chosen by *ggplot2* based on the available space in the current plotting device. The width and height of the device are specified when it is opened in R, either explicitly by you or through default parameters[14]. Moreover, the

[14] E. g., see the manual pages of the `pdf` and `png` functions.

graph dimensions also depend on the presence or absence of additional decorations, like the color scale bars in Figure 3.28.

There are two simple rules that you can apply for scatterplots:

- If the variables on the two axes are measured in the same units, then make sure that the same mapping of data space to physical space is used – i. e., use `coord_fixed`. In the scatterplots above, both axes are the logarithm to base 2 of expression level measurements, that is a change by one unit has the same meaning on both axes (a doubling of the expression level). Another case is principal component analysis (PCA), where the x-axis typically represents component 1, and the y-axis component 2. Since the axes arise from an orthonormal rotation of input data space, we want to make sure their scales match. Since the variance of the data is (by definition) smaller along the second component than along the first component (or at most, equal), well-done PCA plots usually have a width that's larger than the height.
- If the variables on the two axes are measured in different units, then we can still relate them to each other by comparing their dimensions. The default in many plotting routines in R, including *ggplot2*, is to look at the range of the data and map it to the available plotting region. However, in particular when the data more or less follow a line, looking at the typical slope of the line can be useful. This is called banking (Cleveland et al., 1988).

To illustrate banking, let's use the classic sunspot data from Cleveland's paper.

```
library("ggthemes")
sunsp = tibble(year   = time(sunspot.year),
               number = as.numeric(sunspot.year))
sp = ggplot(sunsp, aes(x = year, y = number)) + geom_line()
sp
```

The resulting plot is shown in the upper panel of Figure 3.29. We can clearly see long-term fluctuations in the amplitude of sunspot activity cycles, with particularly low maximum activities in the early 1700s, early 1800s, and around the turn of the 20th century. But now lets try out banking.

```
ratio = with(sunsp, bank_slopes(year, number))
sp + coord_fixed(ratio = ratio)
```

What the algorithm does is to look at the slopes in the curve, and in particular, the above call to `bank_slopes` computes the median absolute slope, and then with the call to `coord_fixed` we shape the plot such that this quantity becomes 1. The result is shown in the lower panel of Figure 3.29. Quite counter-intuitively, even though the plot takes much smaller space, we see more on it! Namely, we can see the saw-tooth shape of the sunspot cycles, with sharp rises and more slow declines.

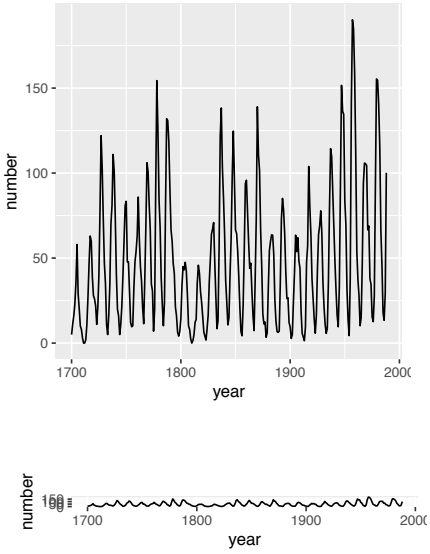

Figure 3.29: The sunspot data. In the upper panel, the plot shape is roughly quadratic, a frequent default choice. In the lower panel, a technique called **banking** was used to choose the plot shape.

3.8 3–5D data

Sometimes we want to show the relations between more than two variables. Obvious choices for including additional dimensions are the plot symbol shapes and colors. The `geom_point` geometric object offers the following aesthetics (beyond `x` and `y`):

- `fill`
- `color`
- `shape`
- `size`
- `alpha`

They are explored in the manual page of the `geom_point` function. `fill` and `color` refer to the fill and outline color of an object, `alpha` to its transparency level. Above, in Figures 3.25 and following, we have used color or transparency to reflect point density and avoid the obscuring effects of overplotting. Instead, we can use them show other dimensions of the data (but of course we can only do one or the other). In principle, we could use all the 5 aesthetics listed above simultaneously to show up to 7-dimensional data; however, such a plot would be hard to decipher, and usually we are better off with sticking to at most one or two additional dimensions and mapping them to a choice of the available aesthetics.

3.8.1 Faceting

Another way to show additional dimensions of the data is to show multiple plots that result from repeatedly subsetting (or "slicing") our data based on one (or more) of the variables, so that we can visualize each part separately. So we can, for instance, investigate whether the observed patterns among the other variables are the same or different across the range of the faceting variable. Let's look at an example[15]

```
library("magrittr")
dftx$lineage %<>% sub("^$", "no", .)
dftx$lineage %<>% factor(levels = c("no", "EPI", "PE", "FGF4-KO"))

ggplot(dftx, aes( x = X1426642_at, y = X1418765_at)) +
  geom_point() + facet_grid( . ~ lineage )
```

[15] The first two lines this code chunk are not strictly necessary – they're just reformatting the `lineage` column of the `dftx` dataframe, to make the plots look better.

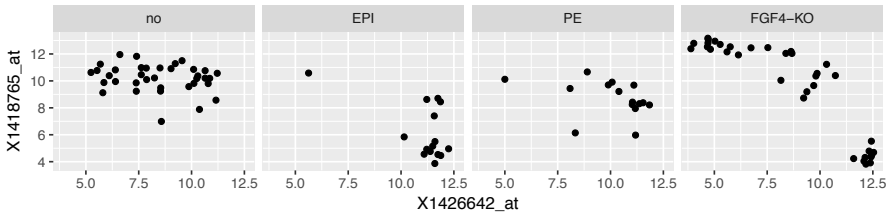

Figure 3.30: An example for **faceting**: the same data as in Figure 3.10, but now split by the categorical variable `lineage`.

The result is shown in Figure 3.30. We used the formula language to specify by which variable we want to do the splitting, and that the separate panels should be in

different columns: `facet_grid( . ~ lineage )`. In fact, we can specify two faceting variables, as follows; the result is shown in Figure 3.31.

```
ggplot( dftx,
  aes( x = X1426642_at, y = X1418765_at)) + geom_point() +
   facet_grid( Embryonic.day ~ lineage )
```

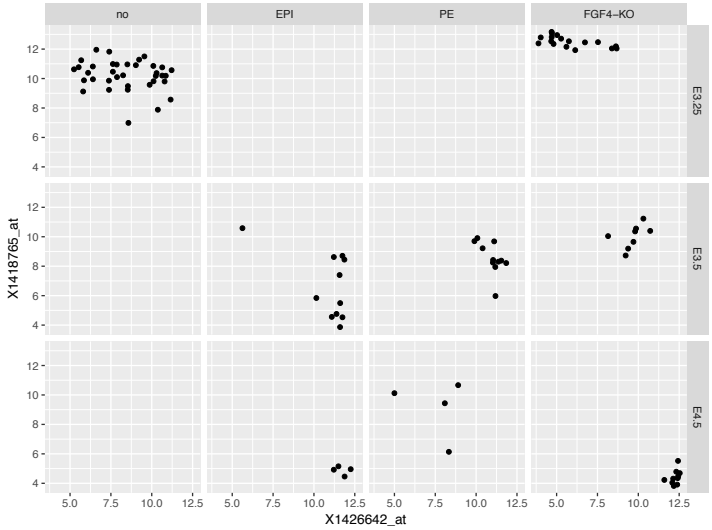

Figure 3.31: **Faceting**: the same data as in Figure 3.10, split by the categorical variables `Embryonic.day` (rows) and `lineage` (columns).

Another useful function is `facet_wrap`: if the faceting variable has too many levels for all the plots to fit in one row or one column, then this function can be used to wrap them into a specified number of columns or rows.

We can use a continuous variable by discretizing it into levels. The function `cut` is useful for this purpose.

```
ggplot(mutate(dftx, Tdgf1 = cut(X1450989_at, breaks = 4)),
   aes( x = X1426642_at, y = X1418765_at)) + geom_point() +
   facet_wrap( ~ Tdgf1, ncol = 2 )
```

We see in Figure 3.32 that the number of points in the four panel is different, this is because `cut` splits into bins of equal length, not equal number of points. If we want the latter, then we can use `quantile` in conjunction with `cut`.

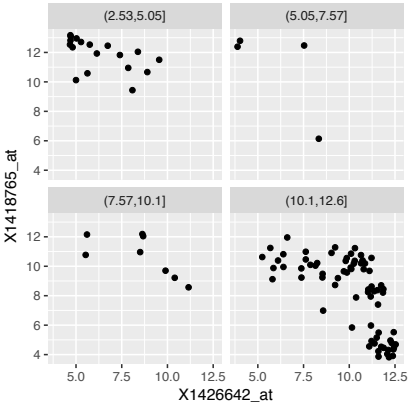

Figure 3.32: **Faceting**: the same data as in Figure 3.10, split by the continuous variable `X1450989_at` and arranged by `facet_wrap`.

Axes scales In Figures 3.30–3.32, the axes scales are the same for all plots. Alternatively, we could let them vary by setting the `scales` argument of the `facet_grid` and `facet_wrap`; this parameters allows you to control whether to leave the x-axis, the y-axis, or both to be freely variable. Such alternatives scalings might allows us to see the full detail of each plot and thus make more minute observations about what is going on in each. The downside is that the plot dimensions are not comparable across the groupings.

Implicit faceting You can also facet your plots (without explicit calls to `facet_grid` and `facet_wrap`) by specifying the aesthetics. A very simple version of implicit faceting is using a factor as your x-axis, such as in Figures 3.16–3.20

3.8.2 Interactive graphics

The plots generated thus far have been static images. You can add an enormous amount of information and expressivity by making your plots interactive. It is impossible here for us to convey interactive visualizations, but we provide pointers to some important resources.

shiny

Rstudio's *shiny* is a web application framework for R. It makes it easy to create interactive displays with sliders, selectors and other control elements that allow changing all aspects of the plot(s) shown – since the interactive elements call back directly into the R code that produces the plot(s). See the shiny gallery for some great examples.

ggvis

ggvis is a graphics system for R that builds upon *shiny* and has an underlying theory, look-and-feel and programming interface similar to *ggplot2*.

As a consequence of interactivity in *shiny* and *ggvis*, there needs to be an R interpreter running with the underlying data and code to respond to the user's actions while she views the graphic. This R interpreter could be on the local machine, or on a server; in both cases, the viewing application is a web browser, and the interaction with R goes through web protocols (http, or https). That is, of course, different from a regular static graphic in a PDF file or in an HTML report, which is produced once and can then be viewed without any

plotly

A great web-based tool for interactive graphic generation is **plotly**. You can view some examples of interactive graphics online at `https://plot.ly/r`. To create your own interactive plots in R, you can use code like

```
library("plotly")
plot_ly(economics, x = date, y = unemploy / pop)
```

Like with *shiny* and *ggvis*, the graphics are viewed in an HTML browser, however, no running R session is required. The graphics are self-contained HTML documents whose "logic" is coded in JavaScript, or more precisely, in the D3.js system.

rgl, webgl

For visualising 3D objects (say, a geometrical structure), there is the package *rgl*. It produces interactive viewer windows (either in specialized graphics device on your screen, or through a web browser) in which you can rotate the scene, zoom and in out, etc. An screenshot of the scene produced by the code below is shown in Figure 3.33.

```
data("volcano")
volcanoData = list(
  x = 10 * seq_len(nrow(volcano)),
  y = 10 * seq_len(ncol(volcano)),
  z = volcano,
  col = terrain.colors(500)[cut(volcano, breaks = 500)]
)
library("rgl")
with(volcanoData, persp3d(x, y, z, color = col))
```

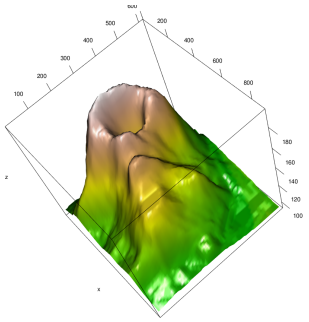

Figure 3.33: *rgl* rendering of the `volcano` data, the topographic information for Maunga Whau (Mt Eden), one of about 50 volcanos in the Auckland volcanic field.

In the code above, the base R function `cut` computes a mapping from the value range of the `volcano` data to the integers between 1 and 500[16], which we use to index the color scale, `terrain.colors(500)`.

For more information, consult the package's excellent vignette.

[16] More precisely, it returns a factor with as many levels, which we let R autoconvert to integers.

3.9 Color

An important consideration when making plots is the coloring that we use in them. Most R users are likely familiar with the built-in R color scheme, used by base R graphics, as shown in Figure 3.34.

```
pie(rep(1, 8), col=1:8)
```

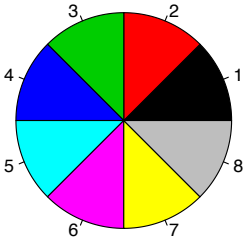

Figure 3.34: Basic R colors.

These color choices date back from 1980s hardware, where graphics cards handled colors by letting each pixel either fully use or not use each of the three basic color channels of the display: red, green and blue (RGB): this leads to $2^3 = 8$ combinations, which lie at the 8 the extreme corners of the RGB color cube[17]. The colors in Figure 3.34 are harsh on the eyes, and there is no good excuse any more for creating graphics that are based on this palette. Fortunately, the default colors used by some of the more modern visualization oriented packages (including *ggplot2*) are much better already, but sometimes we want to make our own choices.

[17] Thus the 8th color should be white; in R, this was replaced by grey, as you can see in Figure 3.34.

In Section 3.7 we saw the function `scale_fill_gradientn`, which allowed us to create the color gradient used in Figures 3.27 and 3.28 by interpolating the basic color palette defined by the function `brewer.pal` in the *RColorBrewer* package. This package defines a great set of color palettes. We can see all of them at a glance by using the function `display.brewer.all` (Figure 3.35).

```
display.brewer.all()
```

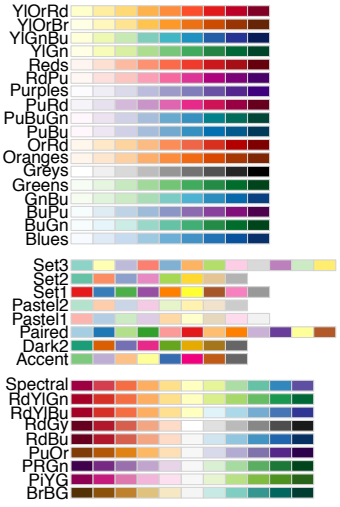

We can get information about the available color palettes from `brewer.pal.info`.

```
head(brewer.pal.info)
```

```
##      maxcolors category colorblind
## BrBG        11      div       TRUE
## PiYG        11      div       TRUE
## PRGn        11      div       TRUE
## PuOr        11      div       TRUE
## RdBu        11      div       TRUE
## RdGy        11      div      FALSE
```

```
table(brewer.pal.info$category)
```

```
##
##  div qual  seq
##    9    8   18
```

The palettes are divided into three categories:

- qualitative: for categorical properties that have no intrinsic ordering. The `Paired` palette supports up to 6 categories that each fall into two subcategories - like **before** and **after**, **with** and **without** treatment, etc.
- sequential: for quantitative properties that go from **low** to **high**
- diverging: for quantitative properties for which there is a natural midpoint or neutral value, and whose value can deviate both up- and down; we'll see an example in Figure 3.37.

To obtain the colors from a particular palette we use the function `brewer.pal`. Its first argument is the number of colors we want (which can be less than the available maximum number in `brewer.pal.info`).

```
brewer.pal(4, "RdYlGn")
```

```
## [1] "#D7191C" "#FDAE61" "#A6D96A" "#1A9641"
```

If we want more than the available number of preset colors (for example so we can plot a heatmap with continuous colors) we can interpolate using the `colorRampPalette` function[18].

```
mypalette  = colorRampPalette(c("darkorange3", "white", "darkblue"))(100)
head(mypalette)
```

```
## [1] "#CD6600" "#CE6905" "#CF6C0A" "#D06F0F" "#D17214" "#D27519"
```

```
par(mai = rep(0.1, 4))
image(matrix(1:100, nrow = 100, ncol = 10), col = mypalette,
        xaxt = "n", yaxt = "n", useRaster = TRUE)
```

[18] `colorRampPalette` returns a function of one parameter, an integer. In the code shown, we call that function with the argument `100`.

Figure 3.36: A quasi-continuous color palette derived by interpolating between the colors `darkorange3`, `white` and `darkblue`.

3.10 Heatmaps

Heatmaps are a powerful of visualising large, matrix-like datasets and giving a quick overview over the patterns that might be in there. There are a number of heatmap drawing functions in R; one that is convenient and produces good-looking output is the function `pheatmap` from the eponymous package[19]. In the code below, we first select the top 500 most variable genes in the dataset `x` and define a function `rowCenter` that centers each gene (row) by subtracting the mean across columns. By default, `pheatmap` uses the **RdYlBu** color palette from *RcolorBrewer* in conjuction with the `colorRampPalette` function to interpolate the 11 color into a smooth-looking palette (Figure 3.37).

[19] A very versatile and modular alternative is the *ComplexHeatmap* package.

```
library("pheatmap")
topGenes = order(rowVars(exprs(x)), decreasing = TRUE)[ seq_len(500) ]
rowCenter = function(x) { x - rowMeans(x) }
pheatmap( rowCenter(exprs(x)[ topGenes, ] ),
  show_rownames = FALSE, show_colnames = FALSE,
  breaks = seq(-5, +5, length = 101),
  annotation_col =
    pData(x)[, c("sampleGroup", "Embryonic.day", "ScanDate") ],
  annotation_colors = list(
    sampleGroup = groupColor,
    genotype = c(`FGF4-KO` = "chocolate1", `WT` = "azure2"),
    Embryonic.day = setNames(brewer.pal(9, "Blues")[c(3, 6, 9)],
                             c("E3.25", "E3.5", "E4.5")),
    ScanDate = setNames(brewer.pal(nlevels(x$ScanDate), "YlGn"),
                        levels(x$ScanDate))
  ),
  cutree_rows = 4
)
```

Let us take a minute to deconstruct this rather massive-looking call to `pheatmap`. The options `show_rownames` and `show_colnames` control whether the row and column names are printed at the sides of the matrix. Because our matrix is large in relation to the available plotting space, the labels would anyway not be readable, and we suppress them. The `annotation_col` argument takes a data frame that carries additional information about the samples. The information is shown in the colored bars on top of the heatmap. There is also a similar `annotation_row` argument, which we haven't used here, for colored bars at the side. `annotation_colors` is a list of named vectors by which we can override the default choice of colors for the annotation bars. Finally, with the `cutree_rows` argument we cut the row dendrogram into four (an arbitrarily chosen number) clusters, and the heatmap shows them by leaving a bit of white space in between. The `pheatmap` function has many further options, and if you want to use it for your own data visualizations, it's worth studying them.

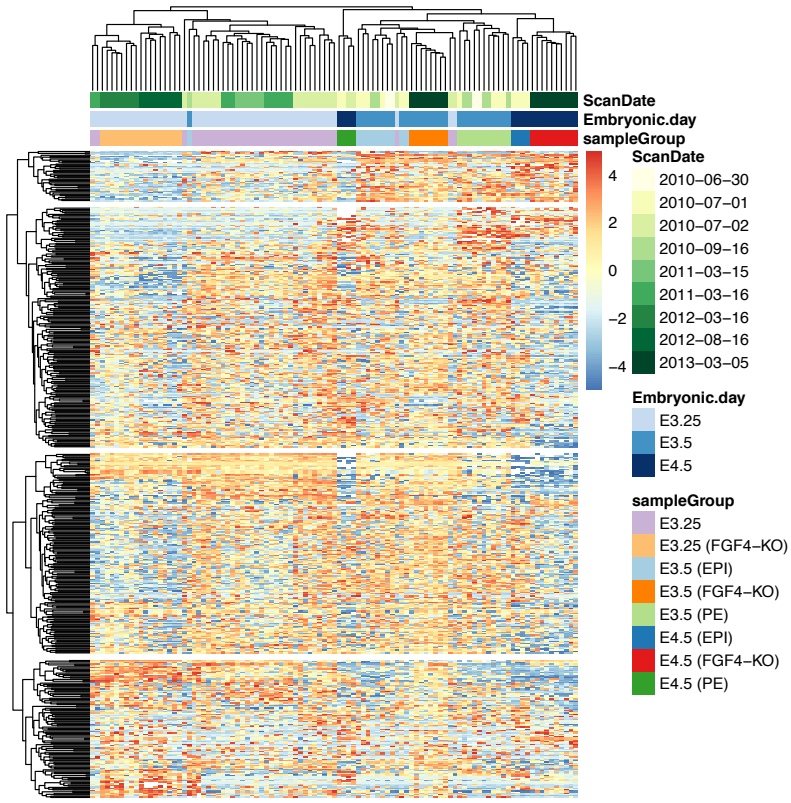

Figure 3.37: A heatmap of relative expression values, i. e., $\log_2$ fold change compared to the average expression of that gene (row) across all samples (columns). The color scale uses a diverging palette, whose neutral midpoint is at 0.

3.10.1 Dendrogram ordering

The ordering of the rows and columns in a heatmap has an enormous impact on the visual impact it makes, and it can be difficult to decide which patterns are real, and which are consequences of arbitrary layout decisions[20]. Let's keep in mind that:

- Ordering the rows and columns by cluster dendrogram (as in Figure 3.37) is an arbitrary choice, and you could just as well make other choices.
- Even if you settle on dendrogram ordering, there is an essentially arbitrary choice at each internal branch, as each branch could be flipped without changing the topology of the tree.

▶ Question **3.10.1.** What other ordering methods can you think of?

▶ Answer **3.10.1.** Among the methods proposed is the travelling salesman problem (McCormick Jr et al., 1972) or projection on the first principal component (for instance, see the examples in the manual page of `pheatmap`).

▶ Question **3.10.2.** Check the manual page of the `hclust` function (which, by default, is used by `pheatmap`) for how it deals with the decision of how to pick which branches of the subtree go left and right.

▶ Question **3.10.3.** Check the argument `clustering_callback` of the `pheatmap` function.

[20] In Chapter 5, we will learn about formal methods for evaluating cluster significance.

3.10.2 Color spaces

Color perception in humans (von Helmholtz, 1867) is three-dimensional[21]. There are different ways of parameterizing this space. Above we already encountered the RGB color model, which uses three values in [0,1], for instance at the beginning of Section 3.4, where we printed out the contents of `groupColor`:

```
groupColor[1]

##      E3.25
## "#CAB2D6"
```

Here, CA is the hexadecimal representation for the strength of the red color channel, B2 of the green and D6 of the green color channel. In decimal, these numbers are 202, 178 and 214, respectively. The range of these values goes from to 0 to 255, so by dividing by this maximum value, an RGB triplet can also be thought of as a point in the three-dimensional unit cube.

The function `hcl` uses a different coordinate system, which consists of the three coordinates hue H, an angle in $[0, 360]$, chroma C, and lightness L as a value in $[0, 100]$. The possible values for C depend on some constraints, but are generally between 0 and 255.

The `hcl` function corresponds to polar coordinates in the CIE-LUV[22] and is designed for area fills. By keeping chroma and luminescence coordinates constant and only varying hue, it is easy to produce color palettes that are harmonious and avoid irradiation illusions that make light colored areas look bigger than dark ones. Our attention also tends to get drawn to loud colors, and fixing the value of chroma makes the colors equally attractive to our eyes.

There are many ways of choosing colors from a color wheel. **Triads** are three colors chosen equally spaced around the color wheel; for example, $H = 0, 120, 240$ gives red, green, and blue. **Tetrads** are four equally spaced colors around the color wheel, and some graphic artists describe the effect as "dynamic". **Warm colors** are a set of equally spaced colors close to yellow, **cool colors** a set of equally spaced colors close to blue. **Analogous color** sets contain colors from a small segment of the color wheel, for example, yellow, orange and red, or green, cyan and blue. **Complementary colors** are colors diametrically opposite each other on the color wheel. A tetrad is two pairs of complementaries. **Split complementaries** are three colors consisting of a pair of complementaries, with one partner split equally to each side, for example, $H = 60,\ 240 - 30,\ 240 + 30$. This is useful to emphasize the difference between a pair of similar categories and a third different one. A more thorough discussion is provided in the references (Mollon, 1995; Ihaka, 2003).

[21] Physically, there is an infinite number of wavelengths of light and an infinite number of ways of mixing them, so other species, or robots, can perceive less or more than three colors.

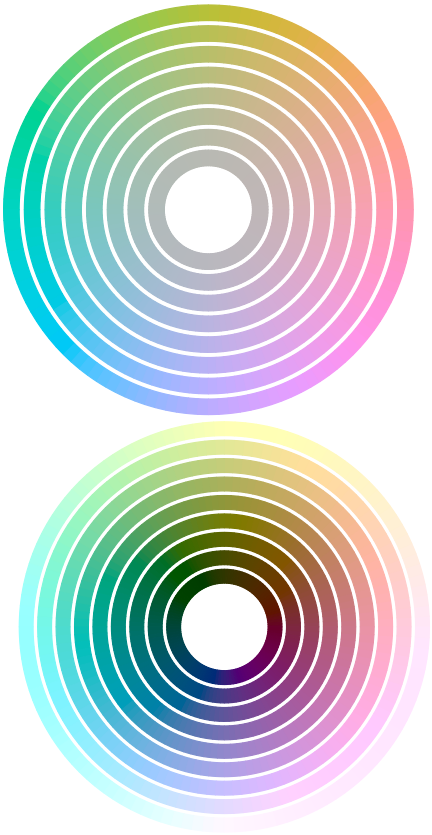

Figure 3.38: Circles in HCL colorspace. Upper panel: The luminosity L is fixed to 75, while the angular coordinate H (hue) varies from 0 to 360 and the radial coordinate $C = 0, 10, \ldots, 60$. Lower panel: constant chroma $C = 50$, H as above, and varying luminosity $L = 10, 20, \ldots, 90$.

[22] CIE: Commission Internationale de l'Éclairage – see e. g. Wikipedia for more on this.

Lines vs areas

For lines and points, we want that they show a strong contrast to the background, so on a white background, we want them to be relatively dark (low lightness L). For area fills, lighter, more pastell-type colors with low to moderate chromatic content are usually more pleasant.

3.11 Data transformations

Plots in which most points are huddled up in one area, with a lot of sparsely populated space, are difficult to read. If the histogram of the marginal distribution of a variable has a sharp peak and then long tails to one or both sides, transforming the data can be helpful. These considerations apply both to `x` and `y` aesthetics, and to color scales. In the plots of this chapter that involved the microarray data, we used the logarithmic transformation[23] – not only in scatterplots like Figure 3.24 for the x and y-coordinates, but also in Figure 3.37 for the color scale that represents the expression fold changes. The logarithm transformation is attractive because it has a definitive meaning - a move up or down by the same amount on a log-transformed scale corresponds to the same multiplicative change on the original scale: $\log(ax) = \log a + \log x$.

Sometimes the logarithm however is not good enough, for instance when the data include zero or negative values, or when even on the logarithmic scale the data distribution is highly uneven. From the upper panel of Figure 3.39, it is easy to take away the impression that the distribution of `M` depends on `A`, with higher variances for lower `A`. However, this is entirely a visual artefact, as the lower panel confirms: the distribution of `M` is independent of `A`, and the apparent trend we saw in the upper panel was caused by the higher point density at smaller `A`.

```
gg = ggplot(tibble(
  A = exprs(x)[, 1],
  M = rnorm(length(A))),
  aes(y = M))
gg + geom_point(aes(x = A))
gg + geom_point(aes(x = rank(A)))
```

▶ Question **3.11.1.** Can the visual artefact be avoided by using a density- or binning-based plotting method, as in Figure 3.28?

▶ Question **3.11.2.** Can the rank transformation also be applied when choosing color scales e. g. for heatmaps? What does **histogram equalization** in image processing do?

[23] We used it implicitly since the data in the *ExpressionSet* object `x` already come log-transformed.

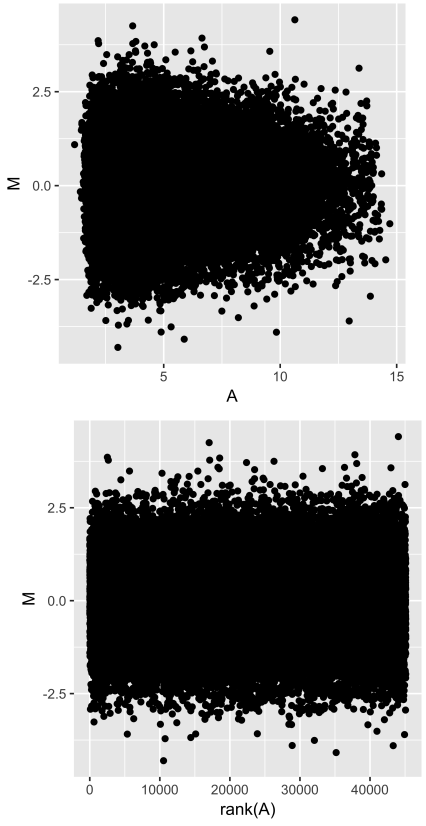

Figure 3.39: The effect of rank transformation on the visual perception of dependency.

3.12 Mathematical symbols and other fonts

We can use mathematical notation in plot labels, using a notation that is a mix of R syntax and LaTeX-like notation (see `help("plotmath")` for details):

```
volume = function(rho, nu)
           pi^(nu/2) * rho^nu / gamma(nu/2+1)

ggplot(tibble(nu    = 1:15,
  Omega = volume(1, nu)), aes(x = nu, y = Omega)) +
geom_line() +
xlab(expression(nu)) + ylab(expression(Omega)) +
geom_text(label =
"Omega(rho, nu)==frac(pi^frac(nu, 2) ~ rho^nu, Gamma(frac(nu, 2) + 1))",
  parse = TRUE, x = 6, y = 1.5)
```

The result is shown in Figure 3.40. It's also easy to switch to other fonts, for instance the serif font Times (Figure 3.41).

```
ggplot(genes, aes( x = value, color = gene)) + stat_ecdf() +
  theme(text = element_text(family = "Times"))
```

In fact, the set of fonts that can be used with a standard R installation are limited, but luckily there is the package *extrafont*, which facilitates using fonts other than R's set of basic PostScript fonts. There's some extra work needed before we can use it, since fonts external to R first need to be made known to it. They could come shipped with your operating system, a with word processor or another graphics application. The set of fonts available and their physical location is therefore not standardized, but will depend on your operating system and further configurations. In the first session after attaching the *extrafont* package, you will need to run the function `font_import` to import fonts and make them known to the package. Then in each session in which you want to use them, you need to call the `loadfonts` function to register them with one or more of R's graphics devices. Finally you can use the `fonttable` function to list the available fonts. You'll need to refer to the documentation of the *extrafonts* package to see how to make this work on your machine.

▶ Question **3.12.1.** Use *extrafont* to produce a version of Figure 3.41 with the font "Bauhaus 93" (or another one available on your system).

▶ Question **3.12.2.** Have a look at the code producing Figure 3.1.

3.13 Genomic data

To visualize genomic data, in addition to the general principles we have discussed in this chapter, there are some specific considerations. The data are usually associated with genomic coordinates. In fact genomic coordinates offer a great organising principle for the integration of genomic data. You will probably have seen genome browser displays such as in Figure 3.43. Here we'll briefly show how to produce such plots programmatically, using your data as well as public annotation. We can only give a short glimpse, and we refer to resources such as Bioconductor for a fuller picture.

The main challenge of genomic data visualization is the size of genomes. We need visualizations at multiple scales, from whole genome down to the nucleotide level.

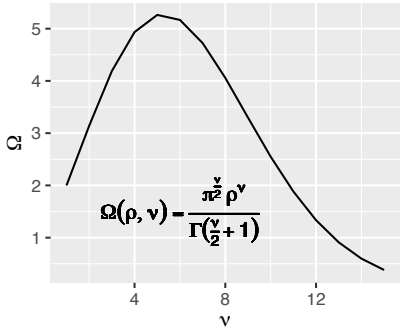

Figure 3.40: Volume Ω of the ν-dimensional sphere with radius $\rho = 1$, for $\nu = 1, \ldots, 15$.

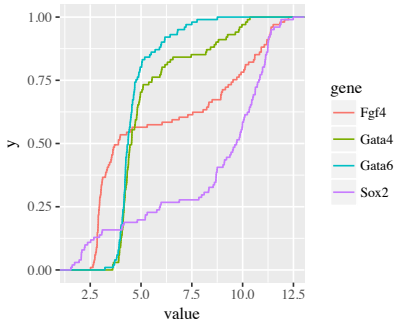

Figure 3.41: As Figure 3.22, with a different font.

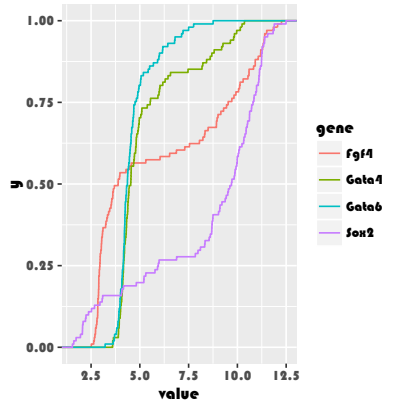

Figure 3.42: As Figure 3.22, with font "Bauhaus 93".

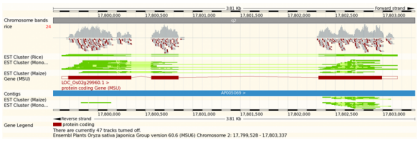

Figure 3.43: Screenshot from Ensembl genome browser, showing gene annotation of a genomic region as well as a read pile-up visualization of an RNA-Seq experiment.

It should be easy to zoom in and and out, and we may need differemt visualization strategies for the different size scales. It can be convenient to visualize biological molecules (genomes, genes, transcripts, proteins) in a linear manner, although their embedding in the 3D physical world can matter (a lot).

Let's start with some fun examples, an ideogram plot of human chromosome 1 (Figure 3.44) and a plot of the genome-wide distribution of RNA editing sites (Figure 3.45).

```
library("ggbio")
data("hg19IdeogramCyto", package = "biovizBase")
plotIdeogram(hg19IdeogramCyto, subchr = "chr1")
```

```
## Warning: 'panel.margin' is deprecated. Please use 'panel.spacing'
property instead
```

```
## Warning: 'panel.margin' is deprecated. Please use 'panel.spacing'
property instead
```

```
## Warning: 'panel.margin' is deprecated. Please use 'panel.spacing'
property instead
```

Figure 3.44: Chromosome 1 of the human genome: ideogram plot.

The `darned_hg19_subset500` lists a selection of 500 RNA editing sites in the human genome. It was obtained from the Database of RNA editing in flies, mice and humans (DARNED, `http://darned.ucc.ie`). The result is shown in Figure 3.45.

```
library("GenomicRanges")
data("darned_hg19_subset500", package = "biovizBase")
autoplot(darned_hg19_subset500, layout = "karyogram",
         aes(color = exReg, fill = exReg))
```

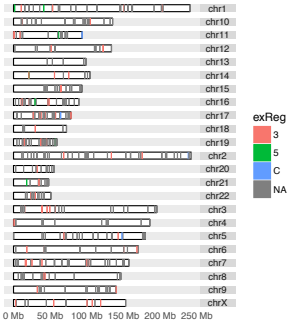

Figure 3.45: Karyogram with RNA editing sites. `exReg` indicates whether a site is in the coding region (C), 3'- or 5'-UTR.

▶ Question **3.13.1.** Fix the ordering of the chromosome in Figure 3.45 and get rid of the warning about chromosome lengths.

▶ Answer **3.13.1.** The information on chromosome lengths in the hg19 assembly of the human genome is (for instance) stored in the `ideoCyto` dataset. In the following, we also use the function `keepSeqlevels` to subset and reorder the chromosomes. See Figure 3.46

```
data("ideoCyto", package = "biovizBase")
dn = darned_hg19_subset500
seqlengths(dn) = seqlengths(ideoCyto$hg19)[names(seqlengths(dn))]
dn = keepSeqlevels(dn, paste0("chr", c(1:22, "X")))
autoplot(dn, layout = "karyogram",
         aes(color = exReg, fill = exReg))
```

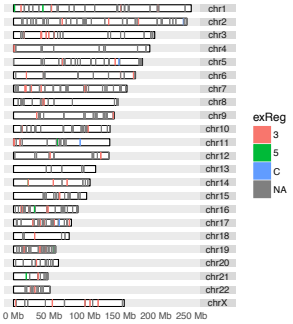

Figure 3.46: Improved version of Figure 3.45.

What type of object is `darned_hg19_subset500`?

```
darned_hg19_subset500[1:2,]
```

```
## GRanges object with 2 ranges and 10 metadata columns:
##       seqnames              ranges strand |       inchr       inrna
##          <Rle>           <IRanges>  <Rle> | <character> <character>
##   [1]     chr5 [86618225, 86618225]      - |           A           I
##   [2]     chr7 [99792382, 99792382]      - |           A           I
##               snp        gene      seqReg       exReg      source
```

```
##       <character> <character> <character> <character> <character>
##   [1]        <NA>        <NA>           0        <NA>    amygdala
##   [2]        <NA>        <NA>           0        <NA>        <NA>
##           ests      esta      author
##       <integer> <integer> <character>
##   [1]         0         0    15342557
##   [2]         0         0    15342557
##   -------
##   seqinfo: 23 sequences from an unspecified genome; no seqlengths
```

It is a *GRanges* object, that is, a specialized class from the Bioconductor project for storing data that are associated with genomic coordinates. Its first three columns are obligatory: `seqnames`, the name of the containing biopolymer (in our case, these are names of human chromosomes), `ranges`, the genomic coordinates of the intervals (in this case, the intervals all have length 1, as they each refer to a single nucleotide), and the DNA strand from which the RNA is transcribed. You can find out more on how to use this class and its associated infrastructure in the documentation, e. g., the vignette of the *GenomicRanges* package. Learning it is worth the effort if you want to work with genome-associated datasets, as it allows for convenient, efficient and safe manipulation of these data and provides many powerful utilities.

To Do

- Along chromosome plots, annotation + data, with sequence as the integrating principle (Gviz).
- HilbertViz

3.14 Recap of this chapter

- You should now be comfortable making beautiful, versatile and easily extendable plots using *ggplot2*'s `ggplot`.
- You should have a basic understanding of the grammar of graphics: the main word classes and the basic vocabulary.
- You understand the importance of choosing the right colors, proportions, and the right geom objects.
- Don't be afraid of setting up your data for faceting – this is a great quick way to look at many different ways to slice the data in different ways.
- Now you are prepared to explore *ggplot2* and plot your data on your own.

3.15 Further reading

The most useful books about *ggplot2* is the second edition of Wickham (2016) and the ggplot2 website. There are a lot of *ggplot2* code snippets online, which you will find through search engines after some exercise (stay critical, not everything online is

true, or up-to-date). Of course, the foundation of the system is based on Wilkinson (2005) and the ideas by Tukey (1977); Cleveland (1988).

3.16 Exercises

▶ Exercise **3.1** (Themes). Explore how to change the visual appearance of plots with themes. For example:

```
ggcars = ggplot(mtcars, aes(x=hp, y=mpg)) + geom_point()
ggcars
ggcars + theme_bw()
ggcars + theme_minimal()
```

▶ Exercise **3.2** (Color names in R). Have a look at `http://research.stowers-institute.org/efg/R/Color/Chart`

▶ Exercise **3.3** (xkcd). On a lighter note, you can even modify *ggplot2* to make plots in the style of the popular webcomic XKCD. You do this through manipulating the font and themes of ggplot2 objects. See `http://stackoverflow.com/questions/12675147/how-can-we-make-xkcd-style-graphs-in-r`.

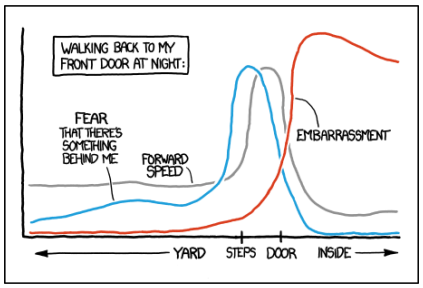

Chapter 13
Supervised Learning

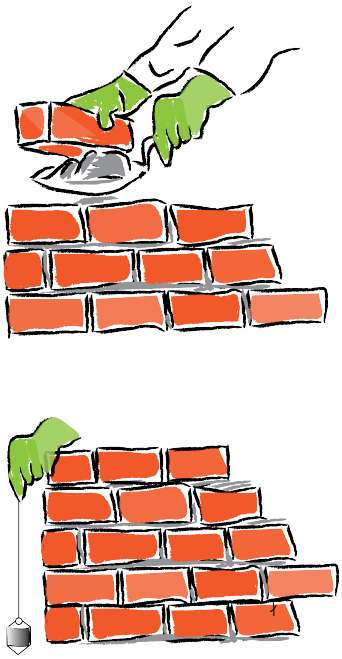

A frequent question in biological and biomedical applications is whether a property of interest (say, disease type, cell type, the prognosis of a patient) can be "predicted", given one or more other properties, called the **predictors**. Often we are motivated by a situation in which the property to be predicted is unknown (it lies in the future, or is hard to measure), while the predictors are known. The crucial point is that we **learn** the prediction rule from a set of training data in which the property of interest is also known. Once we have the rule, we can either apply it to new data, and make actual predictions of unknown outcomes; or we can dissect the rule with the aim of better understanding the underlying biology.

Figure 13.1: In a supervised learning setting, we have a yardstick or plumbline to judge how well we are doing: the response itself.

Compared to unsupervised learning and what we have seen in Chapters 5, 7 and 9, where we do not know what we are looking for or how to decide whether our result is "right", we are on much more solid ground with supervised learning: the objective is clearly stated, and there are straightforward criteria to measure how well we are doing.

The central issue in **supervised learning**[1] is **overfitting** and **generalisability**: did we just learn the training data "by heart" by constructing a rule that has 100% accuracy on the training data, but would perform poorly on any new data? Or did our rule indeed pick up some of the pertinent patterns in the system being studied, which will also apply to yet unseen new data?

[1] Sometimes the term **statistical learning** is used, more or less exchangeably.

13.1 Goals for this chapter

In this chapter we will

- see exemplary applications that motivate the use of supervised learning methods
- learn what discriminant analysis does,
- define measures of performance,
- encounter the curse of dimensionality and see what overfitting is,
- find out about regularisation and understand the concepts of generisability and model complexity,

- see how to use cross-validation to tune parameters of the algorithms,
- get to see a unified framework for machine learning algorithms in R that allows you to use hundreds of methods in a consistent manner,
- discuss method hacking.

13.2 What are the data?

The basic data structure for both supervised and unsupervised learning is (at least conceptually) a dataframe, where each row corresponds to an object and the columns are different features[2] of the objects. While in unsupervised learning we aim to find (dis)similarity relationships between the objects based on their feature values (e. g., by clustering or ordination), in supervised learning we aim to find a mathematical function (or a computational algorithm) that predicts the value of one of the features from the other features. Many implementations require that there are no missing values, whereas other methods can be generalized to work with some amount of missing data.

[2] Features are usually numerical scalars or categorical variables, although some methods can be generalized to work with other data types.

The feature that we select over all the others with the aim of predicting is called the **objective** or the **response**. Sometimes the choice is natural, but sometimes it is also instructive to reverse the roles, especially if we are interested in dissecting the prediction function for the purpose of biological understanding, or in disentangling correlations from causation.

The framework for supervised learning covers both continuous and categorical response variables. In the continuous case we also call it **regression**, in the categorical case, **classification**. It turns out that this distinction is not a detail, as it has quite far-reaching consequences for the choice of loss function (Section 13.5) and thus the choice of algorithm (Friedman, 1997).

The first question to consider in any supervised learning task is how the number of objects compares to the number of predictors. The more data, the better, and much of the hard work in supervised learning has to do with overcoming the limitations of having a finite (and typically, too small) training set.

▶ Question **13.2.1.** Give examples where we have encountered instances of supervised learning with a categorical response in this book.

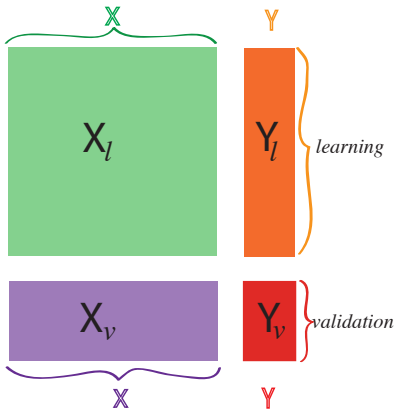

Figure 13.2: In supervised learning, we assign two different roles to our variables. We have labeled the explanatory variables X and the response variable(s) Y. There are also two different sets of observations: the training set X_ℓ and Y_ℓ and the validation set X_v and Y_v.

13.2.1 Motivating examples

Predicting diabetes type

The `diabetes` dataset (Reaven and Miller, 1979) presents three different groups of diabetes patients and five clinical variables measured on them.

```
library("ggplot2")
library("readr")
```

```
library("magrittr")
diabetes = read_csv("../data/diabetes.csv", col_names = TRUE)
diabetes
```

```
## # A tibble: 144 x 7
##       id relwt glufast glutest steady insulin group
##    <int> <dbl>   <int>   <int>  <int>   <int> <int>
## 1      1  0.81      80     356    124      55     3
## 2      3  0.94     105     319    143     105     3
## 3      5  1.00      90     323    240     143     3
## 4      7  0.91     100     350    221     119     3
## 5      9  0.99      97     379    142      98     3
## 6     11  0.90      91     353    221      53     3
## 7     13  0.96      78     290    136     142     3
## 8     15  0.74      86     312    208      68     3
## 9     17  1.10      90     364    152      76     3
## 10    19  0.83      85     296    116      60     3
## # ... with 134 more rows
```

```
diabetes$group %<>% factor
```

We used the forward-backward pipe operator `%<>%` to convert the `group` column into a factor.

```
library("reshape2")
ggplot(melt(diabetes, id.vars = c("id", "group")),
       aes(x = value, col = group)) +
  geom_density() + facet_wrap( ~variable, ncol = 2, scales = "free")
```

The plot is shown in Figure 13.3.

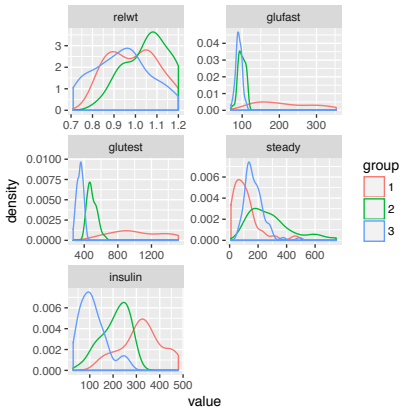

Figure 13.3: We see already from the one-dimensional distributions that some of the individual variables could potentially predict which group a patient is more likely to belong to. Our goal will be to combine variables to improve these one dimensional predictions.

Predicting cellular phenotypes

Neumann et al. (2010) observed human cancer cells using live-cell imaging. The cells were genetically engineered so that their histones were tagged with a green fluorescent protein (GFP). A genome-wide RNAi library was applied to the cells, and for each siRNA perturbation, movies of a few hundred cells were recorded for about two days, to see what effect the depletion of each gene had on cell cycle, nuclear morphology and cell proliferation. Their paper reports the use of an automated image classification algorithm that quantified the visual appearance of each cell's nucleus and enabled the prediction of normal mitosis states or aberrant nuclei. The algorithm was trained on the data from around 3000 cells that were annotated by a human expert. It was then applied to almost 2 billions images of nuclei (Figure 13.4). Using automated image classification provided scalablity (annotating 2 billion images manually would take a long time) and objectivity.

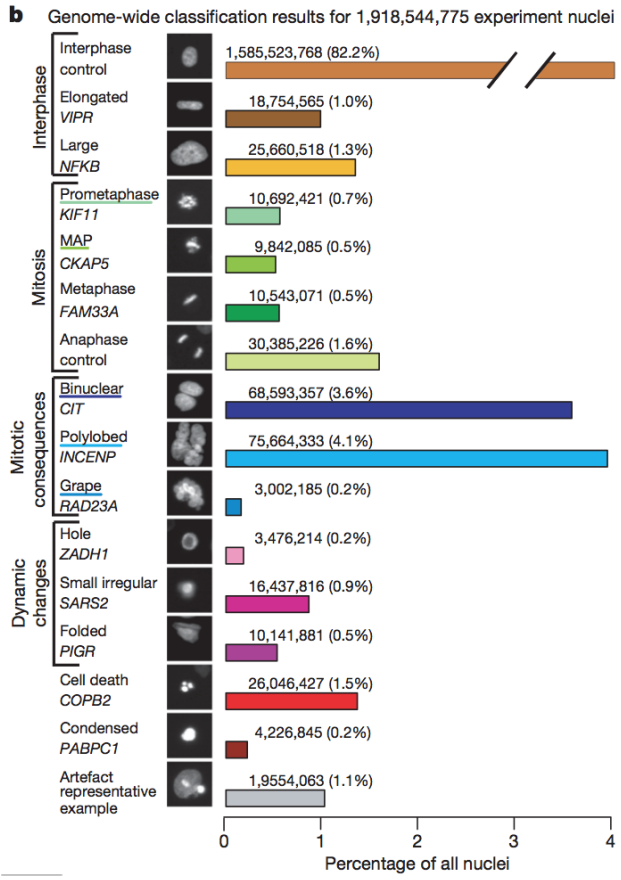

Figure 13.4: The data were images of $2x10^9$ nuclei from movies. The images were segmented to identify the nuclei, and numeric features were computed for each nucleus, corresponding to size, shape, brightness and lots of other more or less abstract quantitative summaries of the joint distribution of pixel intensities. From the features, the cells were classified into 16 different nuclei morphology classes, represented by the rows of the barplot. Representative images for each class are shown in black and white in the center column. The class frequencies, which are very unbalanced, are shown by the lengths of the bars.

Predicting embryonic cell states

We will revisit the mouse embryo data (Ohnishi et al., 2014), which we have already seen in Chapters 3, 5 and 7, and show how we can predict the developmental state (Embryonic Days) from the gene expression measurements.

13.3 Linear discrimination

We start with one of the simplest possible discrimination problems[3], where we have objects described by two continuous features (so the objects can be thought of as points in the 2D plane) and falling into three groups. Our aim is to define class boundaries, which are lines in the 2D space.

[3] Arguably the simplest possible problem is a single continuous feature, two classes, and the task of finding a single threshold to discriminate between the two groups.

13.3.1 Diabetes data

Let's see whether we can predict the feature `group` from the features `insulin` and `glutest` variables in the `diabetes` data. It's always a good idea to first visualise the data (Figure 13.5).

```
ggdb = ggplot(mapping = aes(x = insulin, y = glutest)) +
  geom_point(aes(colour = group), data = diabetes)
ggdb
```

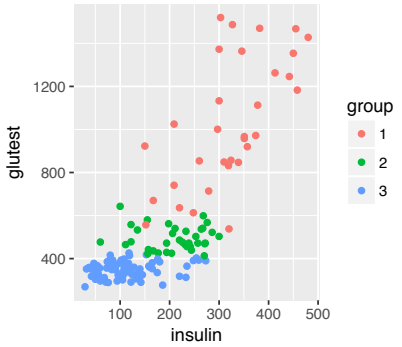

Figure 13.5: Scatterplot of two of the variables in the `diabetes` data. Each point is a sample, and the color indicates the diabetes type as encoded in the `group` variable.

We'll start with a method called **linear discriminant analysis** (**LDA**). This method is a foundation stone of classification, many of the more complicated (and sometimes more powerful) algorithms are really just generalisations of LDA.

```
library("MASS")
diabetes_lda = lda(group ~ insulin + glutest, data = diabetes)
diabetes_lda
```

```
## Call:
## lda(group ~ insulin + glutest, data = diabetes)
##
## Prior probabilities of groups:
##         1         2         3
## 0.2222222 0.2500000 0.5277778
##
## Group means:
##    insulin   glutest
## 1 320.9375 1027.3750
## 2 208.9722  493.9444
## 3 114.0000  349.9737
##
## Coefficients of linear discriminants:
##                  LD1         LD2
## insulin -0.004463900 -0.01591192
## glutest -0.005784238  0.00480830
##
## Proportion of trace:
##    LD1    LD2
## 0.9677 0.0323
```

```
ghat = predict(diabetes_lda)$class
table(ghat, diabetes$group)
```

```
##
## ghat  1  2  3
##    1 25  0  0
##    2  6 24  6
##    3  1 12 70
```

```
mean(ghat != diabetes$group)
```

```
## [1] 0.1736111
```

▶ Question **13.3.1.** What do the different parts of the above output mean?

Now, let's visualise the LDA result[4]. We are going to plot the prediction regions for each of the three groups. We do this by creating a grid of points and using our prediction rule on each of them. We'll then also dig a bit deeper into the mechanics of LDA and plot the class centers (`diabetes_lda$means`) and ellipses that correspond to the fitted covariance matrix (`diabetes_lda$scaling`). Assembling this

[4] Note how we first visualised the data, in Figure 13.5, and are now going to visualise the fitted model (Figure 13.6). The prediction regions can, in principle, be shown for any classification method, including a "black box" method. On the other hand, the cluster centers and ellipses in Figure 13.6 are a method-specific visualisation.

visualization requires us to write a bit of code.

```
make1Dgrid = function(x) {
  rg  = range(x)
  wid = diff(rg)
  rg  = rg + wid * 0.05 * c(-1, 1)
  seq(from = rg[1], to = rg[2], length.out = 100)
}
```

Set up the points for prediction, a 100×100 grid that covers the data range.

```
diabetes_grid = with(diabetes,
  expand.grid(insulin = make1Dgrid(insulin),
              glutest = make1Dgrid(glutest)))
```

Do the predictions.

```
diabetes_grid$ghat =
  predict(diabetes_lda, newdata = diabetes_grid)$class
```

The group centers.

```
centers = diabetes_lda$means
```

Compute a unit circle and an affine transformation of the circle into the ellipse we want to plot.

```
unitcircle = exp(1i * seq(0, 2*pi, length.out = 90)) %>%
          (function(x) cbind(Re(x), Im(x)))
ellipse = unitcircle %*% solve(diabetes_lda$scaling)
```

All three ellipses, one for each group center.

```
ellipses = lapply(seq_len(nrow(centers)), function(i) {
  (ellipse +
   matrix(centers[i, ], byrow = TRUE,
          ncol = ncol(centers), nrow = nrow(ellipse))) %>%
     cbind(group = i)
}) %>% do.call(rbind, .) %>% data.frame
ellipses$group %<>% factor
```

Now we are ready to plot (Figure 13.6).

```
ggdb + geom_raster(aes(fill = ghat),
             data = diabetes_grid, alpha = 0.4, interpolate = TRUE) +
    geom_point(data = as_data_frame(centers), pch = "+", size = 8) +
    geom_path(aes(colour = group), data = ellipses) +
    scale_x_continuous(expand = c(0, 0)) +
    scale_y_continuous(expand = c(0, 0))
```

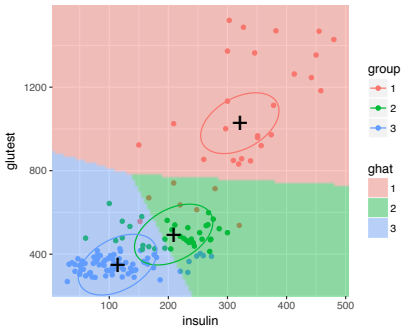

Figure 13.6: As Figure 13.5, with the classification regions from the LDA model shown.

▶ Question **13.3.2.** Why is the boundary between the prediction regions for groups 1 and 2 not perpendicular to the line between the cluster centers?

▶ Question **13.3.3.** How confident would you be about the predictions in those areas of the 2D plane that are far from all of the cluster centers?

▶ Question **13.3.4.** Why is the boundary between the prediction regions for groups 2 and 3 not half-way between the centers, but shifted in favor of class 3? (Hint: have a

look at the `prior` argument of `lda`.) Try again with uniform prior.

▶ Answer **13.3.1.** The result of the following code chunk is shown in Figure 13.7.

```
diabetes_up = lda(group ~ insulin + glutest, data = diabetes,
  prior = with(diabetes, rep(1/nlevels(group), nlevels(group))))

diabetes_grid$ghup =
  predict(diabetes_up, newdata = diabetes_grid)$class

stopifnot(all.equal(diabetes_up$means, diabetes_lda$means))

ellipse_up  = unitcircle %*% solve(diabetes_up$scaling)
ellipses_up = lapply(seq_len(nrow(centers)), function(i) {
  (ellipse_up +
   matrix(centers[i, ], byrow = TRUE,
          ncol = ncol(centers), nrow = nrow(ellipse_up))) %>%
     cbind(group = i)
}) %>% do.call(rbind, .) %>% data.frame
ellipses_up$group %<>% factor

ggdb + geom_raster(aes(fill = ghup),
            data = diabetes_grid, alpha = 0.4, interpolate = TRUE) +
    geom_point(data = data.frame(centers), pch = "+", size = 8) +
    geom_path(aes(colour = group), data = ellipses_up) +
    scale_x_continuous(expand = c(0, 0)) +
    scale_y_continuous(expand = c(0, 0))
```

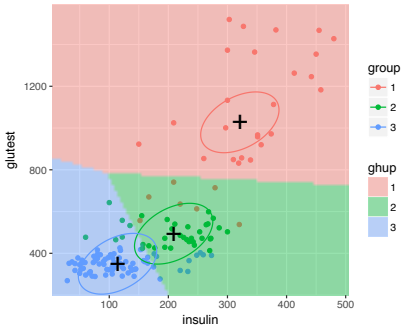

Figure 13.7: As Figure 13.6, but with uniform class priors.

The `stopifnot` line confirms that the class centers are the same –they are independent of the prior–, but the joint covariance is not.

▶ Question **13.3.5.** What is the difference in the prediction accuracy if we use all 5 variables instead of just `insulin` and `glufast`?

▶ Answer **13.3.2.**

```
diabetes_lda5 = lda(group ~ relwt + glufast + glutest +
          steady + insulin, data = diabetes)
diabetes_lda5

## Call:
## lda(group ~ relwt + glufast + glutest + steady + insulin, data = diabetes)
##
## Prior probabilities of groups:
##         1         2         3
## 0.2222222 0.2500000 0.5277778
##
## Group means:
##       relwt   glufast   glutest   steady  insulin
## 1 0.9915625 213.65625 1027.3750 108.8438 320.9375
## 2 1.0558333  99.30556  493.9444 288.0000 208.9722
## 3 0.9372368  91.18421  349.9737 172.6447 114.0000
##
## Coefficients of linear discriminants:
##                   LD1           LD2
```

```
## relwt   -1.339546e+00 -3.7950612048
## glufast  3.301944e-02  0.0373202882
## glutest -1.263978e-02 -0.0068947755
## steady   1.240248e-05 -0.0059924778
## insulin -3.895587e-03  0.0005754322
##
## Proportion of trace:
##    LD1    LD2
## 0.8784 0.1216
```

```
ghat5 = predict(diabetes_lda5)$class
table(ghat5, diabetes$group)
```

```
##
## ghat5  1  2  3
##     1 26  0  0
##     2  5 31  3
##     3  1  5 73
```

```
mean(ghat5 != diabetes$group)
```

```
## [1] 0.09722222
```

▶ Question **13.3.6.** Instead of approximating the prediction regions by classification from a grid of points, compute the separating lines explicitly from the linear determinant coefficients.

▶ Answer **13.3.3.** See Section 4.3, Equation (4.10) in (Hastie et al., 2008).

13.3.2 Predicting embryonic cell state from gene expression

Assume that we already know that the four genes *FN1*, *TIMD2*, *GATA4* and *SOX7* are relevant to the classification task[5]. We want to build a classifier that predict the developmental time (embryonic days, E3.25, E3.5, E4.5). We load the data and select four corresponding probes.

[5] Later in this chapter we will see methods that can drop this assumption and screen all available features.

```
library("Hiiragi2013")
data("x")
probes = c("1426642_at","1418765_at","1418864_at","1416564_at")
embryoCells = as_data_frame(t(exprs(x)[probes, ])) %>%
  mutate(Embryonic.day = x$Embryonic.day) %>%
  filter(x$genotype == "WT")
```

We can use the Bioconductor annotation package associated with the microarray to verify that the probes correspond to the intended genes,

```
annotation(x)
```

```
## [1] "mouse4302"
```

```
library("mouse4302.db")
anno = AnnotationDbi::select(mouse4302.db, keys = probes,
         columns = c("SYMBOL", "GENENAME"))
anno
```

```
##      PROBEID SYMBOL
## 1 1426642_at    Fn1
## 2 1418765_at  Timd2
## 3 1418864_at  Gata4
## 4 1416564_at   Sox7
##                                                GENENAME
## 1                                             fibronectin 1
## 2 T cell immunoglobulin and mucin domain containing 2
## 3                                 GATA binding protein 4
## 4                  SRY (sex determining region Y)-box 7
```

```
mt = match(anno$PROBEID, colnames(embryoCells))
colnames(embryoCells)[mt] = anno$SYMBOL
```

and produce a pairs plot (Figure 13.8).

```
library("GGally")
ggpairs(embryoCells, mapping = aes(col = Embryonic.day),
  columns = anno$SYMBOL, upper = list(continuous = "points"))
```

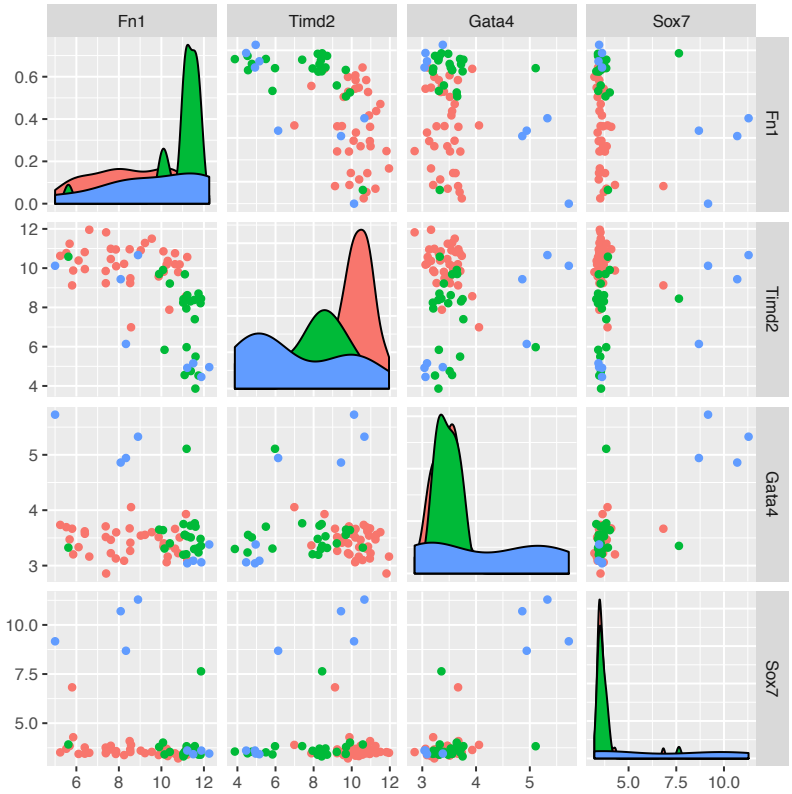

Figure 13.8: Expression values of the discriminating genes, with the prediction target Embryonic.day shown by color.

We can now call `lda` on these data. The linear combinations LD1 and LD2 that serve as discriminating variables are given in the slot `ed_lda$scaling` of the output from `lda`.

```
ec_lda = lda(Embryonic.day ~ Fn1 + Timd2 + Gata4 + Sox7,
             data = embryoCells)
```

```
round(ec_lda$scaling, 1)

##        LD1  LD2
## Fn1   -0.2 -0.4
## Timd2  0.5  0.0
## Gata4 -0.1 -0.6
## Sox7  -0.7  0.5
```

For the visualisation of the learned model in Figure 13.9, we need to build the prediction regions and their boundaries by expanding the grid in the space of the two new coordinates LD1 and LD2.

```
ec_rot = predict(ec_lda)$x %>% as_data_frame %>%
           mutate(ed = embryoCells$Embryonic.day)

ec_lda2 = lda(ec_rot[, 1:2], predict(ec_lda)$class)

ec_grid = with(ec_rot, expand.grid(
  LD1 = make1Dgrid(LD1),
  LD2 = make1Dgrid(LD2)))

ec_grid$edhat = predict(ec_lda2, newdata = ec_grid)$class

ggplot() +
  geom_point(aes(x = LD1, y = LD2, colour = ed), data = ec_rot) +
  geom_raster(aes(x = LD1, y = LD2, fill = edhat),
            data = ec_grid, alpha = 0.4, interpolate = TRUE) +
  scale_x_continuous(expand = c(0, 0)) +
  scale_y_continuous(expand = c(0, 0)) +
  coord_fixed()
```

▶ Question **13.3.7.** Repeat these analyses using quadratic discriminant analysis (qda). What difference do you see in the shape of the boundaries?

▶ Answer **13.3.4.** See Figure 13.10.

```
library("gridExtra")

ec_qda = qda(Embryonic.day ~ Fn1 + Timd2 + Gata4 + Sox7,
             data = embryoCells)

variables = colnames(ec_qda$means)
pairs = combn(variables, 2)
lapply(seq_len(ncol(pairs)), function(i) {
  grid = with(embryoCells,
    expand.grid(x = make1Dgrid(get(pairs[1, i])),
                y = make1Dgrid(get(pairs[2, i])))) %>%
    `colnames<-`(pairs[, i])

  for (v in setdiff(variables, pairs[, i]))
    grid[[v]] = median(embryoCells[[v]])

  grid$edhat = predict(ec_qda, newdata = grid)$class
```

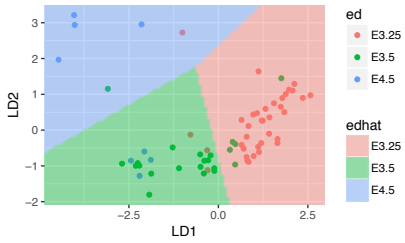

Figure 13.9: LDA classification regions for Embryonic.day.

```
  ggplot() + geom_point(
      aes_string(x = pairs[1, i], y = pairs[2, i],
      colour = "Embryonic.day"), data = embryoCells) +
    geom_raster(
      aes_string(x = pairs[1, i], y = pairs[2, i], fill = "edhat"),
      data = grid, alpha = 0.4, interpolate = TRUE) +
    scale_x_continuous(expand = c(0, 0)) +
    scale_y_continuous(expand = c(0, 0)) +
    coord_fixed() +
    if (i != ncol(pairs)) theme(legend.position = "none")
}) %>% grid.arrange(grobs = ., ncol = 3)
```

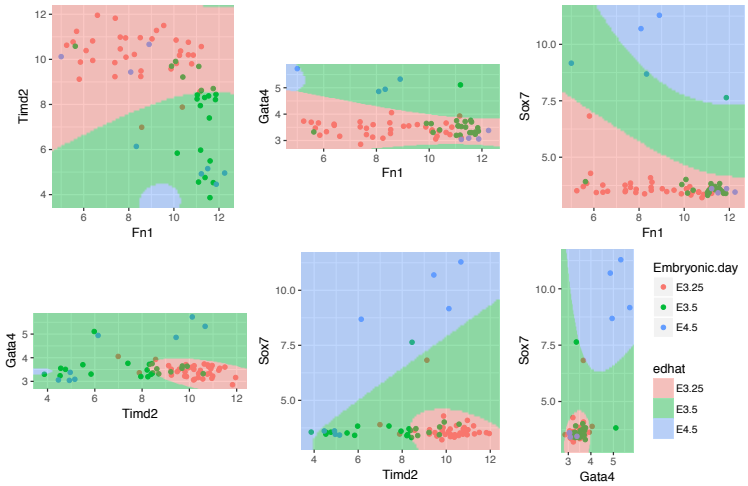

Figure 13.10: QDA for the mouse cell data, all pairwise plots of the four features.

▶ Question **13.3.8.** What happens if you call `lda` or `qda` with a lot more genes, say the first 1000, in the Hiiragi dataset?

▶ Answer **13.3.5.**

```
lda(t(exprs(x))[, 1:1000], x$Embryonic.day)

## Warning in lda.default(x, grouping, ...): variables are collinear

qda(t(exprs(x))[, 1:1000], x$Embryonic.day)

## Error in qda.default(x, grouping, ...): some group is too small for
'qda'
```

13.4 Machine learning vs rote learning

Computers are really good at memorizing facts. In the worst case, a machine learning algorithm is a roundabout way of doing this[6]. The central question in statistical learning is whether the algorithm was able to generalize, i. e., interpolate and extrapolate. Let's look at the following example. We generate random data (`rnorm`) for `n` objects, with different numbers of features (given by `p`). We train a LDA on these data and compute the **misclassification rate**, i. e., the fraction of times the prediction is wrong (`pred != resp`).

[6] The not so roundabout way is database technologies.

```
library("dplyr")
p = 2:21
n = 20

mcl = lapply(p, function(k) {
  replicate(100, {
    xmat = matrix(rnorm(n * k), nrow = n)
    resp = sample(c("apple", "orange"), n, replace = TRUE)
    fit  = lda(xmat[, 1:k], resp)
    pred = predict(fit)$class
    mean(pred != resp)
  }) %>% mean %>% tibble(mcl = .)
}) %>% bind_rows %>% cbind(., p = p)

ggplot(mcl, aes(x = p, y = mcl)) + geom_line() + geom_point() +
  ylab("Misclassification rate")
```

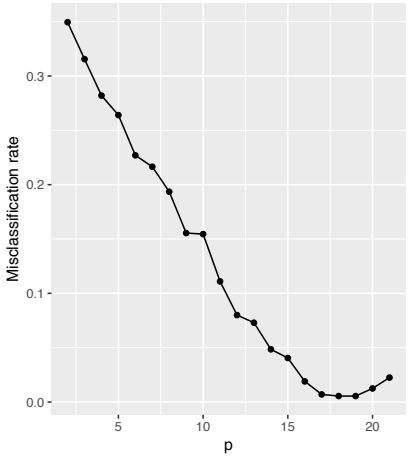

Figure 13.11: Misclassification rate of LDA applied to random data. With increasing number of features (`p`), the misclassification rate becomes almost zero as `p` approaches `n`, the number of objects. (As `p` becomes even larger, the "performance" degrades again, apparently due to numerical properties of the `lda` implementation used here.)

▶ Question **13.4.1.** What is the purpose of the `replicate` loop in the above code? What happens if you omit it (or replace the 100 by 1)?

▶ Answer **13.4.1.** Averaging the misclassification rate over 100 replicates makes the estimate more stable, and since we are working with simulated data, we are at liberty to do so. For each single replicate, the curve is a noisier version of Figure 13.11.

Figure 13.11 seems to imply that we can perfectly predict random labels from random data, if we only fit a complex enough model, i.e., one with many parameters. How can we overcome such an absurd conclusion? The problem with the above code is that the model performance is evaluated on the same data on which it was trained. This generally leads to positive bias, as you see in this crass example. How can we overcome this problem? The key idea is to assess model performance on different data than those on which the model was trained.

13.4.1 Cross-validation

A naive approach might be to split the data in two halves, and use the first half for learning ("training"), the second half for assessment ("testing"). It turns out that this is needlessly variable and needlessly inefficient. Needlessly variable, since by splitting the data only once, our results can be quite affected by how the splitting happens to fall. It seems better to do the splitting many times, and average. This will give us more stable results. Needlessly inefficient, since the performance of machine learning algorithms depends on the number of samples, and the performance measured on half the data is likely[7] to be worse than what it is with all the data. For this reason, it is better to use unequal sizes of training and test data. In the extreme case, we'll use as much as $n - 1$ samples for training, and the remaining one for testing. After we've done this likewise for all samples, we can average our performance metric. This is called **leave-one-out cross-validation**. An alternative is **k-fold cross-validation**, where the samples are repeatedly split into a training set of size of around $n(k-1)/k$ and a test set of size of around n/k. Both alternatives have pros and contras, and there is not a universally best choice. An advantage of leave-one-out is that the amount of data used for training is close to the maximally available data; this is

[7] Unless we have such an excess of data that it doesn't matter.

especially important if the sample size is limiting and "every little matters" for the algorithm. A drawback of leave-one-out is that the training sets are all very similar, so they may not sufficiently model the kind of sampling changes to be expected if a new dataset came along. For large n, leave-one-out cross-validation can be needlessly time-consuming[8].

[8] See Chapter *Model Assessment and Selection* in the book by Hastie et al. (2008) for further discussion on these trade-offs.

```
estimate_mcl_loocv = function(x, resp) {
  vapply(seq_len(nrow(x)), function(i) {
    fit  = lda(x[-i, ], resp[-i])
    ptrn = predict(fit, newdata = x[-i,, drop = FALSE])$class
    ptst = predict(fit, newdata = x[ i,, drop = FALSE])$class
    c(train = mean(ptrn != resp[-i]), test = (ptst != resp[i]))
  }, FUN.VALUE = c(0,0)) %>% rowMeans %>% t %>% as_data_frame
}

xmat = matrix(rnorm(n * last(p)), nrow = n)
resp = sample(c("apple", "orange"), n, replace = TRUE)

mcl = lapply(p, function(k) {
  estimate_mcl_loocv(xmat[, 1:k], resp)
}) %>% bind_rows %>% data.frame(p) %>% melt(id.var = "p")

ggplot(mcl, aes(x = p, y = value, col = variable)) + geom_line() +
  geom_point() + ylab("Misclassification rate")
```

The result is show in Figure 13.12.

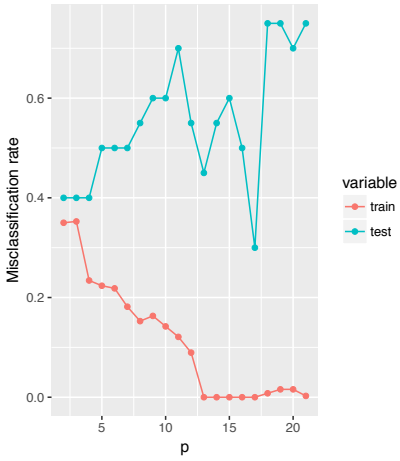

Figure 13.12: Cross-validation: the misclassification rate of LDA applied to random data, when evaluated on test data that were not used for learning, hovers around 0.5 independent of p. The misclassification rate on the training data is also shown. It behaves similar to what we already saw in Figure 13.11.

▶ Question **13.4.2.** Why are the curves in Figure 13.12 more variable ("wiggly") than in Figure 13.11? How can you overcome this?

▶ Answer **13.4.2.** Only one dataset (`xmat`, `resp`) was used to calculate Figure 13.12, whereas for Figure 13.11, we had the data generated within a `replicate` loop. You could similarly extend the above code to average the misclassification rate curves over many replicate datasets.

13.4.2 The curse of dimensionality

In Section 13.4.1 we have seen overfitting and cross-validation on random data, but how does it look if there is in fact a relevant class separation?

```
p   = 2:20
mcl = replicate(100, {
  xmat = matrix(rnorm(n * last(p)), nrow = n)
  resp = sample(c("apple", "orange"), n, replace = TRUE)
  xmat[, 1:6] = xmat[, 1:6] + as.integer(factor(resp))

  lapply(p, function(k) {
    estimate_mcl_loocv(xmat[, 1:k], resp)
  }) %>% bind_rows %>% cbind(p = p) %>% melt(id.var = "p")
}, simplify = FALSE)

mcl = bind_rows(mcl) %>% group_by(p, variable) %>%
```

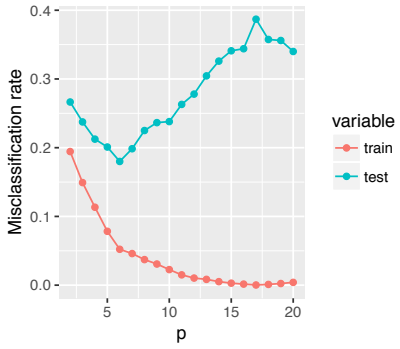

Figure 13.13: As we increase the number of features included in the model, the misclassification rate initially improves; as we start including more and more irrelevant features, it increases again, as we are fitting noise.

```
   summarise(value = mean(value))

ggplot(mcl, aes(x = p, y = value, col = variable)) + geom_line() +
   geom_point() + ylab("Misclassification rate")
```

The result is shown in Figure 13.13. The group centers are the vectors (in $\mathbb{R}^{20}$) given by the coordinates $(1, 1, 1, 1, 1, 1, 0, 0, 0, \ldots)$ (apples) and $(2, 2, 2, 2, 2, 2, 0, 0, 0, \ldots)$ (oranges), and the optimal decision boundary is the hyperplane orthogonal to the line between them. For k smaller than 6, the decision rule cannot reach this hyperplane – it is biased. As a result, the misclassification rate is suboptimal, and it decreases with k. But what happens for k larger than 6? The algorithm is, in principle, able to model the optimal hyperplane, and it should not be distracted by the additional features. The problem is that it is. The more additional features enter the dataset, the higher the probability that one or more of them happen to fall in a way that they *look like* good, discriminating features in the training data – only to mislead the classifier and degrade its performance in the test data. Shortly we'll see how to use penalization to (try to) control this problem.

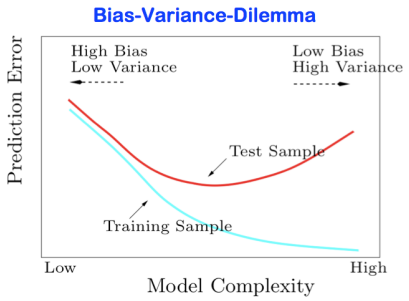

Figure 13.14: Idealized version of Figure 13.13, from Hastie et al. (2008). A recurrent goal in machine learning is finding the sweet spot in the variance–bias trade-off.

The term **curse of dimensionality** was coined by Bellman (1961). It refers to the fact that high-dimensional spaces are very hard to sample. Our intuitions about distances between points in a high-dimensionsal space, and the relationship between its volume and surface, break down.

▶ Question **13.4.3.** Assume you have a dataset with 1 000 000 data points in p dimensions. The data are uniformly distributed in the unit hybercube (i. e., all features lie in the interval $[0, 1]$). What's the side length of a hybercube that can be expected to contain 10 points, as a function of p?

▶ Answer **13.4.3.** See Figure 13.15.

```
sideLength = function(p, pointDensity = 1e6, pointsNeeded = 10)
   (pointsNeeded / pointDensity) ^ (1 / p)
ggplot(tibble(p = 1:750, sideLength = sideLength(p)),
       aes(x = p, y = sideLength)) +
  geom_line(col = "red") + geom_hline(aes(yintercept = 1), linetype = 2)
```

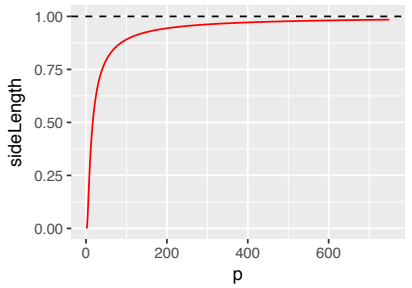

Figure 13.15: Side length of a hybercube expected to contain 10 points out of 1 million uniformly distributed ones, as a function of its dimension p. While for $p = 1$, this length is $10/10^6 = 10^{-5}$, for larger p it approaches 1, i. e., becomes the same as the range of each the features. In genomics, we often aim to fit models to data with thousands of features.

Generally, prediction at the boundaries of feature space is more difficult than in its interior, as it tends to involve extrapolation, rather than interpolation.

▶ Question **13.4.4.** What fraction of a unit cube's total volume is closer than 0.01 to any of its surfaces, as a function of the dimension?

▶ Answer **13.4.4.** See Figure 13.16.

```
p = 1:750
volOuterCube = 1 ^ p
volInnerCube = 0.98 ^ p
ggplot(tibble(p = p, `V(shell)` = volOuterCube - volInnerCube),
       aes(x = p, y =`V(shell)`)) + geom_line(col = "blue")
```

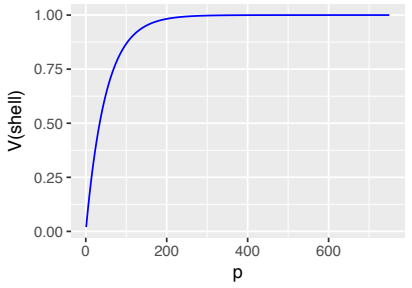

Figure 13.16: Fraction of a unit cube's total volume that is in its "shell" (here operationalised as those points that are closer than 0.01 to its surface) as a function of the dimension p.

▶ Question **13.4.5.** What is the coefficient of variation (ratio of standard deviation over average) of the distance between two randomly picked points in the unit hypercube, as a function of the dimension?

▶ Answer **13.4.5.** We solve this one by simulation. We generate `n` pairs of random points in the hypercube (`x1`, `x2`) and compute their Euclidean distances. See Figure 13.17. This result can also be predicted from the central limit theorem.

```
n = 1000
df = tibble(
  p = round(10 ^ seq(0, 4, by = 0.25)),
  cv = vapply(p, function(k) {
    x1 = matrix(runif(k * n), nrow = n)
    x2 = matrix(runif(k * n), nrow = n)
    d = sqrt(rowSums((x1 - x2)^2))
    sd(d) / mean(d)
  }, FUN.VALUE = NA_real_))
ggplot(df, aes(x = log10(p), y = cv)) + geom_line(col = "orange") +
  geom_point()
```

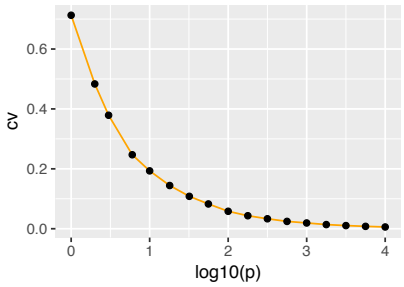

Figure 13.17: Coefficient of variation (CV) of the distance between randomly picked points in the unit hypercube, as a function of the dimension. As the dimension increases, everybody is equally far away from everyone else: there is almost no variation in the distances any more.

13.5 Objective functions

We've already seen the **misclassification rate** (MCR) used to assess our classification performance in Figures 13.11–13.13. Its population version is defined as

$$\mathrm{MCR} = \mathrm{E}\left[\mathbb{1}_{\hat{y}\neq y}\right], \tag{13.1}$$

and for a finite sample

$$\widehat{\mathrm{MCR}} = \frac{1}{n}\sum_{i=1}^{n}\mathbb{1}_{\hat{y}_i\neq y_i}. \tag{13.2}$$

This is not the only choice we could make. Perhaps we care more about the misclassification of apples as oranges than vice versa, and we can reflect this by introducing weights that depend on the type of error made into the sum of Equation (13.2) (or the integral of Equation (13.1)). This can get even more elaborate if we have more than two classes. Often we do not only want to see a single numeric summary, but the whole **confusion table**, which in *R* we can get via expressions like

```
table(truth, response)
```

An important special case is binary classification with asymmetric costs – think about, say, a medical test. Here, the **sensitivity** (a.k.a. **true positive rate** or **recall**) is related to the misclassification of non-sick as sick, and the **specificity** (or **true negative rate**) depends on the probability of misclassification of sick as non-sick. Often, there is a single parameter (e. g., a threshold) that can be moved up and down, allowing a trade-off between sensitivity and specificity (and thus, equivalently, between the two types of misclassification). In those cases, we usually are not content to know the classifier performance at one single choice of threshold, but at many (or all) of them. This leads to **receiver operating characteristic** (**ROC**) or **precision-recall** curves.

▶ Question **13.5.1.** What are the exact relationships between the per-class misclassification rates and sensitivity and specificity?

▶ Answer **13.5.1.** The sensitivity or true positive rate is

$$\text{TPR} = \frac{\text{TP}}{\text{P}},$$

where TP is the number of true positives and P the number of all positives. The specificity or true negative rate is

$$\text{SPC} = \frac{\text{TN}}{\text{N}},$$

where TN is the number of true negatives and N the number of all negatives. See also `https://en.wikipedia.org/wiki/Sensitivity_and_specificity`

Another cost function can be computed from the **Jaccard index**, which we already saw in Chapter 5.

$$J(A, B) = \frac{|A \cap B|}{|A \cup B|}, \tag{13.3}$$

where A is the set of samples for which the true class is 1 ($A = \{i \,|\, y_i = 1\}$) and B is the set of samples for which the predicted class is 1. J is a number between 0 and 1, and a high value of J indicates high overlap of the two sets. Note that J does not depend on the number of samples for which both true and predicted class is 0 – so it is particularly suitable for measuring the performance of methods that try to find rare events.

We can also consider probabilistic class predictions, which come in the form $\hat{P}(Y \,|\, X)$. In this case, a possible risk function would be obtained by looking at distances between the true probability distribution and the estimated probability distributions. For two classes, the finite sample version of the log loss is

$$\text{log loss} = -\frac{1}{n}\sum_{i=1}^{n} y_i \log(\hat{p}_i) + (1 - y_i)\log(1 - \hat{p}_i), \tag{13.4}$$

where $\hat{p}_i \in [0, 1]$ is the prediction, and $y_i \in \{0, 1\}$ is the truth[9].

[9] Note that the log loss will be infinite if a prediction is totally confident ($\hat{p}_i$ is exactly 0 or 1) but wrong.

For continuous continuous response variables (regression), a natural choice is the **mean squared error** (**MSE**). It is the average squared error,

$$\widehat{\text{MSE}} = \frac{1}{n}\sum_{i=1}^{n}(\hat{Y}_i - Y_i)^2. \tag{13.5}$$

The population version is defined analogously, by turning the summation into an integral as in Equations (13.1) and (13.2).

Statisticians call functions like Equations (13.1–13.5) variously (and depending on context and predisposition) **risk function**, **cost function**, **objective function**[10].

[10] There is even an *R* package dedicated to evaluation of statistical learners called *metrics*.

13.6 Variance–bias trade-off

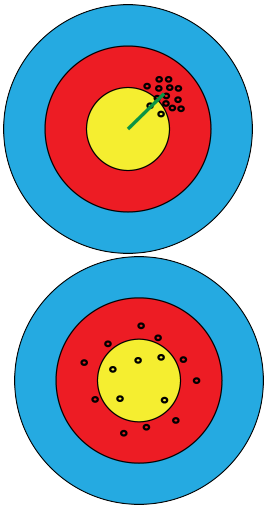

Figure 13.18: In the upper bull's eye, the estimates are systematically off target, but in a quite reproducible manner. The green segment represents the bias. In the lower bull's eye, the estimates are not biased, as they are centered in the right place, however they have high variance. We can distinguish the two scenarios since we see the result from many shots. If we only had one shot and missed the bull's eye, we could not easily know whether that's because of bias or variance.

An important fact that helps us understand the tradeoffs when picking a statistical learning model is that the MSE is the sum of two terms, and often the choices we can make are such that one of those terms goes down while the other one goes up. The bias measures how different the average of all the different estimates is from the truth, and variance, how much an individual one might scatter from the average value (Figure 13.18). In applications, we often only get one shot, therefore being reliably almost on target can beat being right on the long term average but really off today. The decomposition

$$\mathrm{MSE} = \underbrace{\mathrm{Var}(\hat{Y})}_{\text{variance}} + \underbrace{\mathbb{E}[\hat{Y} - Y]^2}_{\text{bias}} \tag{13.6}$$

follows by straightforward algebra.

When trying to minimize the MSE, it is important to remember that sometimes we can pay the price of some bias to obtain a much smaller variance and thus an overall estimator of lower MSE. In classification (with categorical response variables), different objective functions than the MSE are used, and there is usually no such straightforward decomposition as in Equation (13.6). In general, we can go much further in classification applications than in regression with trading biases for variance, since the discreteness of the response neutralizes certain biases (Friedman, 1997).

13.6.1 Penalization

In high-dimensional statistics, we are constantly plagued by variance: there is just not enough data to fit all the possible parameters. One of the most fruitful ideas in high-dimensional statistics is **penalization**: a tool to actively control and exploit the variance-bias tradeoff.

Although generalisation of LDA to high-dimensional settings is possible (Clemmensen et al., 2011; Witten and Tibshirani, 2011), it turns out that logistic regression is a more general approach[11], and therefore we'll now switch to that, using the *glmnet* package.

Multinomial[12] logistic regression models the posterior log-odds between k classes and can be written in the form[13]

$$\log \frac{P(Y = i \,|\, X = x)}{P(Y = k \,|\, X = x)} = \beta_i^0 + \beta_i x, \tag{13.7}$$

where $i = 1, \ldots, k-1$; x is the $n \times p$ data matrix (n: number of samples, p: number of features), and β_i is a p-dimensional vector that determines how the classification odds for class i versus class k depend on x. The numbers β_i^0 are intercepts and depend, among other things, on the classes' prior probabilities. Instead of the log odds (13.7) (i. e., ratios of class probabilities), we can also write down an equivalent model for the class probabilities themselves, and the fact that we here used the k-th

[11] It fits into the framework of generalized linear models.

[12] Or, for the special case of two classes, binomial logistic regression.

[13] See (Hastie et al., 2008) for a complete presentation.

class as a reference is an arbitrary choice, as the model estimates are equivariant under this choice (Hastie et al., 2008). The model is fit by maximising the log-likelihood $\ell(\beta, \beta^0; x)$, where $\beta = (\beta_1, \ldots, \beta_{k-1})$ and analogously for β^0.

So far, so good. But as p gets larger, there is an increasing chance that some of the estimates go wildly off the mark, due to random sampling happenstances in the data. This is true even if for each individual coordinate of the vector β_i, the error distribution is bounded: the probabilty of there being one coordinate that is in the far tails increases the more coordiates there are, i.e., the larger p is.

A related problem can also occur, not in (13.7), but in other, non-linear models, as the model dimension p increases while the sample size n remains the same: the likelihood landscape around its maximum becomes increasingly flat, and the maximum-likelihood estimate of the model parameters becomes more and more variable. Eventually, the maximum is no longer a point, but a submanifold, and the maximum likelihood estimate is unidentifiable.

Both of these limitations can be overcome with a modification of the objective: instead of maximising the bare log-likelihood, we maximise a penalized version of it,

$$\hat{\beta} = \arg\max_{\beta} \ell(\beta, \beta^0; x) + \lambda \, \mathrm{pen}(\beta), \tag{13.8}$$

where $\lambda \geq 0$ is a real number, and pen is a convex function, called the **penalty function**. Popular choices are $\mathrm{pen}(\beta) = |\beta|^2$ (**ridge regression**) and $\mathrm{pen}(\beta) = |\beta|^1$ (**lasso**)[14]. In the **elastic net**, ridge and lasso are hybridized by using the penalty function $\mathrm{pen}(\beta) = (1-\alpha)|\beta|^1 + \alpha|\beta|^2$ with some further parameter $\alpha \in [0, 1]$. The crux is, of course, how to choose the right λ, and we will discuss that in the following.

[14] Here, $|\beta|^\nu = \sum_i \beta_i^\nu$ is the L_ν-norm of the vector β. Variations are possible, for instead we could include in this summation only some but not all of the elements of β; or we could scale different elements differently, for instance based on some prior belief of their scale and importance.

13.6.2 Example: predicting colon cancer from stool microbiome composition

Zeller et al. (2014) studied metagenome sequencing data from fecal samples of 156 humans that included colorectal cancer patients and tumor-free controls. Their aim was to see whether they could identify biomarkers (presence or abundance of certain taxa) that could help with early tumor detection. The data are available from Bioconductor through its **ExperimentHub** service under the identifier EH359.

```
library("ExperimentHub")
eh = ExperimentHub()
zeller = eh[["EH361"]]
```

```
zeller$disease %>% table
```

```
## .
##        cancer large_adenoma             n small_adenoma
##            53            15            61            27
```

▶ Question **13.6.1.** Explore the `eh` object to see what other datasets there are.
▶ Answer **13.6.1.**

```
eh
```

For the following, let's focus on the normal and cancer samples and set the adenomas aside.

```
zellerNC = zeller[, zeller$disease %in% c("n", "cancer")]
```

Before jumping into model fitting, it is always a good idea to do some exploration of the data. First, let's look at the sample annotations for some of the samples. We pick them randomly, since this can be more representative of the whole dataset than only looking at the first or last ones.

```
pData(zellerNC)[ sample(ncol(zellerNC), 3), ]
```

```
##                     subjectID age gender bmi country disease
## CCIS71578391ST-4-0     FR-187  70   male  25  france       n
## CCIS50003399ST-4-0     FR-194  66 female  28  france       n
## CCIS38765456ST-20-0    FR-723  79 female  22  france  cancer
##                     tnm_stage ajcc_stage localization     fobt
## CCIS71578391ST-4-0       <NA>       <NA>         <NA> negative
## CCIS50003399ST-4-0       <NA>       <NA>         <NA> negative
## CCIS38765456ST-20-0    t4n1m1         iv           lc positive
##                     wif-1_gene_methylation_test   group bodysite
## CCIS71578391ST-4-0                    negative control    stool
## CCIS50003399ST-4-0                    negative control    stool
## CCIS38765456ST-20-0                   positive     crc    stool
##                     ethnicity number_reads
## CCIS71578391ST-4-0      white     74021867
## CCIS50003399ST-4-0      white     63416533
## CCIS38765456ST-20-0     white     81682982
```

Next, let's explore the feature names[15].

[15] We define the helper function `formatfn` to line wrap these long character strings for the available space here.

```
formatfn = function(x)
   gsub("|", "| ", x, fixed = TRUE) %>% lapply(strwrap)

rownames(zellerNC)[1:4]
```

```
## [1] "k__Bacteria"                  "k__Viruses"
## [3] "k__Bacteria|p__Firmicutes"    "k__Bacteria|p__Bacteroidetes"
```

```
rownames(zellerNC)[nrow(zellerNC) + (-2:0)] %>% formatfn
```

```
## [[1]]
## [1] "k__Bacteria| p__Proteobacteria| c__Deltaproteobacteria|"
## [2] "o__Desulfovibrionales| f__Desulfovibrionaceae|"
## [3] "g__Desulfovibrio| s__Desulfovibrio_termitidis"
##
## [[2]]
## [1] "k__Viruses| p__Viruses_noname| c__Viruses_noname|"
## [2] "o__Viruses_noname| f__Baculoviridae| g__Alphabaculovirus|"
## [3] "s__Bombyx_mori_nucleopolyhedrovirus|"
## [4] "t__Bombyx_mori_nucleopolyhedrovirus_unclassified"
##
## [[3]]
```

```
## [1] "k__Bacteria| p__Proteobacteria| c__Deltaproteobacteria|"
## [2] "o__Desulfovibrionales| f__Desulfovibrionaceae|"
## [3] "g__Desulfovibrio| s__Desulfovibrio_termitidis|"
## [4] "t__GCF_000504305"
```

As you can see, the features are a mixture of abundance quantifications at different taxonomic levels, from **k**ingdom over **phylum** to **s**pecies. We could select only some of these, but here we continue with all of them. Next, let's look at the distribution of some of the features. Here, we show two; in practice, it is helpful to scroll through many such plots quickly to get an impression.

```
ggplot(melt(exprs(zellerNC)[c(510, 527), ]), aes(x = value)) +
    geom_histogram(bins = 25) +
    facet_wrap( ~ Var1, ncol = 1, scales = "free")
```

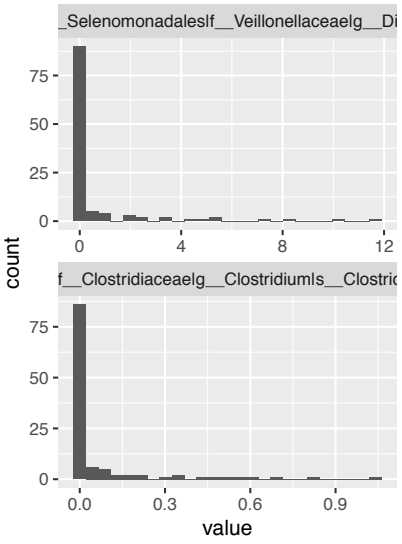

Figure 13.19: Histograms of the distributions for two randomly selected features. The distributions are highly skewed, with many zero values and a thin, long tail of non-zero values.

In the simplest case, we fit model (13.7) as follows.

```
library("glmnet")
glmfit = glmnet(x = t(exprs(zellerNC)),
                y = factor(zellerNC$disease),
                family = "binomial")
```

A remarkable feature of the `glmnet` function is that it fits (13.7) not only for one choice of λ, but for all possible λs at once. For now, let's look at the prediction performance for, say, $\lambda = 0.04$. The name of the function parameter is `s`:

```
predTrsf = predict(glmfit, newx = t(exprs(zellerNC)),
                   type = "class", s = 0.04)
table(predTrsf, zellerNC$disease)
```

```
##
## predTrsf cancer  n
##   cancer     51  0
##   n           2 61
```

Not bad[16]. Let's have a closer look at `glmfit`. The *glmnet* package offers a a diagnostic plot that is worth looking at (Figure 13.20).

```
plot(glmfit, col = brewer.pal(12, "Set3"), lwd = sqrt(3))
```

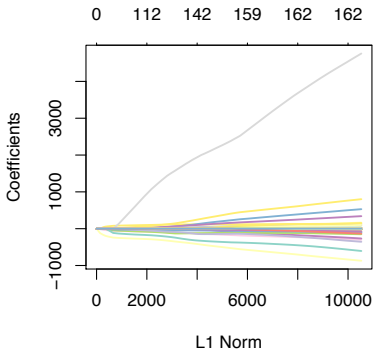

Figure 13.20: Regularization paths for `glmfit`.

▶ Question **13.6.2.** What is the x-axis in Figure 13.20? What are the different lines?

▶ Answer **13.6.2.** Consult the manual page of the function `plot.glmnet` in the *glmnet* package.

Let's get back to the question of how to choose the parameter λ. We could try many different choices –and indeed, all possible choices– of λ, assess classification performance in each case using cross-validation, and then choose the best λ[17]. We could do so by writing a loop as we did in the `estimate_mcl_loocv` function in Section 13.4.1. It turns out that the *glmnet* package already has built-in functionality for that, with the function `cv.glmnet`, which we can use instead.

```
cvglmfit = cv.glmnet(x = t(exprs(zellerNC)),
                     y = factor(zellerNC$disease),
                     family = "binomial")
plot(cvglmfit)
```

[16] But remember that this is on the training data, without cross-validation.

[17] You'll already realize from the description of this strategy that if we optimize λ in this way, the resulting apparent classification performance will likely be exaggerated. We need a truly independent dataset, or at least another, outer cross-validation loop to get a more realistic impression of the generalizability. We will get back to this question at the end of the chapter.

The diagnostic plot is shown in Figure 13.21. We can access the optimal value with

```
cvglmfit$lambda.min

## [1] 0.08830775
```

As this value results from finding a minimum in an estimated curve, it turns out that it is often too small, i. e., that the implied penalization is too weak. A heuristic recommended by the authors of the *glmnet* package is to use a somewhat larger value instead, namely the largest value of λ such that the performance measure is within 1 standard error of the minimum.

```
cvglmfit$lambda.1se

## [1] 0.1015325
```

▶ Question **13.6.3.** How does the confusion table look like for $\lambda =$ `lambda.1se`?
▶ Answer **13.6.3.**

```
s0 = cvglmfit$lambda.1se
predict(glmfit, newx = t(exprs(zellerNC)),type = "class", s = s0) %>%
    table(zellerNC$disease)

##
## .        cancer  n
##   cancer     35  7
##   n          18 54
```

▶ Question **13.6.4.** What features drive the classification?
▶ Answer **13.6.4.**

```
coefs = coef(glmfit)[, which.min(abs(glmfit$lambda - s0))]
topthree = order(abs(coefs), decreasing = TRUE)[1:3]
as.vector(coefs[topthree])

## [1] -28.629194  -4.486355  -1.095961

formatfn(names(coefs)[topthree])

## [[1]]
## [1] "k__Bacteria| p__Candidatus_Saccharibacteria|"
## [2] "c__Candidatus_Saccharibacteria_noname|"
## [3] "o__Candidatus_Saccharibacteria_noname|"
## [4] "f__Candidatus_Saccharibacteria_noname|"
## [5] "g__Candidatus_Saccharibacteria_noname|"
## [6] "s__candidate_division_TM7_single_cell_isolate_TM7b"
##
## [[2]]
## [1] "k__Bacteria| p__Firmicutes| c__Clostridia| o__Clostridiales|"
## [2] "f__Ruminococcaceae| g__Subdoligranulum|"
## [3] "s__Subdoligranulum_variabile"
##
## [[3]]
## [1] "k__Bacteria| p__Firmicutes| c__Clostridia| o__Clostridiales|"
## [2] "f__Lachnospiraceae| g__Lachnospiraceae_noname|"
## [3] "s__Lachnospiraceae_bacterium_7_1_58FAA"
```

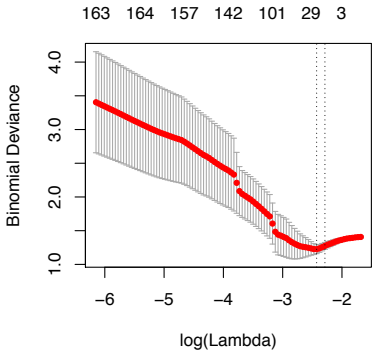

Figure 13.21: Diagnostic plot for `cv.glmnet`: shown is a measure of cross-validated prediction performance, the deviance, as a function of λ. The dashed vertical lines show `lambda.min` and `lambda.1se`.

▶ Question **13.6.5.** How do the results change if we transform the data, say, with the `asinh` transformation as we saw in Chapter 5?

▶ Answer **13.6.5.** See Figure 13.22.

```
cv.glmnet(x = t(asinh(exprs(zellerNC))),
          y = factor(zellerNC$disease),
          family = "binomial") %>% plot
```

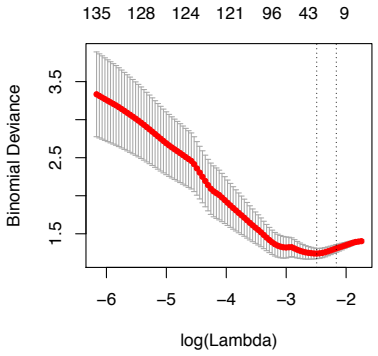

Figure 13.22: like Figure 13.21, but using an asinh transformation of the data.

▶ Question **13.6.6.** Would a good classification performance on these data mean that this assay is ready for screening and early cancer detection?

▶ Answer **13.6.6.** No. The performance here is measured on a set of samples in which the cases have similar prevalence as the controls. This serves well enough to explore the biology. However, in a real-life application, the cases will be much less frequent. To be practically useful, the assay must have a much higher specificity, i. e., not wrongly diagnose disease where there is none. To establish specificity, a much larger set of normal samples need to be tested.

13.6.3 Example: classifying mouse cells from their expression profiles

Figures 13.21 and 13.22 are textbook examples of how we expect the dependence of (cross-validated) classification performance versus model complexity (λ) to look. Now let's get back to the mouse embryo cells data. We'll try to classify the cells from embryonic day E3.25 with respect to their genotype.

```
sx = x[, x$Embryonic.day == "E3.25"]
embryoCellsClassifier = cv.glmnet(t(exprs(sx)), sx$genotype,
                family = "binomial", type.measure = "class")
plot(embryoCellsClassifier)
```

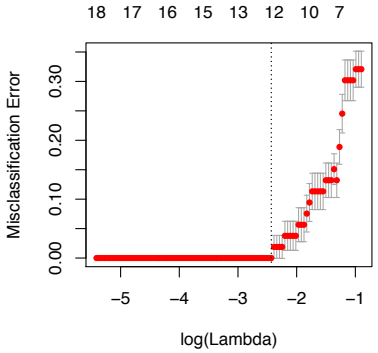

Figure 13.23: Cross-validated misclassification error versus penalty parameter for the mouse cells data.

In Figure 13.23 we see that the misclassification error is (essentially) monotonously increasing with λ, and is smallest for $\lambda \to 0$, i. e., if we apply no penalization at all.

▶ Question **13.6.7.** What is going on with these data?

▶ Answer **13.6.7.** It looks that inclusion of more, and even of all features, does not harm the classification performance. In a way, these data are "too easy". Let's do a t-test for all features:

```
mouse_de = rowttests(sx, "genotype")
ggplot(mouse_de, aes(x = p.value)) +
  geom_histogram(boundary = 0, breaks = seq(0, 1, by = 0.01))
```

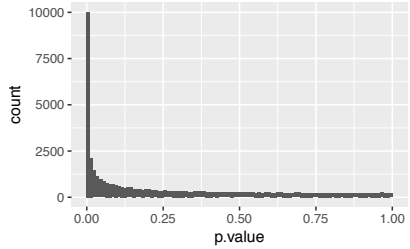

Figure 13.24: Histogram of p-values for the per-feature t-tests between genotypes in the E3.25 samples.

The result, shown in Figure 13.24, shows that large number of genes are differentially expressed, and thus informative for the class distinction. We can also compute the pairwise distances between all samples, using all features.

```
dists = as.matrix(dist(scale(t(exprs(x)))))
diag(dists) = +Inf
```

and then for each sample determine the class of its nearest neighbor

```
nn = sapply(seq_len(ncol(dists)), function(i) which.min(dists[, i]))
table(x$sampleGroup, x$sampleGroup[nn]) %>% `colnames<-`(NULL)
```

```
##
##                  [,1] [,2] [,3] [,4] [,5] [,6] [,7] [,8]
##   E3.25            33    0    0    0    3    0    0    0
##   E3.25 (FGF4-KO)   1   15    0    1    0    0    0    0
##   E3.5 (EPI)        2    0    3    0    6    0    0    0
##   E3.5 (FGF4-KO)    0    0    0    8    0    0    0    0
##   E3.5 (PE)         0    0    0    0   11    0    0    0
##   E4.5 (EPI)        0    0    0    0    2    2    0    0
##   E4.5 (FGF4-KO)    1    0    0    0    0    0    9    0
##   E4.5 (PE)         0    0    0    0    2    0    0    2
```

Using all features, the nearest neighbour classifier is correct in almost all cases, including for the E3.25 wildtype vs FGF4-KO distinction. This means that for these data, there is no apparent benefit in regularisation or feature selection. Limitations of using all features might become apparent with truly new data, but that is out of reach for cross-validation.

13.7 A large choice of methods

We have now seen three classification methods: linear discriminant analysis (`lda`), quadratic discriminant analysis (`qda`) and the elastic net (`glmnet`). In fact, there are hundreds of different learning algorithms[18] available in R and its add-on packages. You can get an overview in the CRAN task view Machine Learning & Statistical Learning. Some examples are:

[18] For an introduction to the subject that uses R and provides many examples and exercises, we recommend (James et al., 2013).

- Support vector machines: the function `svm` in the package *e1071*; `ksvm` in *kernlab*
- Tree based methods in the packages *rpart*, *tree*, *randomForest*
- Boosting methods: the functions `glmboost` and `gamboost` in package *mboost*
- `PenalizedLDA` in the package *PenalizedLDA*, `dudi.discr` and `dist.pcaiv` in *ade4*).

The complexity and heterogeneity of choices of learning strategies, tuning parameters and evaluation criteria in each of these packages can be confusing. You will already have noted differences in the interfaces of the `lda`, `qda` and `glmnet` functions, i. e., in how they expect their input data to presented and what they return. There is even greater diversity across all the other packages and functions. At the same time, there are common tasks such as cross-validation, parameter tuning and performance assessment that are more or less the same no matter what specific method is used. As you have seen, e. g., in our `estimate_mcl_loocv` function, the looping and data shuffling involved leads to rather verbose code.

So what to do if you want to try out and explore different learning algorithms? Fortunately, there are several projects that provide unified interfaces to the large number of different machine learning interfaces in R, and also try to provide "best practice" implementations of the common tasks such as parameter tuning and performance assessment. The two most well-known ones are the packages *caret* and *mlr*.

Here were have a look at *caret*. You can get a list of supported methods through its `getModelInfo` function. There are quite a few, here we just show the first 8.

```
library("caret")
caretMethods = names(getModelInfo())
head(caretMethods, 8)
```

```
## [1] "ada"         "AdaBag"      "AdaBoost.M1" "adaboost"
## [5] "amdai"       "ANFIS"       "avNNet"      "awnb"
```

```
length(caretMethods)
```

```
## [1] 232
```

We will check out a neural network method, the `nnet` function from the eponymous package. The `parameter` slot informs us on the the available tuning parameters[19].

[19] They are described in the manual of the `nnet` function.

```
getModelInfo("nnet", regex = FALSE)[[1]]$parameter
```

```
##   parameter   class         label
## 1      size numeric #Hidden Units
## 2     decay numeric  Weight Decay
```

Let's try it out.

```
trnCtrl = trainControl(
  method = "repeatedcv",
  repeats = 3,
  classProbs = TRUE)

tuneGrid = expand.grid(
  size = c(2, 4, 8),
  decay = c(0, 1e-2, 1e-1))

nnfit = train(
  Embryonic.day ~ Fn1 + Timd2 + Gata4 + Sox7,
  data = embryoCells,
  method = "nnet",
  tuneGrid  = tuneGrid,
  trControl = trnCtrl,
  metric = "Accuracy")
```

That's quite a mouthful, but the nice thing is that this syntax is standardized and applies across many different methods. All you need to do specify the name of the method and the grid of tuning parameters that should be explored via the `tuneGrid` argument.

Now we can have a look at the output (Figure 13.25).

```
nnfit
```

```
## Neural Network
##
## 66 samples
##  4 predictor
```

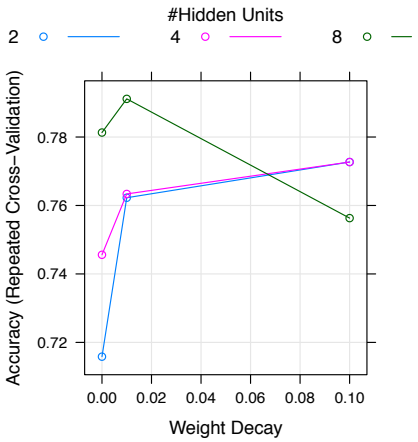

Figure 13.25: Parameter tuning of the neural net by cross-validation.

```
##  3 classes: 'E3.25', 'E3.5', 'E4.5'
##
## No pre-processing
## Resampling: Cross-Validated (10 fold, repeated 3 times)
## Summary of sample sizes: 59, 59, 59, 59, 60, 60, ...
## Resampling results across tuning parameters:
##
##   size  decay  Accuracy   Kappa
##   2     0.00   0.7158333  0.4270723
##   2     0.01   0.7622619  0.5710980
##   2     0.10   0.7726984  0.5926065
##   4     0.00   0.7455952  0.5284067
##   4     0.01   0.7633730  0.5902138
##   4     0.10   0.7726984  0.5919238
##   8     0.00   0.7813095  0.6169179
##   8     0.01   0.7911508  0.6257162
##   8     0.10   0.7563095  0.5595771
##
## Accuracy was used to select the optimal model using  the
##  largest value.
## The final values used for the model were size = 8 and decay = 0.01.
```

```
plot(nnfit)
predict(nnfit) %>% head(10)
```

```
##  [1] E3.25 E3.25 E3.25 E3.25 E3.25 E3.25 E3.25 E3.25 E3.25 E3.25
## Levels: E3.25 E3.5 E4.5
```

▶ Question **13.7.1.** Will the accuracy that we obtained above for the optimal tuning parameters generalize to a new dataset? What could you do to address that?

▶ Answer **13.7.1.** No, it is likely to be too optimistic, as we have picked the optimum. To get a somewhat more realistic estimate of prediction performance when generalized, we could formalize (into computer code) all our data preprocessing choices and the above parameter tuning procedure, and embed this in another, outer cross-validation loop (Ambroise and McLachlan, 2002). However, this is likely still not enough, as we discuss in the next section.

13.7.1 Method hacking

In Chapter 6 we encountered **p-value hacking**. A similar phenomenon exists in statistical learning: given a dataset, we explore various different methods of preprocessing (such as normalization, outlier detection, transformation, feature selection), try out different machine learning algorithms and tune their parameters until we are content with the result. The measured accuracy is likely to be too optimistic, i. e., will not generalize to a new dataset. Embedding as many of our methodical choices into a computational formalism and having an outer cross-validation loop (not to be confused with the inner loop that does the parameter tuning) will ameliorate the problem. But is unlikely to address it completely, since not all our choices can be formalized.

The gold standard remains validation on truly unseen data. In addition, it is never a bad thing if the classifier is not a black box but can be interpreted in terms of domain knowledge. Finally, report not just summary statistics, such as misclassification rates, but lay open the complete computational workflow, so that anyone (including your future self) can convince themselves of the robustness of the result or of the influence of the preprocessing, model selection and tuning choices (Holmes, 2016).

Exercises

▶ Exercise **13.1.** Apply a kernel support vector machine, available in the *kernlab* package, to the `zeller` microbiome data. What kernel function is best?

▶ Exercise **13.2.** It has been quipped that all classification methods are just refinements of two archetypal ideas: discriminant analysis and k nearest neighbors. In what sense might that be a useful classification?

▶ Answer **13.1.** In linear discriminant analysis, we consider our objects as elements of $\mathbb{R}^p$, and the learning task is to define regions in this space, or boundary hyperplanes between them, which we use to predict the class membership of new objects. This is archetypal for **classification by partition**. Generalizations of linear discriminant analysis permit more general spaces and more general boundary shapes.

In k nearest neighbors, no embedding into a coordinate space is needed, but instead we require a distance (or dissimilarity) measure that can be computed between each pair of objects, and the classification decision for a new object depends on its distances to the training objects and their classes. This is archetypal for **kernel-based** methods.

▶ Exercise **13.3.** Use `glmnet` for a prediction of a continous variable, i.e., for regression. Explore the effects of using ridge versus lasso penalty.

▶ Answer **13.2.** There are infinitely many possibilities here. For instance, you could explore the prostate cancer data as in Chapter 3 of (Hastie et al., 2008); the data are available in the CRAN package *ElemStatLearn*.

▶ Exercise **13.4.** Consider smoothing as a regression and model selection problem. What is the equivalent quantity to the penalization parameter λ in Equation (13.8)? How do you choose it?

▶ Answer **13.3.** We refer to Chapter 5 of (Hastie et al., 2008)

▶ Exercise **13.5.** **Scale invariance.** Consider a rescaling of one of the features in the (generalized) linear model (13.7). For instance, denote the ν-th column of x by $x_{\cdot\nu}$, and suppose that $p \geq 2$ and that we rescale $x_{\cdot\nu} \mapsto s\, x_{\cdot\nu}$ with some number $s \neq 0$. What will happen to the estimate $\hat{\beta}$ from Equation (13.8) in (a) the unpenalized case ($\lambda = 0$) and (b) the penalized case ($\lambda > 0$)?

▶ Answer **13.4.** In the unpenalized case, the estimates will be scaled by $1/s$, so that the resulting model is, in effect, the same. In the penalized case, the penalty from the ν-th component of β will be different. If $|s| > 1$, the amplitude of the feature is increased, smaller β-components are required for it to have the same effect in the prediction, and therefore the feature is more likely to receive a non-zero and/or

larger estimate, possibly on the cost of the other features; conversely for $|s| < 1$.

Bibliography

Christophe Ambroise and Geoffrey J. McLachlan. Selection bias in gene extraction on the basis of microarray gene-expression data. **PNAS**, 99(10):6562–6566, 2002.

S. Anders, A. Reyes, and W. Huber. Detecting differential usage of exons from RNA-seq data. **Genome Research**, 22(10):2008–2017, 2012.

Simon Anders and Wolfgang Huber. Differential expression analysis for sequence count data. **Genome Biology**, 11:R106, 2010. URL `http://genomebiology.com/2010/11/10/R106`.

Francis J Anscombe. The transformation of poisson, binomial and negative-binomial data. **Biometrika**, pages 246–254, 1948.

Paul L Auer and RW Doerge. Statistical design and analysis of RNA sequencing data. **Genetics**, 185(2):405–416, 2010.

Rhonda Bacher and Christina Kendziorski. Design and computational analysis of single-cell rna-sequencing experiments. **Genome Biology**, 17(1):1, 2016.

A. Baddeley, J. Moller, and R. Waagepetersen. Non- and semiparametric estimation of interaction in inhomogeneous point patterns. **Statistica Neerlandica**, 54:329–350, 2000.

A.J. Baddeley. Spatial sampling and censoring. In O.E. Barndorff-Nielsen, W.S. Kendall, and M.N.M. van Lieshout, editors, **Stochastic Geometry: Likelihood and Computation**, pages 37–78. Chapman and Hall, 1998.

Daniela Beisser, Gunnar W Klau, Thomas Dandekar, Tobias Müller, and Marcus T Dittrich. BioNet: an R-package for the functional analysis of biological networks. **Bioinformatics**, 26(8):1129–1130, 2010.

Mikhail Belkin and Partha Niyogi. Laplacian eigenmaps for dimensionality reduction and data representation. **Neural computation**, 15(6):1373–1396, 2003.

Richard Ernest Bellman. **Adaptive control processes: a guided tour**. Princeton University Press, 1961.

Sean C Bendall, Garry P Nolan, Mario Roederer, and Pratip K Chattopadhyay. A deep profiler's guide to cytometry. **Trends in immunology**, 33(7):323–332, 2012.

Yoshua Bengio, Jean-François Paiement, Pascal Vincent, Olivier Delalleau, Nicolas Le Roux, and Marie Ouimet. Out-of-sample extensions for lle, isomap, mds, eigenmaps, and spectral clustering. **Advances in neural information processing systems**, 16:177–184, 2004.

Y. Benjamini and Y. Hochberg. Controlling the false discovery rate: a practical and powerful approach to multiple testing. **Journal of the Royal Statistical Society B**, 57:289–300, 1995.

Yoav Benjamini and Marina Bogomolov. Selective inference on multiple families of hypotheses. **Journal of the Royal Statistical Society: Series B (Statistical Methodology)**, 76(1):297–318, 2014.

Yoav Benjamini and Daniel Yekutieli. Hierarchical fdr testing of trees of hypotheses. Technical report, Technical report, Department of Statistics and Operations Research, Tel Aviv University, 2003.

M. V. Boland and R. F. Murphy. A neural network classifier capable of recognizing the patterns of all major subcellular structures in fluorescence microscope images of HeLa cells. **Bioinformatics**, 17(12):1213–1223, 2001.

Remco Bouckaert, Joseph Heled, Denise Kühnert, Tim Vaughan, Chieh-Hsi Wu, Dong Xie, Marc A Suchard, Andrew Rambaut, and Alexei J Drummond. BEAST 2: a software platform for bayesian evolutionary analysis. **PLoS Comput Biol**, 10(4):e1003537, 2014.

Richard Bourgon, Robert Gentleman, and Wolfgang Huber. Independent filtering increases detection power for high-throughput experiments. **PNAS**, 107(21):9546–9551, 2010. URL `http://www.pnas.org/content/107/21/9546.long`.

George EP Box, William G Hunter, and J Stuart Hunter. **Statistics for experimenters: an introduction to design, data analysis, and model building**. John Wiley & Sons, 1978.

Eoin L Brodie, Todd Z DeSantis, Dominique C Joyner, Seung M Baek, Joern T Larsen, Gary L Andersen, Terry C Hazen, Paul M Richardson, Donald J Herman, TK Tokunaga, JM Wan, and MK Firestone. Application of a high-density oligonucleotide microarray approach to study bacterial population dynamics during uranium reduction and reoxidation. **Applied and Environmental Microbiology**, 72(9):6288–6298, 2006.

A. N. Brooks, L. Yang, M. O. Duff, K. D. Hansen, J. W. Park, S. Dudoit, S. E. Brenner, and B. R. Graveley. Conservation of an RNA regulatory map between Drosophila and mammals. **Genome Research**, pages 193–202, 2011. ISSN 1088-9051. doi: 10.1101/gr.108662.110. URL `http://genome.cshlp.org/cgi/doi/10.1101/gr.108662.110`.

Michael George Bulmer. **Francis Galton: pioneer of heredity and biometry**. JHU Press, 2003.

Benjamin Callahan, Diana Proctor, David Relman, Julia Fukuyama, and Susan Holmes. Reproducible research workflow in R for the analysis of personalized human microbiome data. In **Pacific Symposium on Biocomputing**, volume 21, page 183. NIH Public Access, 2016a.

Benjamin J Callahan, Paul J McMurdie, Michael J Rosen, Andrew W Han, Amy J Johnson, and Susan P Holmes. DADA2: High resolution sample inference from amplicon data. **Nature Methods**, pages 1–4, 2016b.

C Cannings and AWF Edwards. Natural selection and the de finetti diagram. **Annals of human genetics**, 31(4):421–428, 1968.

J.G. Caporaso, J. Kuczynski, J. Stombaugh, K. Bittinger, F.D. Bushman, E.K. Costello, N. Fierer, A.G. Peña, J.K. Goodrich, J.I. Gordon, and R. Knight. Qiime allows analysis of high-throughput community sequencing data. **Nature methods**, 7(5):335–336, 2010.

J.G. Caporaso, C.L. Lauber, W.A. Walters, D. Berg-Lyons, C.A. Lozupone, P.J. Turnbaugh, N. Fierer, and R. Knight. Global patterns of 16s rrna diversity at a depth of millions of sequences per sample. **PNAS**, 108(Supplement 1):4516–4522, 2011.

A.E. Carpenter, T.R. Jones, M.R. Lamprecht, C. Clarke, I.H. Kang, O. Friman, D.A. Guertin, J.H. Chang, R.A. Lindquist, J. Moffat, et al. CellProfiler: image analysis software for identifying and quantifying cell phenotypes. **Genome Biology**, 7:R100, 2006.

Daniel B Carr, Richard J Littlefield, WL Nicholson, and JS Littlefield. Scatterplot matrix techniques for large N. **Journal of the American Statistical Association**, 82(398):424–436, 1987.

Ron Caspi, Tomer Altman, Joseph M Dale, Kate Dreher, Carol A Fulcher, Fred Gilham, Pallavi Kaipa, Athikkattuvalasu S Karthikeyan, Anamika Kothari, Markus Krummenacker, et al. The metacyc database of metabolic pathways and enzymes and the biocyc collection of pathway/genome databases. **Nucleic acids research**, 38(suppl 1):D473–D479, 2010.

John Chakerian and Susan Holmes. Computational tools for evaluating phylogenetic and hierarchical clustering trees. **Journal of Computational and Graphical Statistics**, 21(3):581–599, 2012.

Min Chen, Yang Xie, and Michael Story. An exponential-gamma convolution model for background correction of illumina beadarray data. **Communications in Statistics-Theory and Methods**, 40(17):3055–3069, 2011.

Sung Nok Chiu, Dietrich Stoyan, Wilfrid S. Kendall, and Joseph Mecke. **Stochastic geometry and its applications**. Springer, 2013.

Line Clemmensen, Trevor Hastie, Daniela Witten, and Bjarne Ersbøll. Sparse discriminant analysis. **Technometrics**, 53:406–413, 2011.

W. S. Cleveland, M. E. McGill, and R. McGill. The shape parameter of a two-variable graph. **Journal of the American Statistical Association**, 83:289–300, 1988.

William S Cleveland. **The Collected Works of John W. Tukey: Graphics 1965-1985**, volume 5. CRC Press, 1988.

J.R. Cole, Q. Wang, E. Cardenas, J. Fish, B. Chai, R.J. Farris, A.S. Kulam-Syed-Mohideen, D.M. McGarrell, T. Marsh, G.M. Garrity, and J.M. Tiedje. The ribosomal database project: improved alignments and new tools for rrna analysis. **Nucleic acids research**, 37 (Supplement 1):D141–D145, 2009.

1000 Genomes Project Consortium. An integrated map of genetic variation from 1,092 human genomes. **Nature**, 491(7422):56–65, 2012.

R. Dennis Cook. Detection of Influential Observation in Linear Regression. **Technometrics**, February 1977.

N.A.C. Cressie. **Statistics for spatial data**. John Wiley and Sons, 1991.

Fabrice de Chaumont, Stéphane Dallongeville, Nicolas Chenouard, Nicolas Hervé, Sorin Pop, Thomas Provoost, Vannary Meas-Yedid, Praveen Pankajakshan, Timothé Lecomte, Yoann Le Montagner, Thibault Lagache, Alexandre Dufour, and Jean-Christophe Olivo-Marin. Icy: an open bioimage informatics platform for extended reproducible research. **Nature Methods**, 9:690–696, 2012.

Bruno DeFinetti. Considerazioni matematiche sull'ereditarieta mendeliana. **Metron**, 6:3–41, 1926.

T. Z. DeSantis, P. Hugenholtz, N. Larsen, M. Rojas, E. L. Brodie, K. Keller, T. Huber, D. Dalevi, P. Hu, and G. L. Andersen. Greengenes, a Chimera-Checked 16S rRNA Gene Database and Workbench Compatible with ARB. **Appl. Environ. Microbiol.**, 72(7):5069–5072, 2006. doi: 10.1128/AEM.03006-05. URL `http://aem.asm.org/cgi/content/abstract/72/7/5069`.

Persi Diaconis and David Freedman. Finite exchangeable sequences. **The Annals of Probability**, pages 745–764, 1980.

Persi Diaconis and Susan Holmes. Gray codes for randomization procedures. **Statistics and Computing**, 4(4):287–302, 1994.

Persi Diaconis, Susan Holmes, and Richard Montgomery. Dynamical bias in the coin toss. **SIAM review**, 49(2):211–235, 2007.

Edwin Diday and M Paula Brito. Symbolic cluster analysis. In **Conceptual and Numerical Analysis of Data**, pages 45–84. Springer, 1989.

P.J. Diggle. **Statistical analysis of spatial point patterns**. Academic Press, 1983.

Daniel B. DiGiulioa, Benjamin J. Callahan, Paul J. McMurdie, Elizabeth K. Costello, Deirdre J. Lyelle, Anna Robaczewskaa, Christine L. Sun, Daniela S. Aliaga-Goltsman, Ronald J. Wongand Gary M. Shaw, David K. Stevenson, Susan P. Holmes, and David A. Relman. Temporal and spatial variation of the human microbiota during pregnancy. **PNAS**, 2015.

Murat Dundar, Ferit Akova, Halid Z. Yerebakan, and Bartek Rajwa. A non-parametric bayesian model for joint cell clustering and cluster matching: identification of anomalous sample phenotypes with random effects. **BMC Bioinformatics**, 15(1):1–15, 2014. ISSN 1471-2105. doi: 10.1186/1471-2105-15-314. URL `http://dx.doi.org/10.1186/1471-2105-15-314`.

Richard Durbin, Sean Eddy, Anders Krogh, and Graeme Mitchison. **Biological Sequence Analysis**. Cambridge University Press, 1998.

R.C. Edgar and H. Flyvbjerg. Error filtering, pair assembly and error correction for next-generation sequencing reads. **Bioinformatics**, 31(21):3476–3482, 2015.

Bradley Efron. **Large-scale inference: empirical Bayes methods for estimation, testing, and prediction**, volume 1. Cambridge University Press, 2010.

Bradley Efron and Robert J Tibshirani. **An introduction to the bootstrap**. CRC press, 1994.

D Elson and E Chargaff. On the desoxyribonucleic acid content of sea urchin gametes. **Experientia**, 8(4):143–145, 1952.

Steven N Evans and Frederick A Matsen. The phylogenetic Kantorovich–Rubinstein metric for environmental sequence samples. **Journal of the Royal Statistical Society: Series B (Statistical Methodology)**, 74(3):569–592, 2012.

Ronald Aylmer Fisher. **The design of experiments**. Oliver & Boyd, 1935.

Bernard Flury. **A first course in multivariate statistics**. Springer, 1997.

David A Freedman. Statistical models and shoe leather. **Sociological methodology**, 21(2):291–313, 1991.

Jerome H Friedman. On bias, variance, 0/1âĂŤloss, and the curse-of-dimensionality. **Data Mining and Knowledge Discovery**, 1: 55–77, 1997.

Jerome H Friedman and Lawrence C Rafsky. Multivariate generalizations of the wald-wolfowitz and smirnov two-sample tests. **The Annals of Statistics**, pages 697–717, 1979.

Julia Fukuyama, Paul J McMurdie, Les Dethlefsen, David A Relman, and Susan Holmes. Comparisons of distance methods for combining covariates and abundances in microbiome studies. In **Pac Symp Biocomput**. World Scientific, 2012.

Robert C Gentleman, Vincent J Carey, Douglas M Bates, Ben Bolstad, Marcel Dettling, Sandrine Dudoit, Byron Ellis, Laurent Gautier, Yongchao Ge, Jeff Gentry, Kurt Hornik, Torsten Hothorn, Wolfgang Huber, Stefano Iacus, Rafael Irizarry, Friedrich Leisch, Cheng Li, Martin Maechler, Anthony J Rossini, Gunther Sawitzki, Colin Smith, Gordon Smyth, Luke Tierney, Jean Y H Yang, and Jianhua Zhang. Bioconductor: open software development for computational biology and bioinformatics. **Genome Biology**, 5(10):R80, Jan 2004. doi: 10.1186/gb-2004-5-10-r80. URL `http://genomebiology.com/2004/5/10/R80`.

Yoav Gilad and Orna Mizrahi-Man. A reanalysis of mouse encode comparative gene expression data. **F1000Research**, 4, 2015.

David J Glass. **Experimental design for biologists**. Cold Spring Harbor Laboratory Press, 2007.

Anastassia Gorvitovskaia, Susan P Holmes, and Susan M Huse. Interpreting prevotella and bacteroides as biomarkers of diet and lifestyle. **Microbiome**, 4(1):1, 2016.

R_ Grantham, Christian Gautier, Manolo Gouy, M Jacobzone, and R Mercier. Codon catalog usage is a genome strategy modulated for gene expressivity. **Nucleic acids research**, 9(1):213–213, 1981.

M.J. Greenacre. **Correspondence analysis in practice**. Chapman & Hall, 2007.

Bettina Grun, Theresa Scharl, and Friedrich Leisch. Modelling time course gene expression data with finite mixtures of linear additive models. **Bioinformatics**, 28(2):222–228, 2012. doi: 10.1093/bioinformatics/btr653. URL `http://bioinformatics.oxfordjournals.org/content/28/2/222.abstract`.

Alon Halevy, Peter Norvig, and Fernando Pereira. The unreasonable effectiveness of data. **Intelligent Systems, IEEE**, 24(2):8–12, 2009.

Robin M Hallett, Anna Dvorkin-Gheva, Anita Bane, and John A Hassell. A gene signature for predicting outcome in patients with basal-like breast cancer. **Scientific reports**, 2, 2012.

Trevor Hastie and Werner Stuetzle. Principal curves. **Journal of the American Statistical Association**, 84(406):502–516, 1989.

Trevor Hastie, Robert Tibshirani, and Jerome Friedman. **The Elements of Statistical Learning**. Springer, 2nd edition, 2008.

Megan L Head, Luke Holman, Rob Lanfear, Andrew T Kahn, and Michael D Jennions. The extent and consequences of p-hacking in science. **PLoS Biol**, 13(3):e1002106, 2015.

M. Held, M.H.A. Schmitz, B. Fischer, T. Walter, B. Neumann, M.H. Olma, M. Peter, J. Ellenberg, and D.W. Gerlich. CellCognition: time-resolved phenotype annotation in high-throughput live cell imaging. **Nature Methods**, 7:747, 2010.

F. Henderson. Software Engineering at Google. **ArXiv e-prints**, 2017.

Jennifer A Hoeting, David Madigan, Adrian E Raftery, and Chris T Volinsky. Bayesian model averaging: a tutorial. **Statistical science**, pages 382–401, 1999.

S. Holmes. Statistics for phylogenetic trees. **Theoretical population biology**, 63(1):17–32, 2003. ISSN 0040-5809.

Susan Holmes. Phylogenetic trees: an overview. In **Statistics and Genetics**, number 112, pages 81–118. Springer, IMA, New York, 1999.

Susan Holmes. Multivariate analysis: The French way. In D. Nolan and T. P. Speed, editors, **Probability and Statistics: Essays in Honor of David A. Freedman**, volume 56 of **IMS Lecture Notes–Monograph Series**. IMS, Beachwood, OH, 2006. URL `http://www.imstat.org/publications/lecnotes.htm`.

Susan Holmes. Statistical proof? the problem of irreproducibility. **Bulletin AMS**, ???:???, 2016.

Susan Holmes, Michael He, Tong Xu, and Peter P Lee. Memory t cells have gene expression patterns intermediate between naive and effector. **PNAS**, 102(15):5519–5523, 2005.

Susan Holmes, Alexander Alekseyenko, Alden Timme, Tyrell Nelson, P.J. Pasricha, and Alfred Spormann. Visualization and statistical comparisons of microbial communities using R packages on Phylochip data. In **Pacific Symposium on Biocomputing**, page 142, 2011a.

Susan Holmes, Alexander V Alekseyenko, Alden Timme, Tyrrell Nelson, Pankaj Jay Pasricha, and Alfred Spormann. Visualization and statistical comparisons of microbial communities using r packages on phylochip data. In **Pacific Symposium on Biocomputing**, pages 142–153. World Scientific, 2011b.

Susan Holmes Junca. **Outils informatiques pour l'évaluation de la pertinence d'un résultat en analyse des données**. PhD thesis, Université Montpellier II, France, 1985. Diss.

Kurt Hornik. A CLUE for CLUster Ensembles. **Journal of Statistical Software**, 14(12), 2005.

H Hotelling. Analysis of a complex of statistical variables into principal components. **Journal of Educational Psychology**, 24(6): 417–441, 1933.

Harold Hotelling. Some improvements in weighing and other experimental techniques. **The Annals of Mathematical Statistics**, 15 (3):297–306, 1944.

Peter J. Huber. Robust estimation of a location parameter. **The Annals of Mathematical Statistics**, 35:73–101, 1964.

Wolfgang Huber, Vincent J Carey, Robert Gentleman, Simon Anders, Marc Carlson, Benilton S Carvalho, Hector Corrada Bravo, Sean Davis, Laurent Gatto, Thomas Girke, Raphael Gottardo, Florian Hahne, Kasper D Hansen, Rafael A Irizarry, Michael Lawrence, Michael I Love, James MacDonald, Valerie Obenchain, Andrzej K Oleś, Hervé Pagès, Alejandro Reyes, Paul Shannon, Gordon K Smyth, Dan Tenenbaum, Levi Waldron, and Martin Morgan. Orchestrating high-throughput genomic analysis with bioconductor.

Nature Methods, 12(2):115–121, 2015.

Henry R Hulett, William A Bonner, Janet Barrett, and Leonard A Herzenberg. Cell sorting: automated separation of mammalian cells as a function of intracellular fluorescence. **Science**, 166(3906):747–749, 1969.

Trey Ideker, Owen Ozier, Benno Schwikowski, and Andrew F Siegel. Discovering regulatory and signalling circuits in molecular interaction networks. **Bioinformatics**, 18 Suppl 1:S233–40, Jan 2002. URL `http://bioinformatics.oxfordjournals.org/cgi/reprint/18/suppl_1/S233`.

Nikolaos Ignatiadis, Bernd Klaus, Judith Zaugg, and Wolfgang Huber. Data-driven hypothesis weighting increases detection power in genome-scale multiple testing. **Nature Methods**, 2016.

Ross Ihaka. Color for presentation graphics. In Kurt Hornik and Friedrich Leisch, editors, **Proceedings of the 3rd International Workshop on Distributed Statistical Computing**. ISSN 1609-395X, Vienna, Austria, 2003.

Ross Ihaka and Robert Gentleman. R: A language for data analysis and graphics. **Journal of Computational and Graphical Statistics**, 5(3):299–314, 1996.

R. A. Irizarry, B. Hobbs, F. Collin, Y. D. Beazer-Barclay, K. J. Antonellis, U. Scherf, and T. P. Speed. Exploration, normalization, and summaries of high density oligonucleotide array probe level data. **Biostatistics**, 4(2):249–264, 2003.

Rafael A Irizarry, Hao Wu, and Andrew P Feinberg. A species-generalized probabilistic model-based definition of cpg islands. **Mammalian Genome**, 20(9-10):674–680, 2009.

Alan Julian Izenman. **Nonlinear Dimensionality Reduction and Manifold Learning**, pages 597–632. Springer New York, New York, NY, 2008.

Laurent Jacob, Guillaume Obozinski, and Jean-Philippe Vert. Group lasso with overlap and graph lasso. In **Proceedings of the 26th Annual International Conference on Machine Learning**, pages 433–440. ACM, 2009.

Gareth James, Daniela Witten, Trevor Hastie, and Robert Tibshirani. **An introduction to statistical learning**. Springer, 2013.

Pierre Jolicoeur, James E Mosimann, et al. Size and shape variation in the painted turtle. a principal component analysis. **Growth**, 24 (4):339–354, 1960.

Ian Jolliffe. **Principal component analysis**. Wiley Online Library, 2002.

T. Jones, A. Carpenter, and P. Golland. Voronoi-based segmentation of cells on image manifolds. **Computer Vision for Biomedical Image Applications**, page 535, 2005.

Daniel Kahneman. **Thinking, fast and slow**. Macmillan, 2011.

Purna C Kashyap, Angela Marcobal, Luke K Ursell, Samuel A Smits, Erica D Sonnenburg, Elizabeth K Costello, Steven K Higginbottom, Steven E Domino, Susan P Holmes, David A Relman, J.I. Gordon, and J Sonnenburg. Genetically dictated change in host mucus carbohydrate landscape exerts a diet-dependent effect on the gut microbiota. **PNAS**, 110(42):17059–17064, 2013.

Leonard Kaufman and Peter J Rousseeuw. Partitioning around medoids (program pam). **Finding groups in data: an introduction to cluster analysis**, pages 68–125, 1990.

David Kendall. Incidence matrices, interval graphs and seriation in archeology. **Pacific Journal of mathematics**, 28(3):565–570, 1969.

DG Kendall. A mathematical approach to seriation. **Philosophical Transactions of the Royal Society of London. Series A, Mathematical and Physical Sciences**, 269(1193):125–134, 1970.

Marc Kéry and J Andrew Royle. **Applied Hierarchical Modeling in Ecology: Analysis of distribution, abundance and species richness in R and BUGS: Volume 1: Prelude and Static Models**. Academic Press, 2015.

Raffaella Koncan, Aránzazu Valverde, María-Isabel Morosini, María García-Castillo, Rafael Cantón, Giuseppe Cornaglia, Fernando Baquero, and Rosa del Campo. Learning from mistakes: Taq polymerase contaminated with β-lactamase sequences results in false emergence of streptococcus pneumoniae containing tem. **Journal of antimicrobial chemotherapy**, 60(3):702–703, 2007.

James J Kozich, Sarah L Westcott, Nielson T Baxter, Sarah K Highlander, and Patrick D Schloss. Development of a dual-index sequencing strategy and curation pipeline for analyzing amplicon sequence data on the miseq illumina sequencing platform. **Applied and environmental microbiology**, 79(17):5112–5120, 2013.

Erik Kristiansson, Michael Thorsen, Markus J Tamás, and Olle Nerman. Evolutionary forces act on promoter length: identification of enriched cis-regulatory elements. **Molecular biology and evolution**, 26(6):1299–1307, 2009.

Pei Fen Kuan, Dongjun Chung, Guangjin Pan, James A Thomson, Ron Stewart, and Sündüz Keleş. A statistical framework for the analysis of chip-seq data. **Journal of the American Statistical Association**, 106(495):891–903, 2011.

Kenneth Lange. **MM Optimization Algorithms**. SIAM, 2016.

Christina Laufer, Bernd Fischer, Maximilian Billmann, Wolfgang Huber, and Michael Boutros. Mapping genetic interactions in human cancer cells with RNAi and multiparametric phenotyping. **Nature Methods**, 10:427–431, 2013.

Joshua Lederberg and Alexa Mccray. 'Ome Sweet 'Omics– A Genealogical Treasury of Words. **The Scientist**, 17(7), April 2001. URL `http://www.the-scientist.com/article/display/12335/`.

J. T. Leek and J. D. Storey. Capturing heterogeneity in gene expression studies by surrogate variable analysis. **PLoS Genetics**, 3(9): 1724–1735, 2007.

Jeffrey T Leek, Robert B Scharpf, Héctor Corrada Bravo, David Simcha, Benjamin Langmead, W Evan Johnson, Donald Geman, Keith Baggerly, and Rafael A Irizarry. Tackling the widespread and critical impact of batch effects in high-throughput data. **Nature Reviews Genetics**, 11(10):733–739, 2010.

Wen-Hsiung Li. **Molecular evolution.** Sinauer Associates Incorporated, 1997.

Wen-Hsiung Li and Dan Graur. **Fundamentals of molecular evolution**, volume 48. Sinauer Associates Sunderland, MA, 1991.

Arthur Liberzon, Aravind Subramanian, Reid Pinchback, Helga Thorvaldsdóttir, Pablo Tamayo, and Jill P Mesirov. Molecular signatures database (msigdb) 3.0. **Bioinformatics**, 27(12):1739–1740, 2011.

Shin Lin, Yiing Lin, Joseph R Nery, Mark A Urich, Alessandra Breschi, Carrie A Davis, Alexander Dobin, Christopher Zaleski, Michael A Beer, William C Chapman, et al. Comparison of the transcriptional landscapes between human and mouse tissues. **PNAS**, 111(48): 17224–17229, 2014.

Michael I Love, Wolfgang Huber, and Simon Anders. Moderated estimation of fold change and dispersion for rna-seq data with deseq2. **Genome biology**, 15(12):1–21, 2014.

Michael I. Love, Simon Anders, Vladislav Kim, and Wolfgang Huber. Rna-seq workflow: gene-level exploratory analysis and differential expression. **F1000Research**, 4(1070), 2015. doi: 10.12688/f1000research.7035.1.

C.A. Lozupone, M. Hamady, S.T. Kelley, and R. Knight. Quantitative and qualitative {beta} diversity measures lead to different insights into factors that structure microbial communities. **Applied and environmental microbiology**, 73(5):1576, 2007.

Kanti Mardia, John T Kent, and John M Bibby. **Multiariate Analysis**. Academic Press, New York, 1979.

Jean-Michel Marin and Christian Robert. **Bayesian core: a practical approach to computational Bayesian statistics**. Springer Science & Business Media, 2007.

William T McCormick Jr, Paul J Schweitzer, and Thomas W White. Problem decomposition and data reorganization by a clustering technique. **Operations Research**, 20(5):993–1009, 1972.

Geoffrey McLachlan and Thriyambakam Krishnan. **The EM algorithm and extensions**, volume 382. John Wiley & Sons, 2007.

Geoffrey McLachlan and David Peel. **Finite mixture models**. John Wiley & Sons, 2004.

Paul J McMurdie and Susan Holmes. Waste not, want not: Why rarefying microbiome data is inadmissible. **PLoS Computational Biology**, 10(4):e1003531, 2014.

Paul J McMurdie and Susan Holmes. Shiny-phyloseq: Web application for interactive microbiome analysis with provenance tracking. **Bioinformatics**, 31(2):282–283, 2015.

Roger Mead. **The design of experiments: statistical principles for practical applications**. Cambridge University Press, 1990.

Victoria Moignard, Steven Woodhouse, Laleh Haghverdi, Andrew J Lilly, Yosuke Tanaka, Adam C Wilkinson, Florian Buettner, Iain C Macaulay, Wajid Jawaid, Evangelia Diamanti, Shin-Ichi Nishikawa, Nir Piterman, Valerie Kouskoff, Fabian J Theis, Jasmin Fisher, and Berthold Göttgens. Decoding the regulatory network of early blood development from single-cell gene expression measurements. **Nature biotechnology**, 2015.

J. Mollon. Seeing colour. In T. Lamb and J. Bourriau, editors, **Colour: Art and Science**. Cambridge Unversity Press, 1995.

Alexander M Mood. On hotelling's weighing problem. **The Annals of Mathematical Statistics**, pages 432–446, 1946.

AE Mourant, Ada Kopec, and K Domaniewska-Sobczak. The distribution of the human blood groups 2nd edition, 1976.

Daniel Müllner. fastcluster: Fast hierarchical, agglomerative clustering routines for r and python. **Journal of Statistical Software**, 53(9):1–18, 2013.

Serban Nacu, Rebecca Critchley-Thorne, Peter Lee, and Susan Holmes. Gene expression network analysis and applications to immunology. **Bioinformatics**, 23(7):850–8, Apr 2007. doi: 10.1093/bioinformatics/btm019. URL `http://bioinformatics.oxfordjournals.org/cgi/content/abstract/23/7/850`.

TA Nelson, S Holmes, AV Alekseyenko, M Shenoy, T Desantis, CH Wu, GL Andersen, J Winston, J Sonnenburg, PJ Pasricha, and A Spormann. Phylochip microarray analysis reveals altered gastrointestinal microbial communities in a rat model of colonic hypersensitivity. **Neurogastroenterology & Motility**, 23(2):169–e42, 2011.

B. Neumann, T. Walter, J. K. Heriche, J. Bulkescher, H. Erfle, C. Conrad, P. Rogers, I. Poser, M. Held, U. Liebel, C. Cetin, F. Sieckmann, G. Pau, R. Kabbe, A. Wunsche, V. Satagopam, M. H. Schmitz, C. Chapuis, D. W. Gerlich, R. Schneider, R. Eils, W. Huber, J. M. Peters, A. A. Hyman, R. Durbin, R. Pepperkok, and J. Ellenberg. Phenotypic profiling of the human genome by time-lapse microscopy reveals cell division genes. **Nature**, 464(7289):721–727, Apr 2010.

Jerzy Neyman and Egon S Pearson. **Sufficient statistics and uniformly most powerful tests of statistical hypotheses**. University California Press, 1936.

Ann L Oberg and Olga Vitek. Statistical design of quantitative mass spectrometry-based proteomic experiments. **Journal of proteome research**, 8(5):2144–2156, 2009.

Y. Ohnishi, W. Huber, A. Tsumura, M. Kang, P. Xenopoulos, K. Kurimoto, A. K. Oles, M. J. Arauzo-Bravo, M. Saitou, A. K. Hadjantonakis, and T. Hiiragi. Cell-to-cell expression variability followed by signal reinforcement progressively segregates early mouse lineages. **Nature Cell Biology**, 16(1):27–37, 2014.

Kieran O'Neill, Nima Aghaeepour, Josef Špidlen, and Ryan Brinkman. Flow cytometry bioinformatics. **PLoS Comput Biol**, 9(12): e1003365, 2013.

S original by Trevor Hastie R port by Andreas Weingessel <Andreas.Weingessel@ci.tuwien.ac.at>. **princurve: Fits a Principal Curve in Arbitrary Dimension**, 2013. URL `https://CRAN.R-project.org/package=princurve`. R package version 1.1-12.

F. Ozsolak and P. M. Milos. RNA sequencing: advances, challenges and opportunities. **Nature Reviews Genetics**, 12:87–98, 2011.

Emmanuel Paradis. **Analysis of Phylogenetics and Evolution with R**. Springer Science & Business Media, 2011.

Rob Patro, Stephen M Mount, and Carl Kingsford. Sailfish enables alignment-free isoform quantification from RNA-seq reads using lightweight algorithms. **Nature Biotechnology**, 32(5):462–464, 2014.

G. Pau, F. Fuchs, O. Sklyar, M. Boutros, and W. Huber. EBImage - an R package for image processing with applications to cellular phenotypes. **Bioinformatics**, 26:979, 2010.

Sandrine Pavoine, Anne-Béatrice Dufour, and Daniel Chessel. From dissimilarities among species to dissimilarities among communities: a double principal coordinate analysis. **Journal of theoretical biology**, 228(4):523–537, 2004.

Guy Perrière and Jean Thioulouse. Use and misuse of correspondence analysis in codon usage studies. **Nucleic Acids Research**, 30 (20):4548–4555, 2002.

Stan Pounds and Stephan W Morris. Estimating the occurrence of false positives and false negatives in microarray studies by approximating and partitioning the empirical distribution of p-values. **Bioinformatics**, 19(10):1236–1242, 2003.

IC Prentice. Non-metric ordination methods in ecology. **The Journal of Ecology**, pages 85–94, 1977.

Elmar Pruesse, Christian Quast, Katrin Knittel, Bernhard M Fuchs, Wolfgang Ludwig, Jörg Peplies, and Frank Oliver Glöckner. Silva: a comprehensive online resource for quality checked and aligned ribosomal rna sequence data compatible with arb. **Nucleic acids research**, 35(21):7188–7196, 2007.

Elizabeth Purdom. Analysis of a data matrix and a graph: Metagenomic data and the phylogenetic tree. **Annals of Applied Statistics**, Jul 2010.

Elizabeth Purdom and Susan P Holmes. Error distribution for gene expression data. **Statistical applications in genetics and molecular biology**, 4(1), 2005.

S. Rajaram, B. Pavie, L. F. Wu, and S. J. Altschuler. PhenoRipper: software for rapidly profiling microscopy images. **Nature Methods**, 9:635–637, 2012.

GM Reaven and RG Miller. An attempt to define the nature of chemical diabetes using a multidimensional analysis. **Diabetologia**, 16 (1):17–24, 1979.

Soo-Yon Rhee, Matthew J Gonzales, Rami Kantor, Bradley J Betts, Jaideep Ravela, and Robert W Shafer. Human immunodeficiency virus reverse transcriptase and protease sequence database. **Nucleic acids research**, 31(1):298–303, 2003.

John Rice. **Mathematical statistics and data analysis**. Cengage Learning, 2006.

B.D. Ripley. **Statistical inference for spatial processes.** Cambridge University Press, 1988.

Davide Risso, John Ngai, Terence P Speed, and Sandrine Dudoit. Normalization of rna-seq data using factor analysis of control genes or samples. **Nature biotechnology**, 32(9):896–902, 2014.

Christian Robert and George Casella. **Introducing Monte Carlo Methods with R**. Springer Science & Business Media, 2009a.

Christian Robert and George Casella. **Introducing Monte Carlo Methods with R**. Springer Science & Business Media, 2009b.

Garry Robins, Tom Snijders, Peng Wang, Mark Handcock, and Philippa Pattison. Recent developments in exponential random graph (p*) models for social networks. **Social networks**, 29(2):192–215, 2007.

David M Rocke and Blythe Durbin. A model for measurement error for gene expression arrays. **Journal of Computational Biology**, 8(6):557–569, 2001.

Fredrik Ronquist, Maxim Teslenko, Paul van der Mark, Daniel L Ayres, Aaron Darling, Sebastian Höhna, Bret Larget, Liang Liu, Marc A Suchard, and John P Huelsenbeck. Mrbayes 3.2: efficient bayesian phylogenetic inference and model choice across a large model space. **Systematic biology**, 61(3):539–542, 2012.

Michael J Rosen, Benjamin J Callahan, Daniel S Fisher, and Susan P Holmes. Denoising pcr-amplified metagenome data. **BMC Bioinformatics**, 13(1):283, 2012.

Peter J Rousseeuw. Silhouettes: a graphical aid to the interpretation and validation of cluster analysis. **Journal of computational and applied mathematics**, 20:53–65, 1987.

Sam T Roweis and Lawrence K Saul. Nonlinear dimensionality reduction by locally linear embedding. **Science**, 290(5500):2323–2326, 2000.

Kris Sankaran and Susan Holmes. structssi: Simultaneous and selective inference for grouped or hierarchically structured data. **Journal of Statistical Software**, 59(1):1–21, 2014.

Mark F Schilling. Multivariate two-sample tests based on nearest neighbors. **Journal of the American Statistical Association**, 81 (395):799–806, 1986.

Johannes Schindelin, Ignacio Arganda-Carreras, Erwin Frise, Verena Kaynig, Mark Longair, Tobias Pietzsch, Stephan Preibisch, Curtis Rueden, Stephan Saalfeld, Benjamin Schmid, Jean-Yves Tinevez, Daniel James White, Volker Hartenstein, Kevin Eliceiri, Pavel Tomancak, and Albert Cardona. Fiji: an open-source platform for biological-image analysis. **Nature Methods**, 9:676–682, 2012.

P D Schloss, S L Westcott, T Ryabin, J R Hall, M Hartmann, E B Hollister, R A Lesniewski, B B Oakley, D H Parks, C J Robinson, J W Sahl, B Stres, G G Thallinger, D J Van Horn, and C F Weber. Introducing mothur: Open-Source, Platform-Independent, Community-Supported Software for Describing and Comparing Microbial Communities. **Appl. and environmental microbiology**, 75(23): 7537–7541, November 2009.

P.D. Schloss, A.M. Schuber, J.P. Zackular, K.D. Iverson, Young V.B., and Petrosino J.F. Stabilization of the murine gut microbiome following weaning. **Gut microbes**, 3(4):383–393, 2012.

Bernhard Schölkopf, Koji Tsuda, and Jean-Philippe Vert. **Kernel methods in computational biology**. MIT press, 2004.

Stephen Senn. Controversies concerning randomization and additivity in clinical trials. **Statistics in medicine**, 23(24):3729–3753, 2004.

Jean Serra. **Image Analysis and Mathematical Morphology**. Academic Press, 1983.

A Francesca Setiadi, Nelson C Ray, Holbrook E Kohrt, Adam Kapelner, Valeria Carcamo-Cavazos, Edina B Levic, Sina Yadegarynia, Chris M Van Der Loos, Erich J Schwartz, Susan Holmes, and PP Lee. Quantitative, architectural analysis of immune cell subsets in tumor-draining lymph nodes from breast cancer patients and healthy lymph nodes. **PLoS One**, 5(8):e12420, 2010.

Cosma Shalizi. **Advanced Data Analysis from an Elementary Point of View**. Cambridge University Press, 2017. URL `https://www.stat.cmu.edu/~cshalizi/ADAfaEPoV/ADAfaEPoV.pdf`.

David Sims, Ian Sudbery, Nicholas E Ilott, Andreas Heger, and Chris P Ponting. Sequencing depth and coverage: key considerations in

genomic analyses. **Nature Reviews Genetics**, 15(2):121–132, 2014.

Charlotte Soneson, Michael I. Love, and Mark Robinson. Differential analyses for RNA-seq: transcript-level estimates improve gene-level inferences. **F1000Research**, 4(1521), 2015. doi: 10.12688/f1000research.7563.2.

O. Stegle, L. Parts, R. Durbin, and J. Winn. A Bayesian framework to account for complex non-genetic factors in gene expression levels greatly increases power in eQTL studies. **PLoS Computational Biology**, 6(5):e1000770, 2010.

T. Steijger, J. F. Abril, P. G. Engstrom, F. Kokocinski, T. J. Hubbard, R. Guigo, J. Harrow, P. Bertone, J. F. Abril, M. Akerman, T. Alioto, G. Ambrosini, S. E. Antonarakis, J. Behr, P. Bertone, R. Bohnert, P. Bucher, N. Cloonan, T. Derrien, S. Djebali, J. Du, S. Dudoit, P. Engstrom, M. Gerstein, T. R. Gingeras, D. Gonzalez, S. M. Grimmond, R. Guigo, L. Habegger, J. Harrow, T. J. Hubbard, C. Iseli, G. Jean, A. Kahles, F. Kokocinski, J. Lagarde, J. Leng, G. Lefebvre, S. Lewis, A. Mortazavi, P. Niermann, G. Ratsch, A. Reymond, P. Ribeca, H. Richard, J. Rougemont, J. Rozowsky, M. Sammeth, A. Sboner, M. H. Schulz, S. M. Searle, N. D. Solorzano, V. Solovyev, M. Stanke, T. Steijger, B. J. Stevenson, H. Stockinger, A. Valsesia, D. Weese, S. White, B. J. Wold, J. Wu, T. D. Wu, G. Zeller, D. Zerbino, and M. Q. Zhang. Assessment of transcript reconstruction methods for RNA-seq. **Nature Methods**, 10(12):1177–1184, 2013.

Stephen M Stigler. **The seven pillars of statistical wisdom**. Harvard University Press, 2016.

Gilbert Strang and Wellesley-Cambridge Press. **Introduction to linear algebra**, volume 3. Wellesley-Cambridge Press Wellesley, MA, 1993.

Joshua B Tenenbaum, Vin De Silva, and John C Langford. A global geometric framework for nonlinear dimensionality reduction. **science**, 290(5500):2319–2323, 2000.

Cajo ter Braak. Correspondence analysis of incidence and abundance data: Properties in terms of a unimodal respose. **Biometrics**, 41, Jan 1985.

Robert Tibshirani. Regression shrinkage and selection via the lasso. **Journal of the Royal Statistical Society. Series B (Methodological)**, pages 267–288, 1996.

Robert Tibshirani, Guenther Walther, and Trevor Hastie. Estimating the number of clusters in a data set via the gap statistic. **Journal of the Royal Statistical Society: Series B (Statistical Methodology)**, 63(2):411–423, 2001.

Michael W Trosset and Carey E Priebe. The out-of-sample problem for classical multidimensional scaling. **Computational statistics & data analysis**, 52(10):4635–4642, 2008.

George C Tseng and Wing H Wong. Tight clustering: A resampling-based approach for identifying stable and tight patterns in data. **Biometrics**, 61(1):10–16, 2005.

John W Tukey. Exploratory data analysis. **Massachusetts: Addison-Wesley**, 1977.

Amos Tversky and Daniel Kahneman. Heuristics and biases: Judgement under uncertainty. **Science**, 185:1124–1130, 1974.

Amos Tversky and Daniel Kahneman. Judgment under uncertainty: Heuristics and biases. In **Utility, probability, and human decision making**, pages 141–162. Springer, 1975.

Pierre-FranÃğois Verhulst. Recherches mathématiques sur la loi d'accroissement de la population. **Nouveaux Mémoires de l'Académie Royale des Sciences et Belles-Lettres de Bruxelles**, 18:1âĂŞ42, 1845.

Martin Vetterli, Jelena Kovačević, and Vivek Goyal. **Foundations of Signal Processing**. Cambridge University Press, 2014.

H. von Helmholtz. **Handbuch der Physiologischen Optik**. Leopold Voss, Leipzig, 1867.

Wencke Walter and Fatima Sanchez-Cabo. **GOplot: Visualization of Functional Analysis Data**, 2015. URL `https://CRAN`.

R-project.org/package=GOplot. R package version 1.0.1.

Q. Wang, G.M. Garrity, J.M. Tiedje, and J.R. Cole. Naive bayesian classifier for rapid assignment of rrna sequences into the new bacterial taxonomy. **Applied and environmental microbiology**, 73(16):5261, 2007.

Ronald L Wasserstein and Nicole A Lazar. The asa's statement on p-values: context, process, and purpose. **The American Statistician**, 2016.

Hadley Wickham. A layered grammar of graphics. **Journal of Computational and Graphical Statistics**, 19(1):3–28, 2010.

Hadley Wickham. Tidy data. **Journal of Statistical Software**, 59(10), 2014.

Hadley Wickham. **ggplot2: Elegant Graphics for Data Analysis**. Springer New York, 2016. ISBN 978-0-387-98140-6. URL http://had.co.nz/ggplot2/book. Second Edition.

Mark A Wiel, Tonje G Lien, Wina Verlaat, Wessel N Wieringen, and Saskia M Wilting. Better prediction by use of co-data: adaptive group-regularized ridge regression. **Statistics in Medicine**, 35(3):368–381, 2016.

Eugene P Wigner. The unreasonable effectiveness of mathematics in the natural sciences. **Communications on pure and applied mathematics**, 13(1):1–14, 1960.

Leland Wilkinson. Dot plots. **The American Statistician**, 53(3):276, 1999.

Leland Wilkinson. **The Grammar of Graphics**. Springer, 2005.

Quin F Wills, Kenneth J Livak, Alex J Tipping, Tariq Enver, Andrew J Goldson, Darren W Sexton, and Chris Holmes. Single-cell gene expression analysis reveals genetic associations masked in whole-tissue experiments. **Nature biotechnology**, 31(8):748–752, 2013.

D Witten, R Tibshirani, S Gross, and B Narasimhan. Pma: Penalized multivariate analysis. **R package version**, 1(5), 2009a.

Daniela M Witten and Robert Tibshirani. Penalized classification using fisher's linear discriminant. **Journal of the Royal Statistical Society: Series B (Statistical Methodology)**, 73(5):753–772, 2011.

Daniela M Witten, Robert Tibshirani, and Trevor Hastie. A penalized matrix decomposition, with applications to sparse principal components and canonical correlation analysis. **Biostatistics**, page kxp008, 2009b.

Svante Wold, Arnold Ruhe, Herman Wold, and WJ Dunn, III. The collinearity problem in linear regression. the partial least squares (pls) approach to generalized inverses. **SIAM Journal on Scientific and Statistical Computing**, 5(3):735–743, 1984.

Erik S Wright. Decipher: harnessing local sequence context to improve protein multiple sequence alignment. **BMC bioinformatics**, 16(1):1, 2015.

CF Jeff Wu and Michael S Hamada. **Experiments: planning, analysis, and optimization**, volume 552. John Wiley & Sons, 2011.

Hongxiang Yu, Diana L Simons, Ilana Segall, Valeria Carcamo-Cavazos, Erich J Schwartz, Ning Yan, Neta S Zuckerman, Frederick M Dirbas, Denise L Johnson, Susan P Holmes, et al. Prc2/eed-ezh2 complex is up-regulated in breast cancer lymph node metastasis compared to primary tumor and correlates with tumor proliferation in situ. **PloS one**, 7(12):e51239, 2012.

Achim Zeileis, Christian Kleiber, and Simon Jackman. Regression models for count data in R. **Journal of Statistical Software**, 27(8), 2008. URL http://www.jstatsoft.org/v27/i08/.

Georg Zeller, Julien Tap, Anita Y Voigt, Shinichi Sunagawa, Jens Roat Kultima, Paul I Costea, Aurélien Amiot, Jürgen Böhm, Francesco Brunetti, Nina Habermann, Rajna Hercog, Moritz Koch, Alain Luciani, Daniel R Mende, Martin A Schneider, Petra Schrotz-King, Christophe Tournigand, Jeanne Tran Van Nhieu, Takuji Yamada, Jürgen Zimmermann, Vladimir Benes, Matthias Kloor, Cornelia M Ulrich, Magnus von Knebel Doeberitz, Iradj Sobhani, and Peer Bork. Potential of fecal microbiota for early-stage detection of

colorectal cancer. **Molecular Systems Biology**, 10(11):766, 2014. doi: 10.15252/msb.20145645. URL http://msb.embopress.org/content/10/11/766.abstract.

Hui Zou and Trevor Hastie. **elasticnet: Elastic-Net for Sparse Estimation and Sparse PCA**, 2012. URL https://CRAN.R-project.org/package=elasticnet. R package version 1.1.

Hui Zou, Trevor Hastie, and Robert Tibshirani. Sparse principal component analysis. **Journal of computational and graphical statistics**, 15(2):265–286, 2006.